The effect of strip thinning on partitioning of evapotranspiration in a Japanese cypress plantation

January 2014

Xinchao SUN

The effect of strip thinning on partitioning of evapotranspiration in a Japanese cypress plantation

A Dissertation Submitted to
The Graduate School of Life and Environmental Sciences,
The University of Tsukuba
in Partial Fulfillment of the Requirements
for the Degree of Doctor of Philosophy in Science
(Doctoral Program in Integrative Environmental Science)

Xinchao SUN

Contents

Abstract

Forest thinning plays a great role in regulating the hydrological cycle at multiple temporal and spatial scales. Moreover, different management practices could result in different effects on components of forest water cycle. Evapotranspiration (ET) is an important component in water balance and is used to evaluate forest hydrological functions. The quantification of changes in partitioning of ET response to thinning could help to understand the changes in forest stand water balance. Strip thinning requires less time and skill needed for tree selection and has been widely adopted in these abandoned Japanese coniferous plantations. Despite numerous studies on the relations between forest practice and water cycle, few studies attempt to elucidate the effect of strip thinning on partitioning of ET. Thus the major objectives of this study were: 1) to examine the effect of strip thinning on partitioning of ET; and 2) to get an integrated finding for optimizing water and forest management in forested watersheds.

The study was conducted in an unmanaged 32-year-old Japanese cypress stand on Mt. Karasawa, located in Tochigi Prefecture in Central Japan. Intensive field measurements were employed to monitor open rainfall (P_g), throughfall (*TF*), stemflow (*SF*), tree transpiration (E_t), and evaporation from forest floor (E_f). Strip thinning which includes each interval of two lines of trees that were felled, was performed in a catchment in October 2011. Stand density decreased 50% corresponding basal area reduced 48%. Monitoring period was divided into pre-thinning period (November 2010 – October 2011) and post-thinning period (November 2011 – October 2012).

These results demonstrated that strip thinning resulted in an increase in *TF* (from 61.4-73.0%) and decreases in *SF* (from 9.8-6.1%) and canopy interception (E_i) rate (from 28.7-20.8%). Water availability in the soil matrix increased after thinning, particularly in dry season. Based on summarizing the findings of previous studies, the degree of decline in E_i loss/rate caused by thinning was related to P_g and ratio of thinning. These results can be used for researchers to get a

general understanding to manage and implement hydrology-based silviculture.

Xylem sap flow densities (F_d) were elucidated before and after thinning. F_d at the outer xylem (0-20 mm) increased remarkably, whereas the F_d at the inner xylem (20-40 mm) had no significant change after thinning. Mean stand sap flow density values were higher in the post-thinning period, and the differences significantly increased with increasing vapor pressure deficit values. Furthermore, daily single tree E_t increased, particularly in the small tree class. Unlike the daily tree E_t, the daily stand E_t decreased from 1.23±0.48 to 0.74±0.42 mm d^{-1}. Annual stand E_t decreased by 38.3% from 441.0 to 272.1 mm. These results can improve the understanding for the E_t responses at individual tree and stand levels to strip thinning.

The changes in E_f were examined before and after thinning. Daily variations in E_f located at different points had no significant differences and corresponded to solar radiation under the forest canopy in both periods. These results could improve the understanding of changes in spatial variations of E_f and solar radiation by thinning, and will be used to analyze and model the energy balance at the forest floor. Additionally, daily E_f increased from 0.34±0.23 to 0.68±0.47 mm d^{-1}. Annual E_f increased by 97.6% from 124.0 to 245.0 mm. The quantification of changes in E_f by thinning can help understand hydrological processes at the forest floor, and develop predictive and management tools to improve water use and water-use efficiency in forest ecosystems.

The changes in partitioning of ET by thinning were quantified. Thinning caused the annual ET decreased by 15.5% from 980.2 to 780.1 mm. Thinning efficiently increased the water availability, and highlighted the positive thinning effects on water resources in forested watersheds. Thinning resulted in decreases in E_i (from 42.3-33.7%) and E_t (from 45.3-34.9%) and an increase in E_f (from 12.4-31.4%). Although stand E_t was the dominant component of ET in both periods, the relative contribution of each flux to ET were changed to be very close after thinning. These findings could guide us for predicting the changes in stand water balance by thinning, and achieving an optimized water and forest management in forested watersheds.

List of Tables

List of Figures

Chapter 1

Chapter 2

Chapter 3

Chapter 4

List of Symbols

A	area of study site (m^2)
c	canopy cover
c_a	an aerodynamic parameter
c_p	the specific heat of air at constant temperature (MJ kg^{-1} $°C^{-1}$)
D or VPD	the vapor pressure deficit (kPa)
DBH	diameter at breast height (cm)
d	the displacement height (m)
$\overline{E}$	mean evaporation rate (mm h^{-1})
$\overline{E}_c$	mean evaporation from the saturated canopy during rainfall, defined as $\overline{E}/c$
$e_{ss}(T)$	the saturated vapor pressure at 2 m above the forest floor (kPa)
e_{sa}	the local actual vapor temperature at 2 m above the forest floor (kPa)
G	the soil heat flux (MJ m^{-2} d^{-1})
h	the canopy height (m)
I_w	canopy wetting
k	the von Kármán constant
m	the number of trees belonging to a certain DBH class
n	the number of DBH classes
P_t'	the amount necessary to saturate the trunks, defined as S_t/p_t
p	direct throughfall proportion
p_t	the proportion of rain diverted to stemflow
$\overline{R}$	mean rainfall intensity (mm h^{-1})
R_n	net radiation load on the canopy (MJ m^{-2})
R_{sn}	the net radiation at 2 m above the forest floor (MJ m^{-2})
r_a	the aerodynamic resistance above the forest canopy(s m^{-1})
r_{sa}	the aerodynamic resistance of the forest floor (s m^{-1})
r_{sc}	the (bulk) surface resistance of the forest floor (s m^{-1})
S	canopy storage capacity (mm)
S_c	canopy capacity per unit area of cover, defined as S/c
S_n	average stemflow volume (ml)

S_t	trunk storage capacity (mm)
T	temperature (°C)
u	the wind speed at height z (m s^{-1})
z	the reference height above the ground surface (m)
z_o	the roughness length (m)
λ	the latent heat of vaporization of water (MJ/kg)
Δ	the rate of change of saturated vapor pressure with temperature (kPa °C^{-1})
α	the albedo of the forest canopy
ρ	the density of dry air (kg m^{-3})
γ	the psychometric constant (kPa °C^{-1})
ε	the acceptable standard error (%)

List of Abbreviations

A_{S_tree}	tree sapwood area
A_{s_stand}	stand sapwood area
A_G	ground area of the study site
A_i	sapwood areas at the xylem depth of 0 – 20 mm for all trees
B_i	sapwood areas at the xylem depth of 20 – 40 mm for all trees
CV	coefficient of variability
ET	evapotranspiration
E_i	canopy interception
E_t	transpiration
$E_{t\text{-}tree}$	single tree transpiration
$E_{t\text{-}stand}$	stand transpiration
E_f	forest floor evaporation
F_d	sap flow density
G_c	canopy conductance
J_S	the mean stand sap flow density
J_{S_A}	the mean F_d for the xylem bands at 0 – 20 mm for all measured trees
J_{S_B}	the mean F_d for the xylem bands at 20 – 40 mm for all measured trees
N	the total number of Japanese cypress trees in the study plot
PET	potential evapotranspiration
PAR	photosynthetically active radiation
P_g	gross precipitation
SF	stemflow
TF	throughfall
Θ	soil water content

Chapter 1 Introduction

1-1 Relationship between forest and water

Forest and water are inseparable. Forests and water occur together and they interact. Plant a tree and it will use water; cut a tree and its water use ceases. Forest hydrology is the study of water in forests: its distribution, storage, movement, and quality; hydrologic processes within forested areas; and the delivery of water from forested areas. Forest hydrology research used field measurements, experiments, and modeling to characterize and predict hydrologic processes and their response to natural disturbance and management of forests. It draws upon disciplinary knowledge from several branches of hydrological sciences, water resources engineering, and forestry to address primary questions of forests and water: What are the flow paths and storage reservoirs of water in forests and forest watersheds? How do modifications of forest vegetation influence water flow paths and storage? How do changes in forests affect water quantity and quality (Anderson et al., 1976)?

The changes in vegetation cover by forest management will have an impact on catchment water balance and hence water yield and groundwater recharge (Llorens and Domingo, 2007; Zhang et al., 2001). The quantification of hydrological processes in forests is an important component of studies aiming to increase water yields in forests (Bosch and Hewlett, 1982; Stednick, 1996) because a reduction in forest covers increases water yield due to the subsequent reduction in evapotranspiration (Zhang et al., 2001). The degrees to which the effects of forest management modify water quantify and quality over the long term has been the subject of forest hydrology for the past century (National Research Council, 2008). Forest hydrologists use concepts of "balance" or "budgets" of water, energy, sediment, and nutrients, to understand how forests affect water quantity and quality. The water balance traces the transformation of precipitation (input) to runoff (output), which is of interest to the general public and water managers (Fig. 1-1). The amount of

precipitation is the dominant control on the amount of runoff. The timing and type of precipitation (e.g., rain, snow, or fog drip) also affect the amount and timing of runoff. A second major control on runoff is the transfer of water to the atmosphere by evapotranspiration from vegetation, and a third control on runoff is the amount of water that can be infiltrated and stored. A third control on runoff is the amount of water that is stored or flows as groundwater, i.e., water that infiltrates into the soil surface; water that is stored in the soil profile, and water that moves laterally as groundwater flow (Fig. 1-1).
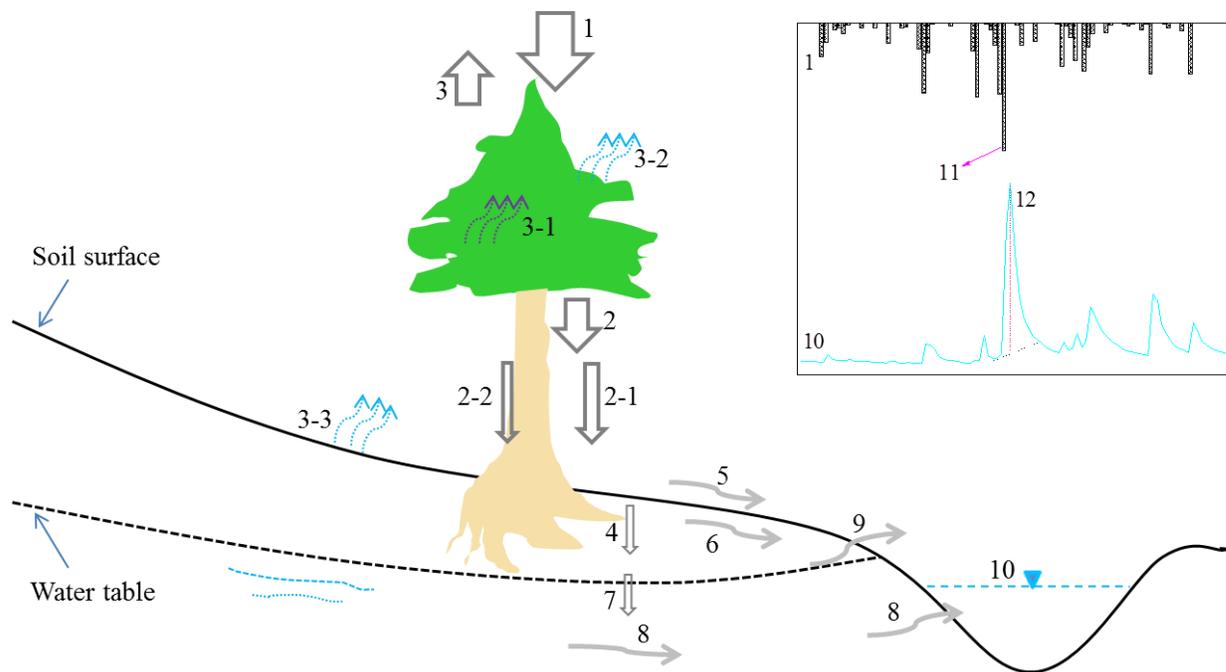
Fig. 1-1 Elements of the water balance in a forest: 1 = precipitation (rain, snow, cloudwater deposition); 2 = net precipitation; 2-1 = throughfall; 2-2 = stemflow; 3 = evapotranspiration; 3-1 = canopy interception; 3-2 = tree transpiration; 3-3 = forest floor evaporation; 4 = infiltration; 5 = surface runoff, or infiltration excess (Horton) overland flow; 6 = subsurface flow, or lateral subsurface flow; 7 = groundwater recharge; 8 = groundwater flow; 9 = saturation excess overland flow; 10 = discharge or streamflow; 11 = precipitation intensity; 12 = peak flow or peak discharge. Although it is not shown, understory vegetation also contributes to these processes.

Forest management (e.g., thinning) plays a great role in regulating the hydrological cycle, as runoff and evapotranspiration, at multiple temporal and spatial scales by altering ecosystem water balances (Andreassian, 2004; Breda et al., 1995; Dung et al., 2012; Simonin et al., 2007). Thinning is a common silvicultural practice to manage between-tree competition, aimed at increasing the dimensions and quality of trees harvested at the end of a rotation. Removal of trees alters the cover and structure of the forest canopy (Crockford and Richardson, 1990; Dung et al., 2012; Lesch and Scott, 1997; Stogsdill et al., 1989) and then leads to increase the amount and density of understory vegetation and the growth rate of residual trees by changing the light conditions under the forest canopy (Aussenac et al., 1982; Dodson et al., 2008; Maleque et al., 2007b; Thomas et al., 1999). These changes can also enhance biodiversity of forest ecosystems (Maleque et al., 2007a; Nagaike et al., 2006). Furthermore, forest thinning alters the hydrological processes of forested watershed by reducing canopy interception (Breda et al., 1995; Crockford and Richardson, 1990; Limousin et al., 2008; Molina and del Campo, 2012; Teklehaimanot et al., 1991), decreasing the evapotranspiration rate (Breda et al., 1995; Serengil et al., 2007) and increasing runoff generation (Dung et al., 2012; Dung et al., 2011; Lane and Mackay, 2001; Lesch and Scott, 1997). Therefore, examining changes in components of forest water cycle by forestry practice has been a critical topic in forest hydrology and could improve the understanding of changes in water resources in forested watersheds.

1-2 Forest conditions in Japan

In Japan, forests cover 67% of total land area, and approximately 40% of forested land area or 25% of the national land area is composed of coniferous plantation forests (National Astronomical Observatory, 2009). The two species in the family Cupressaceae, Japanese cedar (*Cryptomeria japonica* D. Don) and Japanese cypress (*Chamaecyparis obtusa* Endl.), are dominant coniferous plantation species in Japan. These plantations were planted mainly after the Second World War to meet the high demand for timber in Japan (Iwamoto, 2002). However, these plantations are now approaching harvesting age, but they have not been managed properly because

of an increase in import of cheap timbers and woody products from other countries and an increase in employment cost (Iwamoto, 2002). As a result, many overstocked stands of these plantations are abandoned. And they have sparse or no understory vegetation cover due to the low light conditions that occur under the dense forest canopy, particularly Japanese cypress forests (Onda et al., 2010).

Therefore, these plantations pose major environmental problems, even if a forest appears healthy from a distance (Fig. 1-2a) (Onda et al., 2010; Teramage et al., 2013). The direct impact of throughfall raindrops decreases the infiltration rate (Nanko et al., 2010), causes splash erosion (Mizugaki et al., 2010; Nanko et al., 2008) and soil surface sealing (Onda and Yukawa, 1994), increases suspended sediment sources (Mizugaki et al., 2008) and nutrient loss (Zhang et al., 2008) from the watershed. Besides, forests cover most mountainous regions upstream of agricultural and urban areas, and are considered water resources in Japan (Sawano et al., 2005). Kuraji (2003) reported that abandoned plantations could consume more water by evapotranspiration (ET) from dense canopies, and reduce catchment runoff and water resources. Komatsu et al. (2008a) summarized 43 annual ET observations in Japanese forest catchments from earlier publications. They reported that the annual ratio of ET to P_g ranged from 15.1 to 74.6% with a mean of 41.3% based on different forest types and meteorological conditions around Japan. Canopy interception, a major component of ET, is crucial in regulating water resources for forests, and comprised 12-30% of gross precipitation in Japanese cypress plantations (Komatsu et al., 2007). Overall, an examination of hydrological processes in forested watersheds is particularly critical for water resources management in Japan. Such examinations on components of forest water cycle (e.g., runoff, ET, canopy interception, tree transpiration, and forest floor evaporation) could enhance the understanding of water resources of forested watershed, and can also provide a basis for future studies of forest management (e.g., thinning).
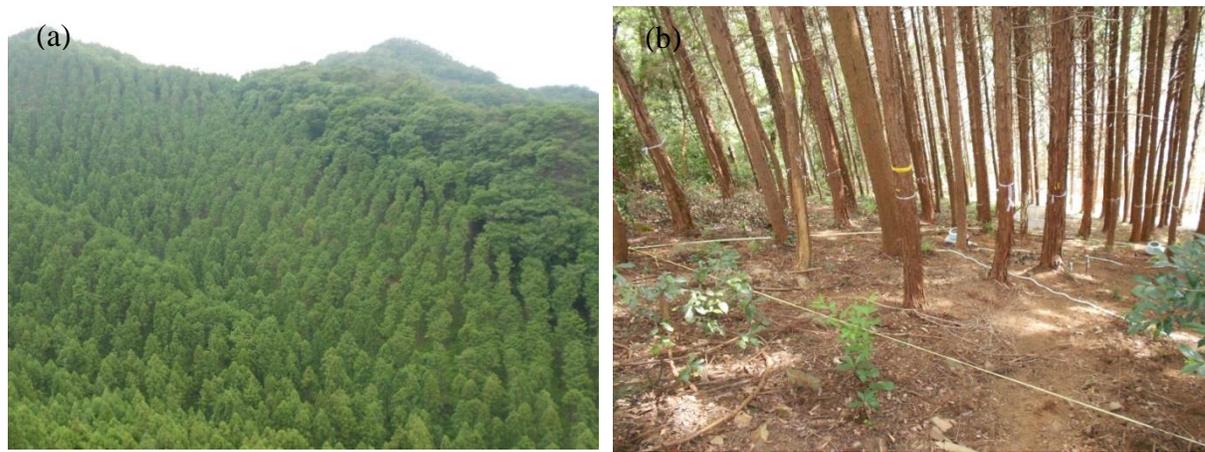
Fig. 1- 2 Abandoned Japanese cypress plantations (a) general view (b) inside of the forest.

In Japan, it is highly required to clarify the effect of thinning on components of forest water cycle especially for coniferous plantations (Komatsu et al., 2013). These plantations need to be thinned twice or three times before they are harvested. Recently, they are subjected to management such as thinning because of many environmental issues in these dense and mature Japanese coniferous plantations (Onda et al., 2010; Teramage et al., 2013). Recovery of understory vegetation is also a management goal during thinning. In general, the 40-60% thinning induced changes in biomass of understory vegetation is caused by increased radiation. Therefore, there has been a partial removal of trees in mature (30-60 years old) plantations. Many studies have been examined changes in various components of forest water cycle (e.g., runoff, canopy interception and transpiration) by forestry practice (e.g., Dung et al., 2011, 2012; Sado and Kurita, 2004; Morikawa et al., 1986). For example, Dung et al. (2011, 2012) reported that heavy thinning of 58.3% in a Japanese cypress plantation resulted in a 2.1 mm increase in overland flow in response to individual storms and a 240.7 mm increase in catchment annual runoff. These examinations could enhance the understanding of underlying processes of the changes in catchment runoff, and will help guide integrated forest and water management.

1-3 Evapotranspiration

1-3-1 Partitioning of evapotranspiration

Precipitation on forested hill slopes can be partitioned into two basic components: one is the water infiltrated to soil, the other is the evapotranspiration (ET) returned to atmosphere. ET is composed of three sub-components: canopy interception (E_i), tree transpiration (E_t) and forest floor evaporation (E_f). ET is an important component in water balance and is used to evaluate forest hydrological functions. In general, ET is in the range of 15-75 % of total precipitation in temperate forest (Komatsu et al., 2008a). The variability of ET related to the amount of precipitation (Laio et al., 2001), land-atmosphere interactions influence weather and climate (Eltahir, 1998; Pielke, 2001), and plant physiology (Lauenroth and Sala, 1992; Porporato et al., 2001; Rodriguez-Iturbe, 2000).

In ecosystem studies, understanding of partitioning of ET helps researchers to identify the influences of biotic and abiotic factors that are involved in the evaporation pathway of the hydrological cycle (Williams et al., 2004). Several studies have focused on partitioning of ET for different forest species and climates. In *Abies fabri* (Mast.) Craib in subalpine climate, ET accounted for 61.4% of gross precipitation (P_g) of 1,199 mm. E_i was the dominant component and represented > 70% of ET, while E_f was the smallest component and only accounted for 6% of ET (Lin et al., 2012). In *Pinus caribaea* Morelet in a tropical climate, ET accounted for > 80% of annual P_g (P_g = 2,054 mm); E_t was the dominant component, accounting for about 70% of ET, while E_i and E_f only accounted for about 20% and 8.5%, respectively (Waterloo et al., 1999). In *Pinus halepensis* Miller in a semi-arid climate, ET sometimes exceeded precipitation and accounted for 85-102% of annual P_g (P_g = 285 mm). E_t and E_f were the main two components, accounting for approximately 49, and 39% of ET, respectively (Raz-Yaseef et al., 2012).

Shimizu et al. (2003) and Kosugi and Katsuyama (2007) focused on the total ET using eddy covariance method in a Japanese cypress plantation and found that the ratio of ET to P_g was in the range of 37.5–62.3%. However, the current information has limited usefulness in drawing concrete

comparisons and conclusions. For example, Hattori (1983) measured the seasonal variation of E_f using soil evaporimeters in a Japanese cypress stand and found that E_f accounted for 8.9% of annual P_g with a mean value of 0.38 mm d^{-1}. Tanaka et al. (2005) observed E_i in mature Japanese coniferous stands and reported that total E_i represented approximate 15.0% of total P_g during a 4-year period. Takagi (2013) quantified the partitioning of ET in a small catchment covered by a mature Japanese cypress plantation, but the study mainly focused on deep percolation into underlying rock. Until now, few data has been available to document all the components of ET at a time and to make comparisons related to its partitioning. The combined monitoring of E_i, E_t and E_f could reveal the partitioning of ET in plantation and could provide better a better understanding of water cycle in forests.

1-3-2 Canopy interception

Precipitation (P_g) partitioning into throughfall (TF), stemflow (SF) and canopy interception (E_i) after it reaches the canopy represents the initial interaction between water cycle and forest. E_i is the proportion of incident precipitation that is intercepted, stored and subsequently evaporated from forest leaves, branches and stems during and after rainfall events. It is a major component of evapotranspiration (Price and Carlyle-Moses, 2003; Schellekens et al., 1999; Viville et al., 1993), and strongly influences the generation of runoff and sediment from forest stands (Wallace and McJannet, 2006). E_i has been investigated in different species, including coniferous forests (Gash, 1979; Llorens et al., 1997; Shi et al., 2010), broad-leaved forest (Andre et al., 2011; Deguchi et al., 2006; Price and Carlyle-Moses, 2003), tropical rainforests (Dykes, 1997; Lloyd et al., 1988; Wallace and McJannet, 2006), cultural cropping system (van Dijk and Bruijnzeel, 2001), and agro-forestry system (Jackson, 2000). In general, E_i is between 9% and 48% of P_g for different canopies (Hormann et al., 1996). The E_i varies greatly, and is determined by forest structural parameters (forest density, canopy structure, and leaf area index) (Deguchi et al., 2006; Komatsu and Hotta,

2007; Staelens et al., 2006) and climatic parameters (evaporation rate and rainfall rate) (Gash, 1979; Link et al., 2004; Wallace and McJannet, 2006).

Previous studies have shown that E_i comprised 12–30% of P_g in Japanese coniferous plantations (Komatsu et al., 2007). Most investigations lack sufficiently high-resolution TF and detailed within-canopy weather data to assess the influence of temporal changes in canopy structure and within-event weather variations on evaporation of intercepted water. Link et al. (2004) reported that E_i in closed canopies is largely controlled by the direct throughfall proportion (p), the fraction that drains from the canopy, and the canopy storage capacity (S). Determination of these E_i parameters is therefore needed to improve understanding of the interception process and test generalized models (Link et al., 2004; Loustau et al., 1992a). However, few interception studies have attempted to determine S and/or p for coniferous forests in Japan.

TF is known to be extremely variable in space, even at the plot scale. Spatial patterns of TF input can affect the heterogeneity of hydrological, biogeochemical, and ecological processes on the forest floor and in the mineral soil (Staelens et al., 2006). The spatial distribution of TF has been reported to either increase (Frost and Edinger, 1991; Nanko et al., 2011) or to be invariant (Loustau et al., 1992b; Shachnovich et al., 2008; Vellak et al., 2003) with distance from the trunk. The spatial distribution is also related to canopy cover, and is greater during leafed periods than leafless periods (Staelens et al., 2006). Nanko et al. (2011) conducted an indoor experiment using 9.8 m-tall transplanted Japanese cypress to evaluate TF spatial variability under a single canopy. They indicated that the spatial distribution was dominated by canopy shape and position of branches inside the canopy; TF rate varied greatly adjacent to the trunk and increased with radial distance from it. However, little is known about the spatial variability in abandoned Japanese cypress forests.

Models of E_i have been developed to assess and predict the magnitude of interception based on rainfall and canopy characteristics (Gash, 1979; Gash et al., 1995; Rutter et al., 1971). The first conceptual interception model, called the Rutter model (Rutter et al., 1971; Rutter and Morton, 1977;

Rutter et al., 1975), calculates water balance for the wetted canopy-derived canopy parameters p and S, and wet-canopy evaporation is computed with the Penman method. The Rutter model was a fundamental, representative model requiring much data. A simpler, storm-based version based on that model, originally called the Gash analytical model, was proposed by Gash (1979). It requires fewer data and has been demonstrated effective for a wide range of canopies. However, the original Gash model overestimates for sparse forest areas (Gash et al., 1995; Valente et al., 1997) since it assumes that the evaporation area extends to the entire plot area. Therefore, the original Gash model was reformulated by introducing a canopy cover fraction for application to sparse forests, by Gash et al. (1995) and Valente et al. (1997), and also removing some mathematical inconsistencies when it dealt with low rainfall rates. Hence, this revised Gash analytical model was more robust and accurate and can be applied widely for different species with range of canopy cover fraction (Deguchi et al., 2006; Gash et al., 1995; Jackson, 2000; Llorens, 1997; Shi et al., 2010; van Dijk and Bruijnzeel, 2001). However, few studies have applied the revised model to abandoned Japanese coniferous forest plantations, parameterizing the interception model and conducting validation.

1-3-3 Tree transpiration

Tree transpiration (E_t) is a main part in forest water balance and for modeling water, energy and carbon exchange in forest ecosystem. In coniferous forests, E_t may account for approximately 19.0-72.4% of ET for different climates summarized from previous studies. To quantify E_t in forests, several methods are available that assess forest water use at both temporal and spatial scales. Thermal dissipation sap flow technique (Granier, 1987) is the most useful, particularly in a mountainous country like Japan, because complex terrain and spatial heterogeneity does not limit its applicability (e.g., Wilson et al., 2001).

To estimate stand-scale E_t, appropriate scaling procedures are required to extrapolate from sap flow measurements made on individual trees. The scaling procedure requires: (1) estimation of the total sapwood area of the stand (A_{S_stand}) from the relationship between the stem diameter at

breast height (DBH; measured for all trees in the stand) and tree sapwood area (A_{S_tree}) measured the sampled trees; (2) estimation of mean stand sap flux density (J_S) from tree-level measurements of xylem sap flow density (F_d) in a limited sample size in the stand; and (3) calculation of stand transpiration as the product of A_{S_stand} and J_S. Several sources of errors must be taken into account at each step in the scaling process because of tree-to-tree variations in F_d (Granier et al., 1996a; Kumagai et al., 2005a; Pataki and Oren, 2003) and A_{S_tree} (Kumagai et al., 2005c) and radial variation in F_d across the sapwood of individual trees (Delzon et al., 2004; Kumagai et al., 2005a; Lu et al., 2000; Shinohara et al., 2013; Zang et al., 1996).

This technique can be effectively applied to estimate the tree water use on a continuous basis, which has made it feasible to examine the thinning effects on water uptake and E_t at both tree and stand levels, at a high temporal resolution. Several studies have used it to examine changes in tree water use induced by thinning (e.g., Breda et al., 1995; Lagergren and Lindroth, 2004; Medhurst et al., 2002; Morikawa et al., 1986). When climatic data are properly collected simultaneously with sap flow data, this method can supply forceful insights into atmospheric-biological controls of tree water use (Whitehead, 1998).

1-3-4 Forest floor evaporation

Forest floor evaporation (E_f) is one component of ET in forests, defined as the evaporation from the A_o horizon and underlying soil surface (Bristow et al., 1986; Deguchi et al., 2008). The A_o horizon consists of litter, fermentation and humus layers. The litter layer is an important fact and helps to prevent excessive loss of soil moisture by evaporation. E_f was in the range of 3 to 21% of total ET in forest stands without an understory (Kelliher et al., 1993). Compared with forests with closed canopies (Moore et al., 1996; Schaap and Bouten, 1997), E_f constituted a high proportion of ET from deciduous forests in the dormant season or in forests with open canopies (Kelliher et al., 1997; Wilson et al., 2000). Additionally, E_f accounted for approximately 6.0-42.1% of ET for

different climates in coniferous forests summarized from previous studies. However, E_f has received little attention compared with research on E_i and E_t, and considered to be much less than them, because the forest floor environment is highly humid, with low wind speed and low available energy, compared with the canopy surface (Hattori, 1983).

In general, E_f can be measured by means of a lysimeter system (Kelliher et al., 1997; Kelliher et al., 1990; Schaap and Bouten, 1997), a closed-chamber system (Deguchi et al., 2008; Norman et al., 1992) or eddy covariance techniques (Baldocchi et al., 2000; Baldocchi and Meyers, 1991; Wilson et al., 2000). Lysimeter systems are useful for simultaneously measuring many points at low cost, and have been applied extensively in different ecosystems (e.g., agriculture, agroforestry and forest) to estimate E_f (e.g., Allen, 1990; Boast and Robertson, 1982; Hattori, 1983; Jackson and Wallace, 1999), although they are unsuitable for long-term measurements because the moisture and heat conditions inside the container change over long periods (Hattori, 1983). Eddy covariance techniques can be used to simulate the average efflux with minimal impact on the local environment, but they need strict requirements that meet for the technique to be applicable (Fang and Moncrieff, 1996). The closed-chamber system was developed to measure CO_2 efflux from soils and designed that air circulates in a loop between the chamber and an external gas analyzer (Goulden and Crill, 1997; Norman et al., 1992). This system could estimate E_f as well as the lysimeter system (Daikoku et al., 2008).

1-4 Thinning effect on partitioning of evapotranspiration

1-4-1 Reviews of forest management effect on forest water cycle

A number of attempts have been made to evaluate how forest management, including thinning, affects components of forest water cycle (e.g., runoff, canopy interception, and transpiration). Bosch and Hewlett (1982) found that increases in water yield depended on the area of harvesting treatments in a given watershed. The increased water yield also related to rates of canopy removal (Baker, 1986; Lane and Mackay, 2001). For example, Lesch and Scott (1997) found that

forest thinning of 22-46% in a 27.2 ha catchment increased annual runoff by 10-71% in the first 3 years after thinning, and annual streamflow decreased slightly after a 46% forest thinning in a 191 ha catchment in South Africa. The rate of increase in catchment runoff after thinning may be related to annual precipitation. For example, Ruprecht et al. (1991) observed a 260 mm increase in annual runoff after 74% of basal area removal for 1300 mm of annual precipitation while Baker (1986) found a 32 mm increase of annual runoff after 31-68% thinning for 668 mm annual precipitation. It implied that areas with more annual precipitation have greater increases in catchment runoff after thinning treatment compared to areas with less precipitation. Besides, hydrological responses to any given precipitation are also strongly scale dependent (Gomi et al., 2008; Sidle et al., 2000). The differences in vegetation type, topography, and soil properties in hillslope, headwater, and downstream areas may result in dominant hydrological processes differ (Sidle et al., 2011; Stomph et al., 2002). Dung et al. (2012) reported that despite annual runoff increased in 240.7 mm at the catchment scale, overland flow at hillslope plot did not increase significantly. Therefore, it is of important to evaluate the complex interactions between vegetation and hydrological processes at various scales when assessing runoff responses associated with forest managements, and to optimize water and forest management in forested watersheds (Castro et al., 1999; Dung et al., 2012; Miyata et al., 2010; Stomph et al., 2002).

Canopy interception (E_i) is one of the major components of the water cycle in forest ecosystems, and is of importance in influencing the water yield of forested areas (Komatsu et al., 2007; Llorens and Domingo, 2007; Hormann et al., 1996). Forest structural parameters (e.g., stand density and leaf area index) strongly determine the variation of E_i (e.g., Deguchi et al., 2006; Link et al., 2004). The changes in characteristics of forest stand caused by thinning would greatly affect E_i. A number of attempts have been made to evaluate how forest management, including thinning, affects E_i in different tree species in the worldwide (e.g. Aussenac et al., 1982; Breda et al., 1995; Limousin et al., 2008; Molina and del Campo, 2012; Teklehaimanot et al., 1991). For example,

Teklehaimanot et al. (1991) found that mean annual E_i rate was 33, 24, 15 and 9% in the 2, 4, 6 and 8 m spacing treatments, respectively, in a *Picea sitchensis* forest in Cloich, Edinburgh. And the difference in E_i between the spacing treatments was attributed to the difference in the boundary layer conductance. Many thinning experiments have shown that the degree of decline in E_i rate is not proportional to the amount of biomass removed. Whitehead and Kelliher (1991) reported that, for instance, removing 56% of the stems with respect to control value only resulted in a 27.2% decrease in E_i in a *Pinus radiata* forest in New Zealand. Furthermore, environmental conditions (e.g., fog entrapment) can also influence the changes in rainfall partitioning by thinning. For example, Aboal et al. (2000) reported that the importance of fog entrapment that reducing leaf area index and surface roughness has a negative effect on throughfall. Hydrological responses to land management and cover change vary greatly because of the complex interactions among climate, soil, and vegetation from individual tree to landscape scales (Bosch and Hewlett, 1982; Zhang et al., 2001). Therefore, it is very necessary to evaluate quantitatively the effect of forestry practice on E_i in forest watersheds. An understanding of relationship between canopy water balance and forest could play an important role on predicting the changes in interception processes caused by forest management.

Tree transpiration (E_t) is influenced by environmental variables, including vapor pressure deficit, solar radiation, wind speed and temperature (Morikawa et al., 1986; Granier et al., 1996a; Oren et al., 1999; Clausnitzer et al., 2011), and by the availability of soil water within the rooting zone (Black et al., 1980; Breda et al., 1995; Simonin et al., 2007). The thinning of forests results in stand canopies more open. Accordingly, the remained individual trees have apportioned a higher availability of site resources (e.g., soil water) due to thinning treatment (Black et al., 1980; Breda et al., 1995; Morikawa et al., 1986). However, thinning can vary various factors that affect the growth rate of trees, and it is difficult to determine the single most important factor affecting tree water use (Medhurst et al., 2002). Therefore, studies regarding changes in E_t that are induced by thinning are

quite necessary for predicting tree water use and for guiding integrated forest and water management.

Several studies have focused on the changes in E_t by thinning in different species (e.g., Breda et al., 1995; Lagergren et al., 2008; Morikawa et al., 1986; Reid et al., 2006; Simonin et al., 2006, 2007; Stogsdill et al., 1992). For example, Morikawa et al. (1986) reported that the stand E_t decreased by 21.2% after 24% thinning in a Japanese cypress forest. In addition, the daily single tree E_t was higher at a given range of solar radiation, except in suppressed trees. Breda et al. (1995) reported that thinning caused the stand E_t value to decrease in the thinned plot of an oak forest for the first year, whereas the stand E_t approached the same level as that on the control plot after two years of thinning. Furthermore, the difference in the stand E_t between the thinned and the control plot may not significantly decrease due to the drought periods. Simonin et al. (2007) found that the difference in the stand E_t between the thinned and the control plot was much less when the soil water content was low in semi-arid *Pinus ponderosa* forests. Lagergren et al. (2008) reported that the stand E_t in the thinned plot was rather higher than that in the control plot during the drought period in a mixed pine-spruce forest in Sweden. However, previous studies only examined changes in E_t by light thinning (removing 24% of stems) (Morikawa et al., 1986) or during a short measuring period (two months before and after thinning, respectively) (Komatsu et al., 2013) for Japanese coniferous plantations. Until now, little data have been available to document the changes in E_t induced by heavy thinning during a long measurement period for coniferous plantations in Japan.

E_f is affected by the photoenvironments (e.g., solar radiation) and the soil water content of the forest floor surface. Kelliher et al. (1993) described the soil environment in relation to leaf area of the vegetation overhead. E_f is constrained by soil water of topsoil and is higher in open sites because forest canopy reduces light penetration and soil temperature. Thinning alters forest structure and changes environmental factors influencing E_f (e.g., solar radiation) inside the forest, and could result in an increase in solar radiation at the forest floor and lead to an increase in E_f contributed to

the higher solar radiation and increased net precipitation. Therefore, it is considered that the proportion of E_f will be relative high where thinning has occurred, and it must not be negligible to evaluate the effect of thinning on E_f in forested watersheds. Some studies have examined the effects of tree shade on spatial variations of E_f (Jackson and Wallace, 1999; Raz-Yaseef et al., 2010). For example, Raz-Yaseef et al. (2010) reported that E_f measured in sun-exposed areas was on average double that in shaded areas, and solar radiation was 92% higher in exposed compared to shaded sites in a semi-arid pine forest in Southern Israel. Furthermore, Simonin et al. (2006) reported that after 82% basal area thinning (corresponding to 45% leaf area index reduced), understory evapotranspiration was greater in thinned compared with unthinned plots in a semi-arid ponderosa pine stand of the southwestern US. The quantification of changes in E_f by thinning is of important for understanding the hydrological processes at the forest floor, and improving water use and water-use efficiency in forest ecosystems. However, until now, few studies have attempted to elucidate the change in E_f induced by thinning.

The changes in forest structure by thinning could alter the relative contributions of E_i, E_t and E_f to total ET in forest watersheds. The reduction of forest canopies and stems may result in decreases in E_i and E_t, and an increase in E_f. The partitioning of ET in forest ecosystems is a dominant control on climate and hydrology at local to global scales. For instance, ET returning to the atmosphere may support future precipitation events and influence canopy gas exchange through a boundary layer feedback (Jarvis and Mcnaughton, 1986). Thus examination of changes in partitioning of ET response to thinning could provide useful information for predicting the changes in forest stand water balance. However, data on the changes in partitioning of ET induced by thinning are still limited.

1-4-2 Strip thinning effect on partitioning of evapotranspiration

Strip thinning is a form of heavy and cost-effective thinning method, in which corridors are opened at regular intervals and the remaining strips are thinned from below, and the width of the

remained sections is usually two to three crown widths. Linear sections of the plantation are harvested paralled to the direction of the slope and often perpendicular to the forest road to extract timber efficiently (Fig. 1-3). Strip thinning has been extensively carried out in these poorly managed plantation stands in Japan primarily because this method does not need select tree that is involved in conventional selective thinning operations and thus requires less time and skill (Taniguchi, 1999) (Fig. 1-3).

Furthermore, strip thinning results in different changes in canopy cover and structure of forest compared with other forestry practices (e.g., selective thinning and partial cutting). The different forest structures can lead to resultant changes in environmental variables (Oguntunde and Oguntuase, 2007; Wilson et al., 2000), the availability of soil water (Aboal et al., 2000; Molina and del Campo, 2012; Stogsdill et al., 1989), and in boundary layer conductance (Teklehaimanot et al., 1991). For example, Teklehaimanot et al. (1991) reported that reported that the greater ventilation (i.e., wind speed) with an increase in tree spacing resulted in greater boundary layer conductance per tree in *Picea sitchensis* (Bong.) Carr forest stands. Recently, Dung et al. (2012) summarized previous studies on the different thinning methods (e.g., partial cutting, clear cutting and selective thinning) and reported that the increase in catchment runoff after selective thinning was less than those after partial cutting. Thus changes in components of forest water cycle response to different management strategies would be different. However, studies on the strip thinning effect on partitioning of ET are quite limited and are quite necessary for achieving an optimized water and forest management.
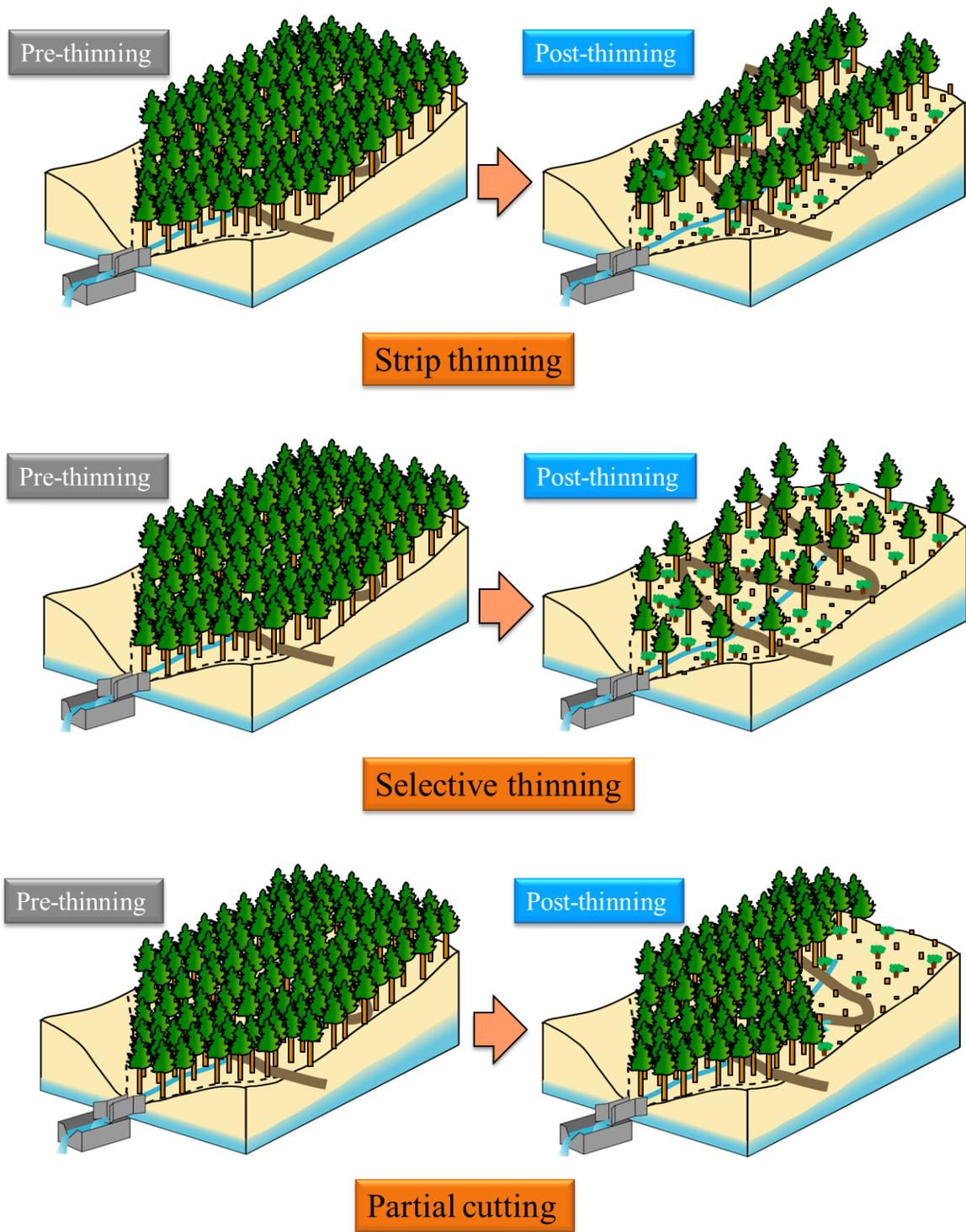
Fig. 1-3 Schematic views of different forest managements (e.g., strip thinning, selective thinning and partial cutting).

1-5 Objectives of this study

Based on the foregoing literature review, this study aimed to (1) quantify partitioning of ET in an abandoned Japanese cypress plantation, and (2) evaluate the effect of strip thinning on ET and its three sub-components (E_i, E_t, and E_f) after 50% strip thinning. The study was conducted in a dense and mature Japanese cypress stand of central Japan.

The rest of the paper is organized as follows. In chapter 2, study site, thinning treatment, measurements, and data analysis were described. In chapter 3, the partitioning of ET was quantified during the growing season and the three components of ET were modeled for an abandoned Japanese cypress plantation. Furthermore, the effect of strip thinning on partitioning of ET was elucidated in chapter 4. Finally, chapter 5 summarized the findings and offered some suggestions for future studies.

Chapter 2 Methodology

2-1 Study area

The study was conducted the catchment K2 on Mt. Karasawa, located in Sano City, Tochigi Prefecture, in central Japan (139°36'E, 36°22'N; 198 m above sea level) (Fig. 2-1). The site is located on a southwest-aspect hill slope with an average slope of 31°. The catchment is covered by Japanese cypress plantations planted in the 1980. However, these plantations received no management practice and have been abandoned since planting. At the time of study, the stand density was high as 2198 trees ha^{-1}, and the corresponding basal area was 50.4 m^2 ha^{-1}. The mean height and diameter at breast height (DBH) were 16.0 m and 19.1 ± 3.9 cm, respectively. The canopy cover fraction was 0.974, as calculated with CanopOn 2 software (http://takenaka-akio.org/etc/canopon2/index.html) from hemispherical photographs of the site. Understory vegetation was sparse, mainly including a fern species (*Gleichenia japonica*) and evergreen shrubs (e.g. *Cleyera japonica* and *Ardisia japonica*). The soil is an orthic brown cambisol with silt–loam texture. The mineral soil is covered by a 1.0-cm thin humus layer with an average bulk density of 1.2 g cm^{-3}.

The humid, temperate climate has a 20-year average annual temperature of 14.1 ± 0.6°C and annual P_g of 1,265 ± 220 mm. The area has two dominant storm periods: the Baiu rainy season from late June to mid-July and the typhoon season from late August to October both of which have abundant precipitation. Rainy season precipitation (from July to October) accounts for 54 ± 10% of mean annual P_g.
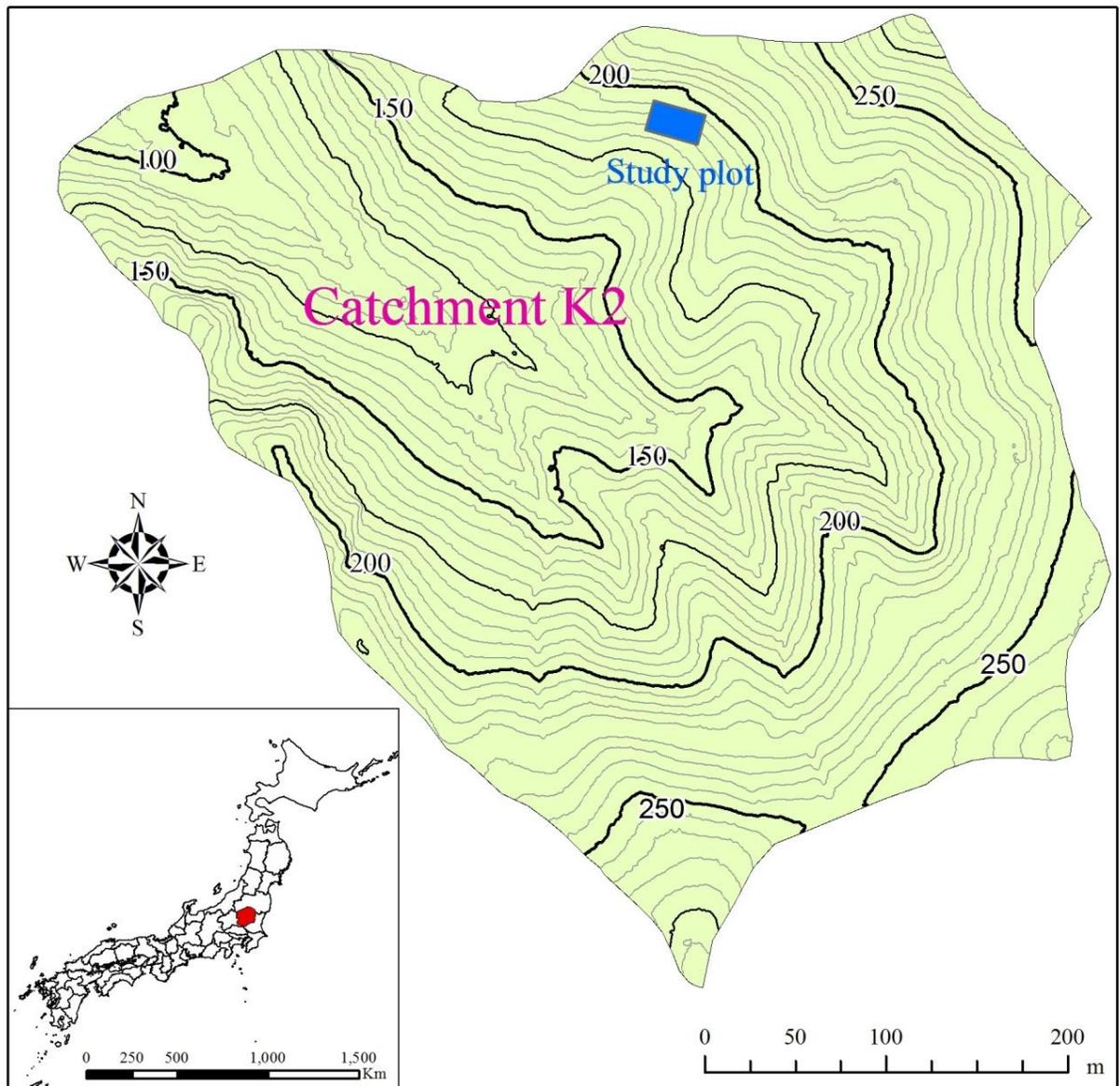
Fig. 2-1 Location map and topography of the Japanese cypress forest field site on Mt. Karasawa, Tochigi Prefecture, Japan.

2-2 Thinning treatment

Strip thinning, which includes each interval of two lines of trees that were felled, was performed in catchment K2 in October 2011 (Fig. 2-2). All thinning operations were conducted by forest workers using no-heavy machinery except for chainsaws, in order to minimize soil disturbance on the hillslope. All twigs, branches, and timber from thinned trees were removed from the stand. In total, 50% of the stems were felled, corresponding to 48% of the basal area. The

number of trees in the plot decreased from 27 to 13. The stand density decreased from 2198 to 1099

trees ha^{-1}. The basal area was reduced from 50.4 to 26.2 m^2 ha^{-1}. The canopy cover diminished from

0.974 to 0.758. The change in DBH was relatively small, decreasing from 19.1 to 18.9 cm (Table 2-

1).
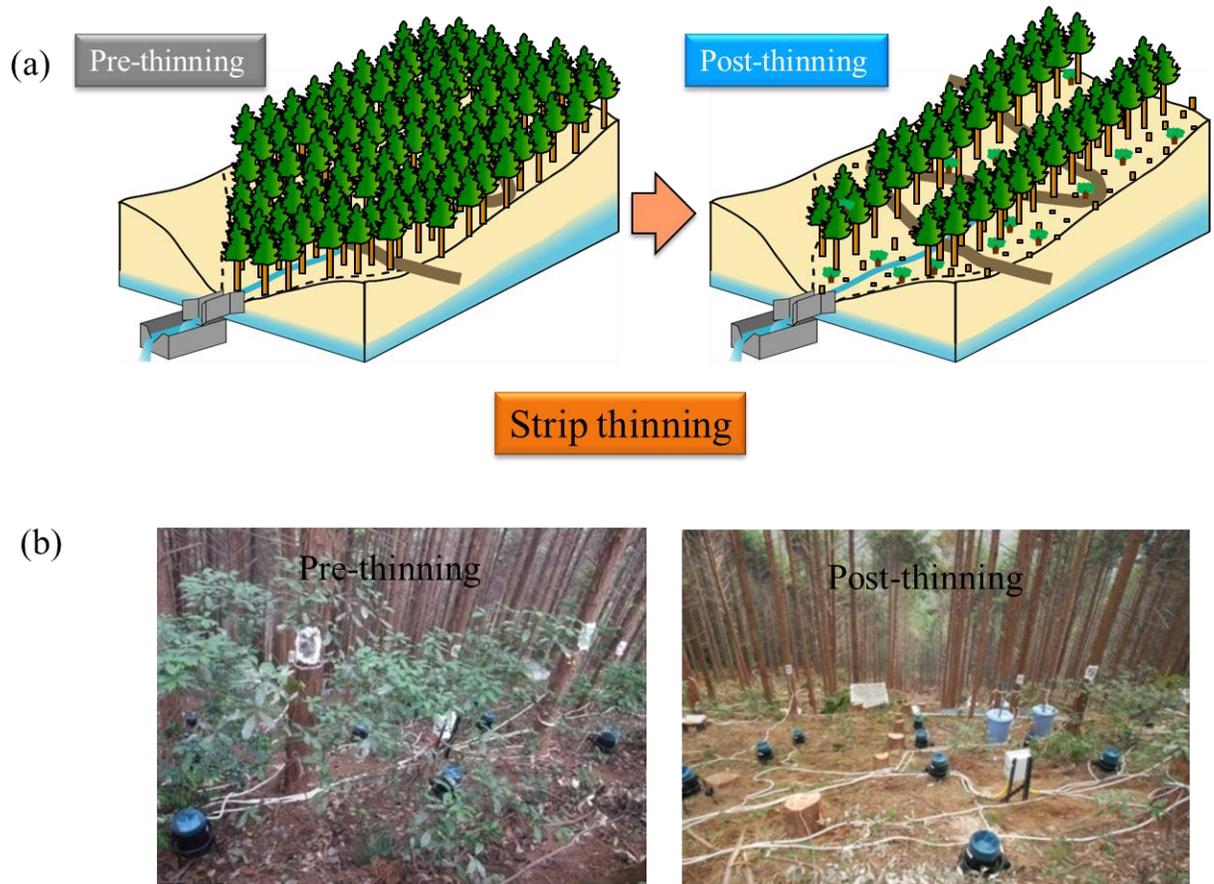
Fig. 2-2 Schematic views of (a) strip thinning in this study and (b) photos in pre-thinning and post-thinning.

Table 2-1 Stand characteristics of the study plot in the pre- and post-thinning periods.

Characteristic	Pre-thinning	Post-thinning	Ratio of thinning (%)
Plot area (m^2)	156	156	
Age (year)	32	32	
Mean height (m)	16	16	
Mean DBH (m)	19.1	18.9	
Canopy cover (%)	97.4	75.8	22.2
Density (trees ha^{-1})	2198	1099	50.0
Basal area ($m^2\,ha^{-1}$)	50.4	26.2	48.0
Sapwood area ($m^2\ ha^{-1}$)	26.1	14.0	46.4
Sapwood area at xylem band ($m^2\ ha^{-1}$)			
0-20 mm	17.7	9.3	47.5
20-40 mm	8.4	4.7	44.0
Sap flux measurements (trees)	10	6	

2-3 Meteorological measurements

P_g was measured by an automatic weather station (Davis Instruments 7852M, Hayward, CA, USA) using a recording rain gauge with 0.2 per tipping, on an open field 250 m from the monitoring hill slope. The data was stored every 5 min with a data logger (SQ1250; Grant Instruments Ltd., Cambridgeshire, UK) along with other meteorological parameters: wind speed and direction, solar radiation, temperature and humidity.

We also measured meteorological conditions under the forest canopy. Wind speed and direction was measured using a three-up anemometer (AC750, Makino Applied Instruments Corp., Tokyo, Japan) at a height of 2 m above the forest floor. Solar radiation, humidity and temperature inside the forest stand were recorded every 30 min at 1 m from the forested ground surface with a data logger (HOBO U30 station; Onset Computer Corporation, MA, USA).

2-4 Canopy interception
2-4-1 Throughfall measurements

TF within a 12 m × 13 m plot was measured by 20 rain gauges (Davis Instruments 7852M) with 0.2 mm per tipping. Numbers of tips were recorded simultaneously at 10-min intervals using

the data logger. The average *TF* was computed from all functioning rain gauges. The rain gauges were distributed on an approximately 2 m × 2 m grid under the forest canopy. To prevent litterfall and dust from blocking the inside hole of rain gauges, they were equipped with a small piece of metal net (grid: 0.2 mm × 0.2 mm) inside and covered by a plastic gauze outside the rain gauge. Each gauge was set on a platform that was 40 cm above the forest floor. The rain gauges were maintained in the same positions throughout the study (Fig. 2-3).
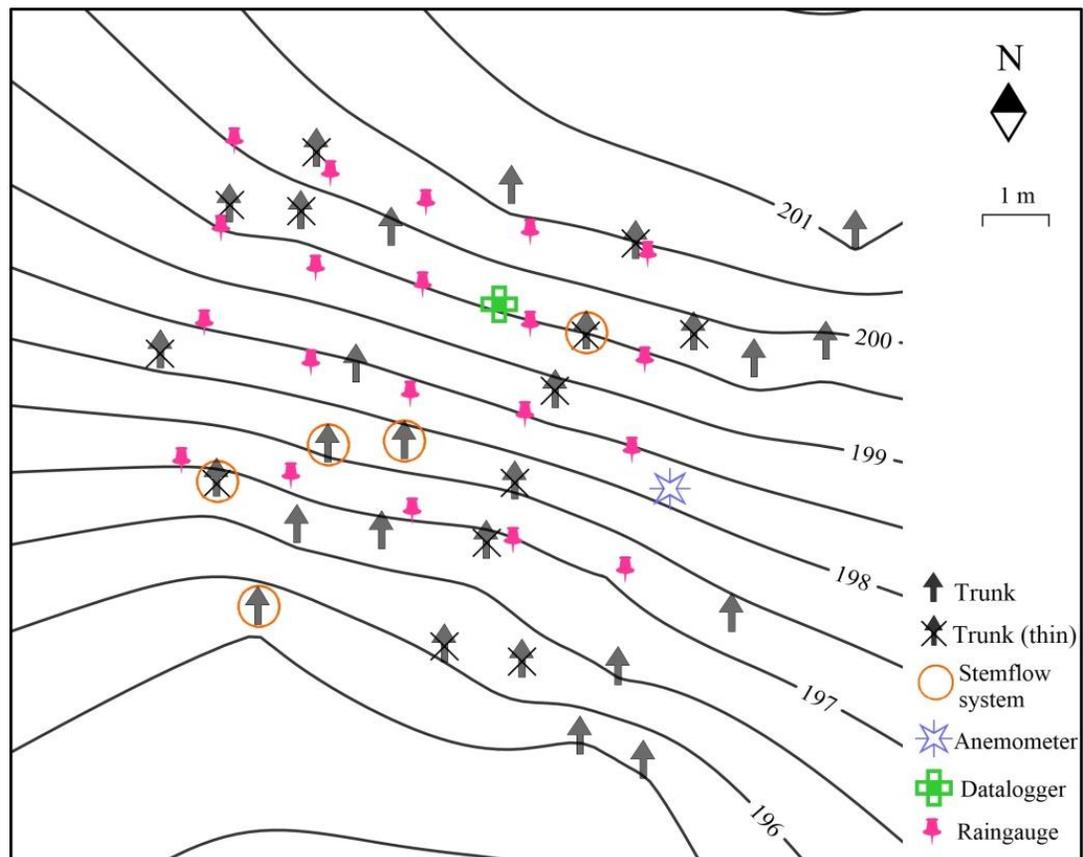
Fig. 2-3 Throughfall and stemflow observation design in the study plot

2-4-2 Stemflow measurements

For *SF* measurements, five experimental individuals were selected with mean DBH of 17.5 cm (13.8–23.0 cm) during the pre-thinning period. Because two trees were thinned, three individuals were left during the post-thinning period (Fig. 2-3). The ratio of measured tree circumstances to all tree circumstances was 0.169 (2.7 m of 16.0 m) for the pre-thinning period and 0.193 (1.5 m of 8.0

m) for the post-thinning period. Each sample tree was equipped with a polyvinyl tube placed around the trunk at about 1.3 m height, with a draining hole connected to a bucket. Then, a flexible plastic board was attached to the tube with staples and silicon sealant, which formed a small channel to drain SF to the bucket directly and smoothly. The distance from the top of the plastic board to the tube was 5–8 cm. The polyvinyl tube was fastened to the tree bole with metal wire at moderate slope, and the gap between tube and bole was sealed with silicon. All buckets were connected to a V-notch weir to measure SF when it exceeded the bucket capacity (82 L). Water level in the bucket and V-notch weir was measured every 5 min with a water level probe (Odyssey capacitance water level probe; Dataflow Systems Pty Ltd., Christchurch, New Zealand). SF volume was calculated from the water level data.

All trees in the stand were classified according to their DBH, and SF depth (mm) of the stand was computed using the following (Hanchi and Rapp, 1997):

$$SF = \sum_{i=1}^{n} \frac{S_n \cdot m}{A \cdot 10^4} \qquad (2.1)$$

where SF is estimated SF depth (mm) of the stand; S_n is average SF volume (ml) from sampled trees in a certain DBH class; A is area of study site (m^2); n is the number of DBH classes, which is 2 (n_1 ≤16 cm and n_2＞16 cm) in this study; and m is the number of trees belonging to a certain DBH class in the stand.

In this study, tree DBH was divided into three classes (n1 ≤ 16cm, 16 < n2 < 20 cm and n3 ≥20cm) according to the range of trees' DBH in the stand (11.3 - 25.1 cm). However, the experimental tree with DBH of 23.0 cm was excluded because of some problems in measurement. Hence, the classes of DBH were reduced to only two dividing at 16 cm. The number of trees belonging to each DBH class, n1 ≤ 16 cm and n2＞16 cm, was 7, and 21, respectively.

2-4-3 Calculation of canopy interception

E_i was calculated according to the water balance of rainfall partitioning. A rainfall event was defined as a period with more than 0.8 mm of total rainfall and separated two subsequent dry period events of a minimum of 6 h. During and after a rainfall event, P_g was partitioned into three fractions, E_i, SF and TF. The water balance of rainfall partitioning is expressed by the following equation:

$$E_i = P_g - TF - SF \qquad (2.2)$$

2-4-4 Canopy parameters

TF components are described based on the analytical model developed by Gash (1979), and composed of p and drainage from the canopy. When a rainfall event begins, TF is composed entirely of the direct component, because rainfall has not contacted the foliage. Then, TF increases approximately linearly with P_g, until the canopy becomes saturated (Fig. 2-4). Once the accumulated precipitation required to saturate the canopy has been reached, an inflection point (P_G') in the cumulative P_g versus cumulative TF plot occurs, as cumulative TF increases as a result of water dripping from the foliage (Fig. 2-4). The slope of the relationship between cumulative P_g and cumulative TF before canopy saturation was determined as p in each event (Link et al., 2004). When a sudden increase in P_g occurred before canopy saturation, p was not determined because it was impossible to find the inflection point from the data. In this study, p was determined using within-event, 10-minute interval rainfall data.
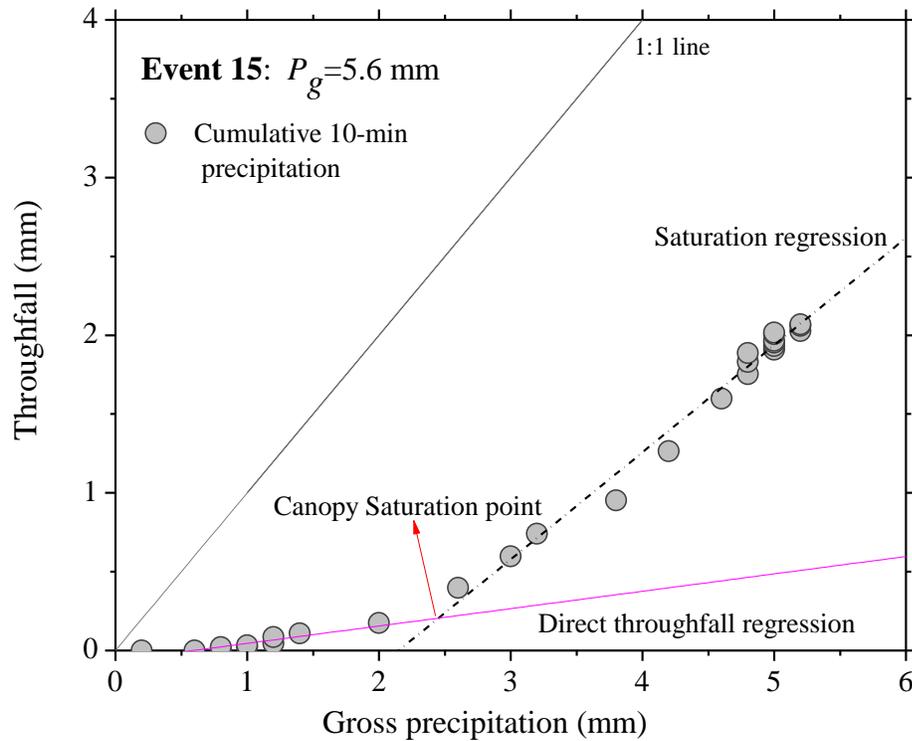
Fig. 2-4 Example (rainfall event 15 in the pre-thinning period) of data used to determine direct throughfall proportion (p) and saturation storage capacity by Link et al. (2004) method. Linear regressions are fit to a scatter plot of throughfall vs. gross precipitation.

S is defined as the amount of water remaining on the canopy in zero evaporation conditions, when rainfall and TF have ceased. S was determined by the original method of Leyton et al. (1967), the simplest method for determining S, using within-event rainfall data. The canopy saturation point was estimated by identifying (P_G') in the P_g versus TF linear relationship, which was determined by the least-squares method. The method to determine S assumed negligible evaporation during canopy wetting (I_w).

2-4-5 Revised Gash analytical model

2-4-5-1 Description of the model

The interception model used is the revised Gash analytical model developed for sparse canopies (Gash et al., 1995). This reduces to the original Gash model for complete canopies (Gash, 1979) when canopy cover is 100%. The canopy cover was 97% in this study, but we used the

revised model since it has a formulation that removes certain mathematical inconsistencies in the original model when treating low rainfall rates (Gash et al., 1995). The revised model assumes that P_g is intercepted in a series of discrete storm events, with sufficient time to dry the canopy between them. Each event can be distinguished by three sequential phases: (1) a wetting phase, during which rainfall is less than required to saturate the canopy; (2) a saturation phase; and (3) a drying phase after rainfall ceased. It is necessary to estimate storage of water on the investigated canopy using S, the minimum depth of water required to saturate the canopy, which is given by the product of canopy capacity per unit area of cover (S_c) and canopy cover (c). The p is the amount of rain that falls directly to the forest floor without touching the canopy. The trunk storage capacity (S_t) is water evaporated from the trunks, and the proportion of rain that is diverted to SF is p_t. The mean rainfall intensity ($\overline{R}$, mm h^{-1}) onto the saturated canopy and mean evaporation rate ($\overline{E}$, mm h^{-1}) during rainfall are also required. Table 2-2 summarizes the five separate components of interception in the revised Gash analytical model.

Table 2-2 Components of interception in revised Gash model.

1	I_c	For m small storms insufficient to saturate the canopy ($P_G<P_G'$)	$c\sum_{j=1}^{m}P_{G,j}$
		For n storms ($P_G>P_G'$) which saturate the canopy,	
2	I_w	Wetting up the canopy	$ncP_G' - ncS_c$
3	I_s	Wet canopy evaporation during the storms	$c\dfrac{\overline{E_c}}{\overline{R}}\sum_{j=1}^{n}(P_{G,j}-P_G')$
4	I_a	Evaporation after storms ceases	ncS_c
5	I_t	Evaporation from trunks for q storms, which saturate the trunks ($P_G>S_t/p_t$)	$qS_t + p_t\sum_{j=1}^{n-q}P_{G,j}$

The amount of rain necessary to saturate the canopy P_G' is given by

$$P_G' = -\frac{\overline{R}}{\overline{E_c}}S_c\ln[1-(\overline{E_c}/\overline{R})] \qquad (2.3)$$

where S_c is S per unit area of cover, defined by $S_c=S/c$; $\overline{E_c}$ is mean evaporation rate from the saturated canopy during rainfall, defined as $\overline{E_c}=\overline{E}/c$.

The amount necessary to saturate the trunks P_t' is given by

$$P_t' = S_t / p_t \qquad (2.4)$$

where S_t is trunk storage capacity and p_t is the proportion of rain diverted to SF.

2-4-5-2 Estimation of model parameters

S was determined using within-event rainfall data, as mentioned above. The p was estimated from the slope of the regression line for all points less than P_G'. p_t and S_t were determined as the slope and negative intercept from a linear regression of SF versus P_g.

$\overline{R}$ was determined using the data recorded by the tipping-bucket rain gauge. $\overline{E}$ was determined using the Penman-Monteith equation with canopy resistance r_s set to zero, namely:

$$\overline{E} = (\Delta R_n + \rho c_p D / r_a) / \lambda(\Delta + \gamma) \qquad (2.5)$$

where λ is the latent heat of vaporization of water, Δ the rate of change of saturated vapor pressure with temperature, R_n net radiation load on the canopy (because we did not measure net radiation, R_n was approximated by $(1-\alpha) R_s$, where R_s is incident solar radiation and α is albedo of the forest canopy, taken as 0.13) (Monteith and Unsworth, 1990). ρ is density of dry air, c_p the specific heat of air at constant temperature, D the vapor pressure deficit, r_a the aerodynamic resistance and γ the psychometric constant. r_a is calculated from the recorded wind speed and surface roughness, using the momentum method:

$$r_a = \ln^2\{(z-d)/z_0\}/(k^2 u) \qquad (2.6)$$

where k is the von Kármán constant (0.41), z the reference height above the ground surface (taken here as $h+2$, where h is canopy height), d the zero plane displacement height, z_0 the roughness length, and u the wind speed at height z. Following Monteith and Unsworth (1990), the displacement height d and roughness length z_0 were taken as 0.7 and 0.1 of vegetation height h (16 m), respectively.

2-5 Tree transpiration

2-5-1 Granier method

Sap flow densities (F_d) were measured by the thermal dissipation method with Granier-type sensors (Granier, 1987), and used to estimate E_t. Each sensor consisted of a pair of probes 20 mm long and 2 mm in diameter containing a copper–constantan thermocouple. The probes were inserted in the sapwood about 0.15 mm apart. The upper probe included a heater that was supplied with 0.2 W constant power. The temperature difference between the upper heated probe and the lower unheated reference probe was measured and converted to F_d according to Granier (1987). Sap flow signals were recorded on a data logger (CR1000, Campbell Scientific, Logan, UT, USA) with a multiplexer (AM 16/32, Campbell Scientific) every 30 s and averaged over 30 min.

F_d was measured in 10 and 6 trees in the pre- and post-thinning period, respectively, so that the number of trees measured in each DBH class corresponded to the frequency distributions of DBH (Table 2-1; Fig. 2-5). In this study, three sensors were positioned about 0.15 mm circumferentially apart at height of about 1.3 m. The upper two sensors were inserted in each selected tree at depths of 0-20 and 20-40 mm to cover the entire sapwood, with a heating element of constantan, powered by 0.2 W constant supply. The lower probe was inserted at a depth of 0-20 mm, representing sapwood temperature. The Japanese cypress plantations are characterized by a circular stem cross section and circumferentially constant sapwood thickness; therefore, we assumed the azimuthal variation in F_d to be small. To avoid the sun-exposed side of the trunk, all the sensors were placed on the north side of the trees, and the part of the trunk into which the sensors were inserted was fully insulated to prevent direct radiation. Sap flow measurements were installed from April 28, 2011.
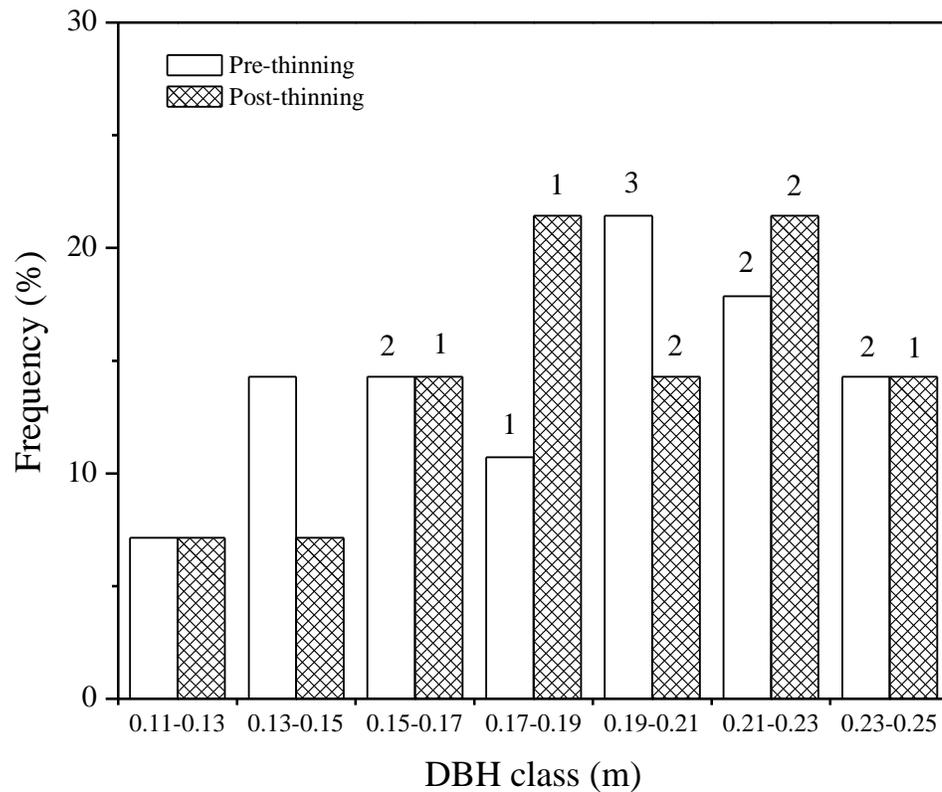
Fig. 2-5 Frequency distributions of stem diameters at breast height (DBH) in the pre- and post-thinning periods, respectively. Note that the number at the top of each bar denotes the number of trees used for the sap flow measurements in each DBH class.

Sapwood thickness (in mm) of each tree in the study plot was measured with a ruler on a core extracted within a 5-mm increment borer at about 1.3 mm aboveground, and assessed as the mean of two orthogonal measurements. Distinct color differences were taken to identify the boundary between sapwood and heartwood. The tree sapwood area (A_{S_tree}) was obtained as the difference between stem cross-sectional area beneath the bark and stem cross-sectional heartwood area assuming that the stem cross sections were circular.

The value calculated from F_d measurements represents tree water uptake, rather than whole-tree transpiration (E_{t-tree}), because of a time lag between the sap flow measured at the stem and

transpired at the canopy (e.g., Kumagai, 2001; Phillips et al., 1997). However, for Japanese cypress

plantations, Kumagai et al. (2009) found that there were no significant differences between daily

stem sap flow and daily E_{t-tree}. Therefore, we regarded daily stem sap flow as daily E_{t-tree}. In this

study, daily E_{t-tree} (kg d^{-1}) was calculated by the following equation:

$$E_{t-tree} = \sum_{i=1}^{2} F_{d\_i} \cdot A_{s\_tree\_i} \quad (2.7)$$

where F_{d_i} is the sap flow density (m^3 m^{-2} d^{-1}) at xylem depths of 0-20 (i=1) and 20-40 mm

(i=2) for the measured tree, respectively; $A_{s\_tree\_i}$ is the sapwood area (m^2) at xylem depths of 0-20

(i=1) and 20-40 mm (i=2) for the measured tree, respectively.

Individual tree-scale measurements were integrated upward for daily stand-level

transpiration ($E_{t-stand}$) (mm d^{-1}) using the following equation (Kumagai et al., 2007; Pataki and

Oren, 2003; Wilson et al., 2001):

$$E_{t-stand} = J_s \frac{A_{s\_stand}}{A_G} \quad (2.8)$$

where J_s is the mean sap flux (m^3 m^{-2} d^{-1}); A_{s_stand} is the stand sapwood area (m^2); and A_G is ground

area of the study site (m^2).

J_s is calculated as

$$J_s = \frac{J_{S\_A} \sum_{i=1}^{N} A_i + J_{S\_B} \sum_{i=1}^{N} B_i}{\sum_{i=1}^{N} (A_i + B_i)} \quad (2.9)$$

where J_{S_A} and J_{S_B} are the mean F_d for the xylem bands at $0 - 20$ and $20 - 40$ mm for all measured

trees, respectively; A_i and B_i are sapwood areas at xylem depths of $0 - 20$ and $20 - 40$ mm for all

trees, respectively; and N is the total number of Japanese cypress trees in the study plot.

2-5-2 Canopy conductance model

The environmental control of stand E_t has been characterized in terms of the response of G_c to environmental factors (e.g., Cienciala et al., 2000; Granier et al., 1996b; Kumagai et al., 2004; Meinzer and Grantz, 1990; Wullschleger et al., 2000). G_c was calculated using the following simplified form of the Penman-Monteith equation (McNaughton and Black, 1973):

$$G_c = \frac{\gamma \cdot \lambda \cdot E_{t-stand}}{c_p \cdot \rho \cdot VPD}$$

(2.10)

where γ is the psychrometric constant, λ is the latent heat of vaporization of water, c_p is the specific heat of air at constant pressure, ρ is the air density, and VPD is the above canopy atmospheric vapor pressure deficit.

This equation is derived under the assumption of complete coupling with the canopy and with the atmosphere. Furthermore, the G_c was calculated as a daily average conductance using thermodynamic variables based on the mean daytime temperature (T) and on the mean daytime VPD, under the assumption that this period is when the VPD has an effect on transpiration and, therefore, uptake. However, the $E_{t-stand}$ was summed over 24 h but was divided by daylight hours only because 1) this value accounted for all of the water uptake driven by the VPD over the day and because 2) this period provided a consistent averaging period compared with that used for the daily VPD. The daily integration period may be subject to large relative errors. These errors are introduced under conditions of low absolute daily $E_{t-stand}$ (Phillips and Oren, 1998). Daylight hours refer to photosynthetically active radiation (PAR) > 0 μ mol m^{-2} s^{-1}. In this study, the starting and ending points for days were from 06:00 h to 18:00 h. In general, the boundary conductance of conifers is sufficiently large. We confirmed that Japanese cypress canopies are aerodynamically well coupled to the atmosphere. Under these conditions, we removed the G_c values obtained on rainy days because the F_d data could be subject to noise on rainy days (Kumagai et al., 2008).

2-6 Forest floor evaporation

2-6-1 Lysimeter measurements

The E_f was measured with three weighing lysimeters placed randomly in the study site (Daikoku et al., 2008; Kelliher et al., 1990; Schaap and Bouten, 1997). The lysimeters were containers of 0.2-m diameter filled with forest soil that was disturbed as little as possible. Their weight was measured with an electrical weighing platform (SB-15K10, A&D Co. Ltd., Tokyo, Japan) and recorded with a data logger (CR10X, Campbell Scientific) every 30 s and averaged over 30 min. The weight losses were regarded as evaporation and the average weight losses of the three lysimeters was considered as the diurnal average evaporation from the forest floor.

2-6-2 Modified Penman-Monteith equation

Lysimeters were installed from13 September to 10 October 2011. Because of the short E_f measuring period, a modified Penman-Monteith equation was used to compute E_f over the same timescale as E_i and E_t (i.e., 1 July to10 October 2011). The physically realistic Penman-Monteith equation is amongst the most widely used models and is effective in predicting E_f of forests (Bond-Lamberty et al., 2011; Schaap and Bouten, 1997; Tian et al., 2011). In the present study, the modified Penman-Monteith equation recommended by Tian et al. (2011) was selected to compute E_f.

$$E_f = \frac{\Delta \times (R_{sn} - G) + \rho_a \times c_p \times \{e_{ss}(T) - e_{sa}\}/r_{sa}}{[\Delta + \gamma \times (1 + r_{sc}/r_{sa})]/\lambda} \qquad (2.11)$$

where Δ is the slope of the saturation vapor pressure curve at air temperature T (kPa $°C^{-1}$) above the forest floor, R_{sn} is the net radiation (MJ m^{-2} s^{-1}) at 2 m above the forest floor, G is the soil heat flux (MJ m^{-2} s^{-1}), ρ_a is air density (kg m^{-3}), c_p is the specific heat of the air (MJ kg^{-1} $°C^{-1}$), $e_{ss}(T)$ is the saturated vapor pressure (kPa) at 2 m above the forest floor when the air temperature is T (°C), e_{sa} is the local actual vapor temperature (kPa) at 2 m above the forest floor, γ is the

psychometric constant γ (kPa °C^{-1}), λ is the latent heat of vaporization of water, r_{sa} and r_{sc} are the aerodynamic and (bulk) surface resistance of the forest floor (s m^{-1}), respectively.

In the present study, we adopted r_{sa} and r_{sc} from a study in dense Douglas fir stand without understory vegetation reported by Schaap and Bouten (1997). r_{sa} was expressed by an aerodynamic parameter (c_a) and the wind speed (u) at 2 m height (m s^{-1}):

$$r_{sa} = \frac{1}{c_a u} \qquad (2.12)$$

Following Schaap and Bouten (1997), c_a was taken as 0.01. r_{sc} was assumed to be a simple empirical function of soil water content (θ) (m^3 m^{-3}):

$$r_{sc} = \max\{0, -1.29 \times 10^4 (\theta - 0.199)\} \quad (2.13)$$

Soil water content was measured from 23 August to 10 October 2011. Because of the short θ measuring period, we assumed that θ was the mean of observed values adjusted to represent non-measuring period (i.e., 1 July to 22 August 2011). Besides, the abundant rainfall would be expected to maintain a high soil content consistently during the study period. The computed E_f was validated with the observed E_f, and the acceptability of these estimates was shown later in this paper.

2-7 Soil water content

Volumetric soil water content (θ) (m^3 m^{-3}) was measured with reflectrometry sensors (ECH$_2$O-10, Decagon Devices Inc., Pullman, WA, USA) and recorded at a 30 min time resolution. The soil moisture sensors were installed nearby each lysimeter and at one of the trees used for measuring sap flow. They were positioned horizontally at depths of 5, 10, 15, 30, 50 and 80 cm in an undisturbed soil column. The hole dug for the sensor installation was backfilled with the original mineral soil and duff.

2-8 Calculation of potential evapotranspiration

In this study, PET (mm d^{-1}) was calculated using following equation:

$$\text{PET} = \frac{\Delta}{\Delta + \gamma} \cdot \frac{R_n - G}{\lambda} \quad (2.14)$$

where Δ is the slope of the vapor saturation curve, γ is the psychrometric constant, R_n is the net radiation, G is the soil heat storage and λ is the latent of water vaporization. For this equation, we assumed $R_n = (1-\alpha)R_s$ and that α is the albedo of the forest canopy, which is taken as 0.13 (Monteith and Unsworth, 1990). G was assumed to be zero because G is usually far less than R_n for forests. The other parameters in the above equation were obtained from the automatic whether station.

2-9 Calculation of evapotranspiration and data analysis

In this study, ET was calculated as the sum of the three components of ET expressed by the following equation:

$$\text{ET} = E_i + E_t + E_f \quad (2.15)$$

where ET is evapotranspiration, E_i is canopy interception, E_t is tree transpiration, and E_f is forest floor evaporation.

The positions of trees and all measurements in the present study were shown in Fig. 2-6. The observation period was divided into pre-treatment (November 2010 – October 2011) and post-treatment (November 2011 – October 2012). In pre-thinning, E_i, E_t and E_f were measured at different time with the shortage of measuring period. Therefore, we will estimate them on the basis of measured values and then extend to the annual scale. TF and SF measurements were estimated according to the strong relationships between TF, SF, and P_g ($TF = 0.650P_g - 0.79$, R^2=0.998; $SF = 0.114P_g - 0.284$, R^2=0.992; respectively), which we obtained from 29 measured rainfall events from July to October, 2011. E_t was estimated using the canopy conductance model, and E_f was simulated by means of the modified Penman-Monteith equation. We thus filled the data gap and analyzed the data from November 2010 to November 2011. In post-thinning, all data were collected completely.

Therefore, we can get annual data in pre- and post-thinning and then analyze the effect of strip thinning on partitioning of ET at annual scale.
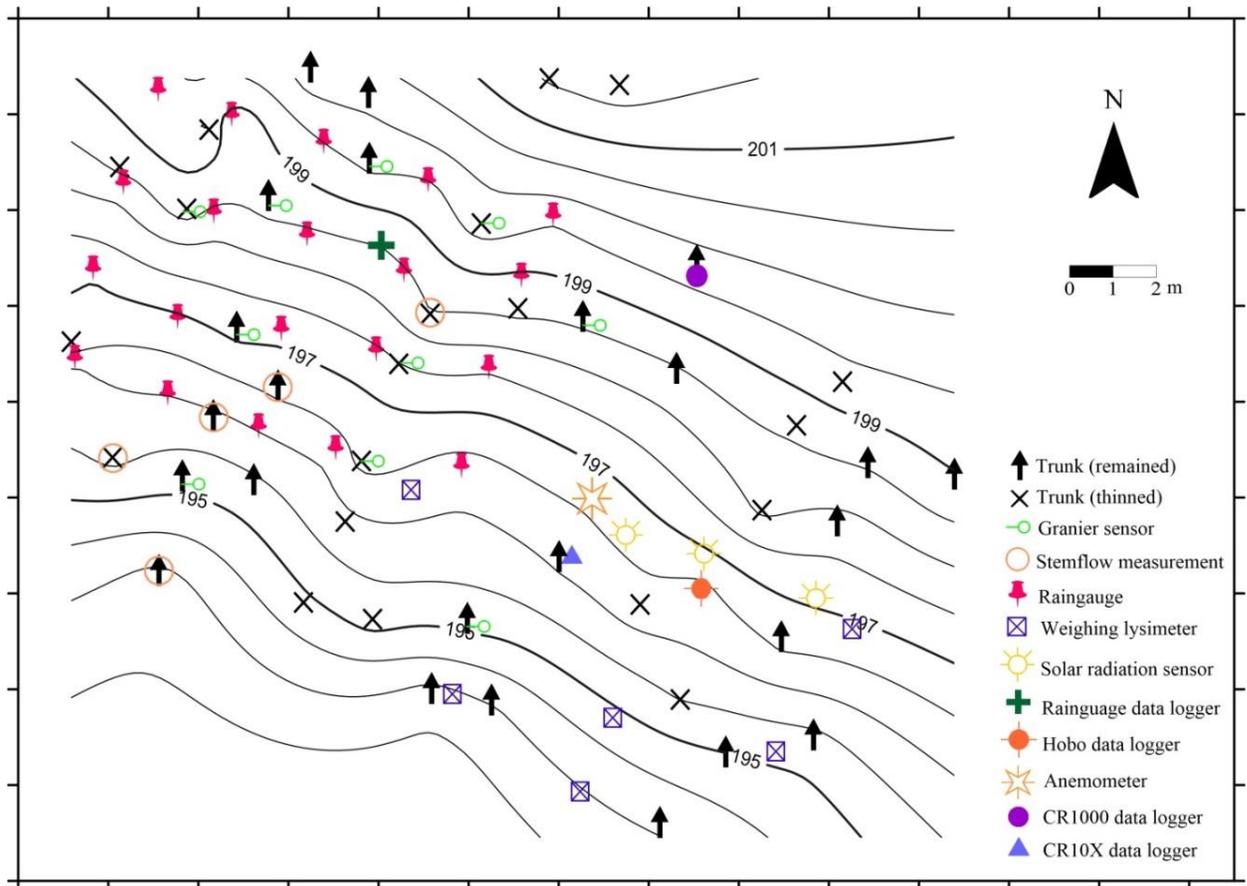
Fig. 2-6 Plot design in this study.

The Wilcoxon-Mann-Whitney (W) non-parametric test for paired samples was used, because the data samples were not distributed normally. A significance level of $P \leq 0.05$ was used for all analysis. Data were performed with the aid of SPSS version 19.0.

Chapter 3 Quantifying and modeling partitioning of the total evapotranspiration in an abandoned Japanese cypress plantation

3-1 Incident rainfall partitioning and canopy interception modeling

3-1-1 Incident rainfall partitioning

Both event-based and total water balance during the measured period are summarized in Table 3-1. It should be noted that data were missed from July 2 to July 18, 2011. Therefore, a total of 29 events were collected with 880.8 mm total rainfall. Event-based P_g ranged from 0.8-176.8 mm with a mean of 30.4 mm. Rainfall duration ranged from 1-51 h with a mean of 12 h. Time since previous event ranged from 6-303 h with a mean 64 h. Total $TF\pm$SD was 565.9±32.1 mm, representing 64.2±3.6% of P_g. Event-based TF was 0–125.8 mm (0–76.5% of P_g). Total $SF\pm$SD was 93.0±5.6 mm, representing 10.6±0.6% of P_g. Event-based SF was 0–19.7 mm (0–13.1% of P_g). Total $E_i\pm$SD was 221.8±9.4 mm, representing 25.2±1.1% of P_g. Event-based E_i was 0.8–36.6 mm (18.2–100% of P_g).

During the study period, p comprised 14±7% of TF, but it was 4–33% between events. Drainage from the canopy was 50±21% of TF, but it was 8–76% between events. Mean S was 2.4±0.7 mm, with range 1.2–3.8 mm (Table 3-1).

The relationships between P_g and the canopy water balance (TF, SF and E_i) are expressed by the following equations (n=29) (Fig. 3-1a, c, e):

$$TF = 0.683\ P_g - 1.25 \quad (r^2 > 0.99) \quad (3.1)$$

$$SF = 0.118\ P_g - 0.387 \quad (r^2 = 0.99) \quad (3.2)$$

$$E_i = 0.198\ P_g + 1.637 \quad (r^2 = 0.97) \quad (3.3)$$

The above equations show strong positive linear correlations between TF, SF, E_i and P_g. These imply that P_g must exceed 1.8 mm and 3.3 mm to initiate TF and SF, respectively.

Table 3-1 Detailed interception summary during the measuring period from July 1 to October 10, 2011.

Event	Start (Julian day)	Duration (h)	Time since previous event (h)	P_g (mm)	TF (mm)	SF (mm)	E_i (mm)	TF/P_g (%)	SF/P_g (%)	E_i/P_g (%)	p (dimensionless)	S (mm)
1	40725.67	5	44	42.8	30.5	3.4	8.9	71.3	7.9	20.8	na	
2	40743.21	20	202	176.8	125.8	18.8	32.2	71.2	10.6	18.2	na	
3	40750.92	3	146	1.2	0.1	0.0	1.1	11.7	0.0	88.3	0.11	
4	40751.71	18	16	54.2	37.7	5.4	11.2	69.6	9.9	20.6	0.24	2.9
5	40752.71	42	6	77.8	49.0	10.2	18.7	62.9	13.1	24.0	0.33	1.6
6	40754.83	5	9	0.8	0.0	0.0	0.8	2.8	0.0	97.2	na	
7	40760.29	14	122	4.2	0.0	0.0	4.2	0.0	0.0	100.0	na	
8	40762.71	5	44	13.8	10.6	0.6	2.7	76.5	4.3	19.3	0.09	3.8
9	40769.88	3	162	2.2	0.6	0.0	1.6	26.3	0.0	73.7	0.15	
10	40771.88	3	45	4.4	2.6	0.0	1.8	58.0	0.0	42.0	0.15	2.3
11	40773.92	2	46	2.8	1.9	0.0	0.9	69.4	0.0	30.6	na	
12	40774.46	16	11	14.0	7.9	0.6	5.5	56.4	4.5	39.1	0.21	2.3
13	40775.79	40	13	33.2	18.4	3.7	11.2	55.3	11.0	33.7	0.13	2.0
14	40777.83	8	9	2.0	0.5	0.0	1.5	22.8	0.0	77.2	0.05	
15	40780.08	10	40	5.6	2.1	0.0	3.5	37.9	0.0	62.1	0.11	2.3
16	40781.58	4	26	29.2	18.5	3.2	7.5	63.2	11.1	25.7	na	
17	40786.08	4	104	3.8	1.2	0.0	2.6	30.9	0.0	69.1	0.13	2.1
18	40786.67	1	10	2.2	0.4	0.0	1.8	16.4	0.0	83.6	0.11	
19	40787.21	29	12	117.8	79.5	14.3	24.0	67.5	12.1	20.4	0.16	2.1
20	40788.88	8	11	3.2	0.5	0.0	2.7	14.6	0.0	85.4	0.06	
21	40789.58	2	10	1.0	0.1	0.0	0.9	8.0	0.0	92.0	0.04	
22	40789.92	6	6	16.4	11.0	2.0	3.4	67.4	11.9	20.7	na	
23	40790.50	1	8	6.6	2.9	0.4	3.3	43.2	6.7	50.1	0.08	2.5
24	40791.46	21	22	21.0	12.3	2.3	6.4	58.4	11.0	30.7	0.11	3.6
25	40803.08	7	258	4.6	1.6	0.0	3.0	35.1	0.0	64.9	0.19	1.9
26	40805.75	51	57	157.0	100.7	19.7	36.6	64.1	12.5	23.3	0.15	2.5
27	40808.58	5	17	14.8	8.3	1.8	4.7	56.2	11.9	32.0	0.05	3.3
28	40821.42	22	303	64.4	40.3	6.8	17.3	62.6	10.6	26.8	0.23	2.3
29	40826.04	2	89	3.0	1.1	0.0	1.9	37.9	0.0	62.1	0.13	1.2
Total				880.8	565.9	93.0	221.8	64.2	10.6	25.2		
Mean		12	64	30.4	19.5	3.2	7.6	45.4	5.1	49.4	0.14	2.4
Min		1	6	0.8	0.0	0.0	0.8	0.0	0.0	18.2	0.04	1.2
Max		51	303	176.8	125.8	19.7	36.6	76.5	13.1	100.0	0.33	3.8

na: Not available. The parameter p and S were not determined due to immediate increase of cumulative P_g in the beginning of the event.
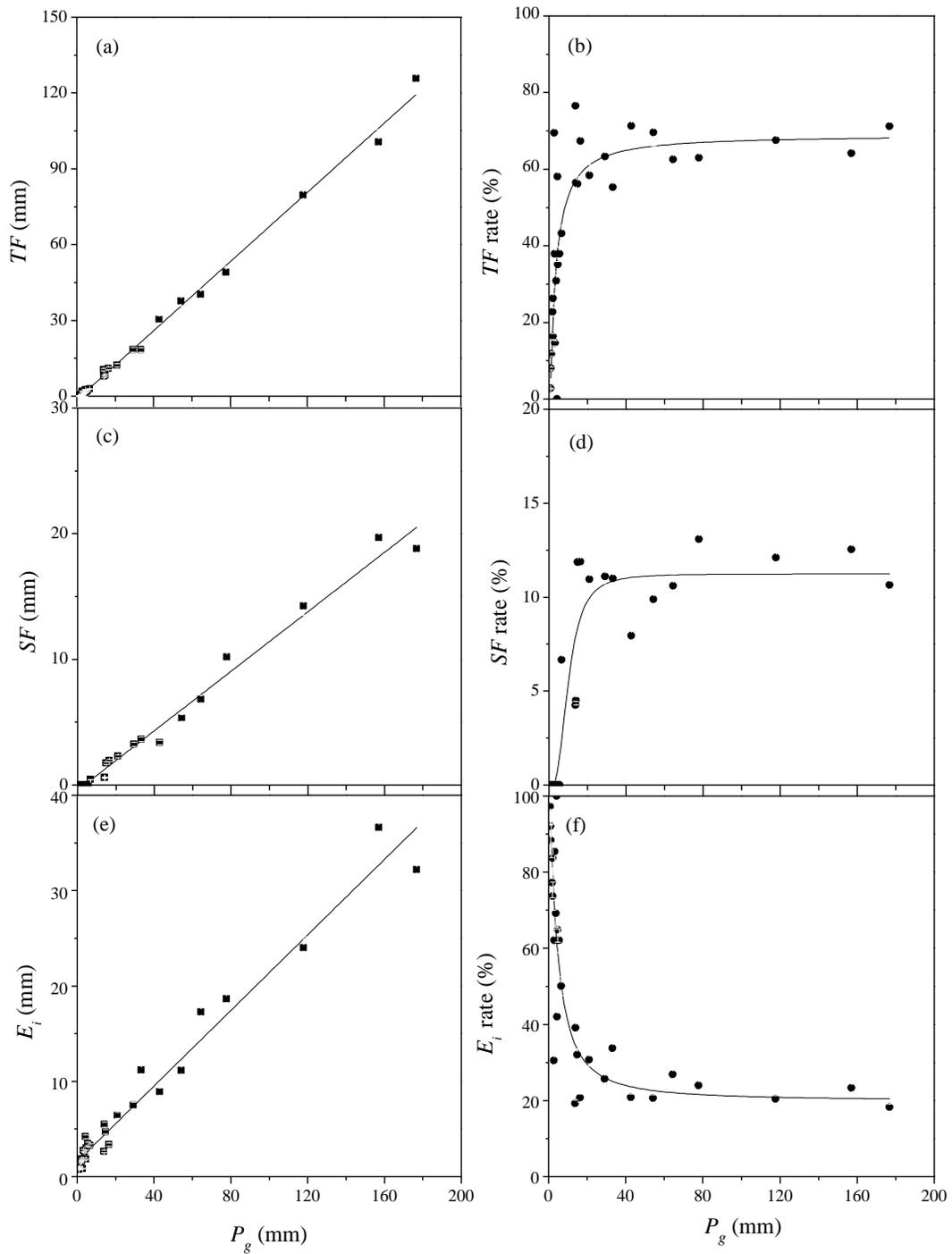
Fig. 3-1 Throughfall (*TF*), stemflow (*SF*), canopy interception (E_i) depth (mm) and rates (%) as a function of gross precipitation (P_g) depth (mm) using 29 event-based data. (a) *TF* amount, (b) *TF* rate, (c) *SF* amount, (d) *SF* rate, (e) E_i amount, (f) E_i rate.

The relationships between P_g and the rate of canopy water balance are expressed by the following equations (n=29) (Fig. 3-1b, d, f):

$$TF\ (\%) = 68.96 - 257.74/\ (3.28 + P_g^{1.12}) \qquad (r^2 = 0.68) \quad (3.4)$$

$$SF\ (\%) = 11.25 - 6916.57/\ (597.18 + P_g^{2.79}) \quad (r^2 = 0.88) \quad (3.5)$$

$$E_i\ (\%) = 1.64\ P_g^{0.43} \qquad\qquad\qquad (r^2 = 0.66) \quad (3.6)$$

The TF rate stabilized with increasing P_g (Fig. 3-1b). For smaller-magnitude events with rainfall depth less than 40 mm, the TF rate varied greatly, from 0% to 77% with mean 39%. For larger-magnitude events with rainfall depth greater than 40 mm, that rate was relatively stable, from 63% to 71% with mean 67%. The SF rate stabilized with increasing P_g (Fig. 3-1d). For smaller-magnitude events with rainfall depth less than 20 mm, the SF rate strongly varied, from 0% to 12% with mean 2%. For larger-magnitude events with rainfall depth greater than 20 mm, the SF rate was relatively stable, from 8% to 13% with mean 11%. The E_i rate also stabilized with increasing P_g (Fig. 3-1f). For smaller-magnitude events with rainfall depth less than 40 mm, the E_i rate varied greatly, from 20% to 100% with mean 58%. For larger-magnitude events with rainfall depth greater than 40 mm, the E_i rate was relatively stable, from 18% to 27% with mean 22%. When rainfall was slight, the E_i rate was relatively large because precipitation was insufficient to saturate the canopy. The stability of this rate was strongly correlated with that of TF.

In the present study, 93.0 mm (10.6% of P_g) was partitioned as SF. This value agrees with other studies of coniferous forest, ranging from the 0.3% reported by Valente et al. (1997) to 12.1% by Hattori and Chikaarashi (1988) (Table 3-2). Nevertheless, the present value is considerably larger than results for other coniferous stands. It was found that SF is affected by stand structure (e.g., stand density and branch inclination angle) (Levia and Frost, 2003). For example, total SF was greater in denser stands (Huber and Iroume, 2001), and horizontal branches were linked to smaller SF values (Crockford and Richardson, 2000). In the present study, stand density was high and stems were vertical on the hillslope; angles between stems and branches were small and nearly vertical.

These factors may partially explain the relatively large *SF* rate generated in the abandoned Japanese cypress plantation.

TF depth was 565.9 mm (64.2% of P_g). This percentage agrees with those of related studies of coniferous forest, from the 60% reported by Viville et al. (1993) to 85% by Shi et al. (2010) (Table 3-2). The present percentage is considerably lower than for other coniferous forests, such as Japanese cypress (74.2%; Tanaka et al., 2005) and natural pine forest (85%; Shi et al., 2010). *TF* in forest ecosystems is affected by multiple factors such as stand characteristics (e.g., stand density, basal area, and canopy cover) (Crockford and Richardson, 2000; Staelens et al., 2006; Molina and Del Campo, 2012), and meteorological conditions (e.g., rainfall intensity) (Llorens et al., 1997). For example, *TF* was negatively and linearly related to the tree density, basal area, and forest canopy cover (Molina and Del Campo, 2012). In the present study, the canopy cover fraction (0.974) was almost close due to high stand density (2198 trees ha^{-1}). These factors may partially explain the relatively low *TF*.

The result of E_i rate (25.2% of P_g) agrees with other studies in coniferous forest that ranges from 12% reported by Haibara and Aiba (1982) to 39.3% by Viville et al. (1993) (Table 3-2). E_i varies greatly, and depends on meteorological conditions and forest properties (Crockford and Richardson, 2000). At the event-based scale, E_i rate stabilized with increasing P_g (Fig. 3-1f). However, at an annual scale, E_i rate decreased with P_g amount (Komatsu et al., 2008b). E_i rate increased with stand density (Komatsu et al., 2008b) and was affected by forest cover and branch architecture (Staelens et al., 2006). Canopy storage capacity (*S*) is one of the useful parameters for examining variation on E_i induced by forest properties (Komatsu et al., 2008b). In the present study, the mean of *S* was 2.4 mm, and in the range of 0.5-4.3 mm which was summarized for different coniferous forests by Hormann et al. (1996) and Link et al. (2004). The quantification of rainfall partitioning can improve understanding of the water resources of forested watersheds, and can also guide forest practices (e.g., thinning) and improve the condition of abandoned coniferous forests

such as Japanese cypress plantations.

Table 3-2 Interception loss for coniferous forests from earlier studies.

Species	Age	Stand density (trees ha^{-1})	Height (m)	DBH (cm)	P_g (mm)	TF/P_g (%)	SF/P_g (%)	E_i/P_g (%)	References
Chamaecyparis obtusa	31	1325	14	18	1087	72.9	8.2	18.9	Hattori and Chikaarashi (1988)
Chamaecyparis obtusa	31	1750	14	18	1336	64.5	12.1	23.4	Hattori and Chikaarashi (1988)
Chamaecyparis obtusa	60-70	3200	8	8	1793	68.7	5.8	25.5	Iwatsubo and Tsutsumi (1967)
Chamaecyparis obtusa	29	2051	11	16	1543	67.7	11.0	21.3	Hattori et al. (1982)
Chamaecyparis obtusa	70	923	19	34	2053	74.2	11.4	14.4	Tanaka et al.(2005)
Cryptomeria japonica	70	513	27	39	2304	78.6	5.6	15.8	Tanaka et al.(2005)
Cryptomeria japonica	30	1467	15	23	1584	63.7	10.2	26.1	Sato et al. (2003a,b)
Cryptomeria japonica	71	750	25	29	1150	-	-	12.0	Haibara and Aiba (1982)
C. japonica/C. obtusa	93	783	18	32	1734	-	-	13.0	Murakami et al. (2000)
Pinus densiflora	40-70	1575	7	12	1513	83.0	3.0	14.0	Mitsudera et al. (1984)
Pinus densiflora	-	2300	12	30	1291	78.1	0.5	20.7	Taniguchi et al. (1996)
Pinus pinaster	60	312	24	34	1366	82.6	0.3	17.1	Valente et al. (1997)
Pinus armandii	27	575	12	20	545	85.0	0.9	14.2	Shi et al. (2010)
Pinus armandii	25	1420	-	12	926	67.4	5.9	26.7	Li et al. (2007)
Pinus pseudostrobus	-	246	12	32	974	80.2	0.6	19.2	Silva and Rodriguez (2001)
Picea sitchensis	29	4250	9	-	1795	-	-	26.7	Gash et al. (1980)
Picea rubens	-	-	-	-	-	76.0	2.3	21.7	Mahendrappa (1990)
Pinus strobus	-	-	-	-	-	65.0	5.3	30.7	Mahendrappa (1990)
Pinus resinosa	-	-	-	-	-	69.0	0.7	28.3	Mahendrappa (1990)
Pseudotsuga menziesii etc.	500	427	19	34	619	75.0	-	25.0	Link et al. (2004)
Picea abies	90	575	25	-	583	67.3	0.3	32.4	Viville et al. (1993)
Picea abies	90	575	25	-	588	65.3	0.5	31.2	Viville et al. (1993)
Picea abies	90	575	25	-	539	60.0	0.7	39.3	Viville et al. (1993)
Pinus sylvestris	33	2400	10	14	850	74.7	1.3	24.0	Llorens et al. (1997)
Chamaecyparis obtusa	32	2198	16	19	881	64.2	10.6	25.2	This study

Entries with dashes indicate that data could not be found in the paper.

3-1-2 Spatial variability of throughfall

The spatial variability of TF amount is expressed via the coefficient of variability (CV), i.e., the standard deviation as a proportion of the mean. Fig. 3-2 shows the CV of TF rate for all rainfall events. At the event-based level, the CV decreased asymptotically with increasing P_G amount. The CV was 16–56%, with median 26%. CV values for smaller-magnitude events were much higher than for larger-magnitude ones. The TF rate and its CV at each rain gauge are shown in Fig. 3-3a, b. The TF rate was 43–70% with mean 55% (Fig. 3-3a). The rate was substantially lower than 100%, because of E_i and the distribution of SF. The CV of TF rate at each rain gauge was 36–61%, with median 46% (Fig. 3-3b).
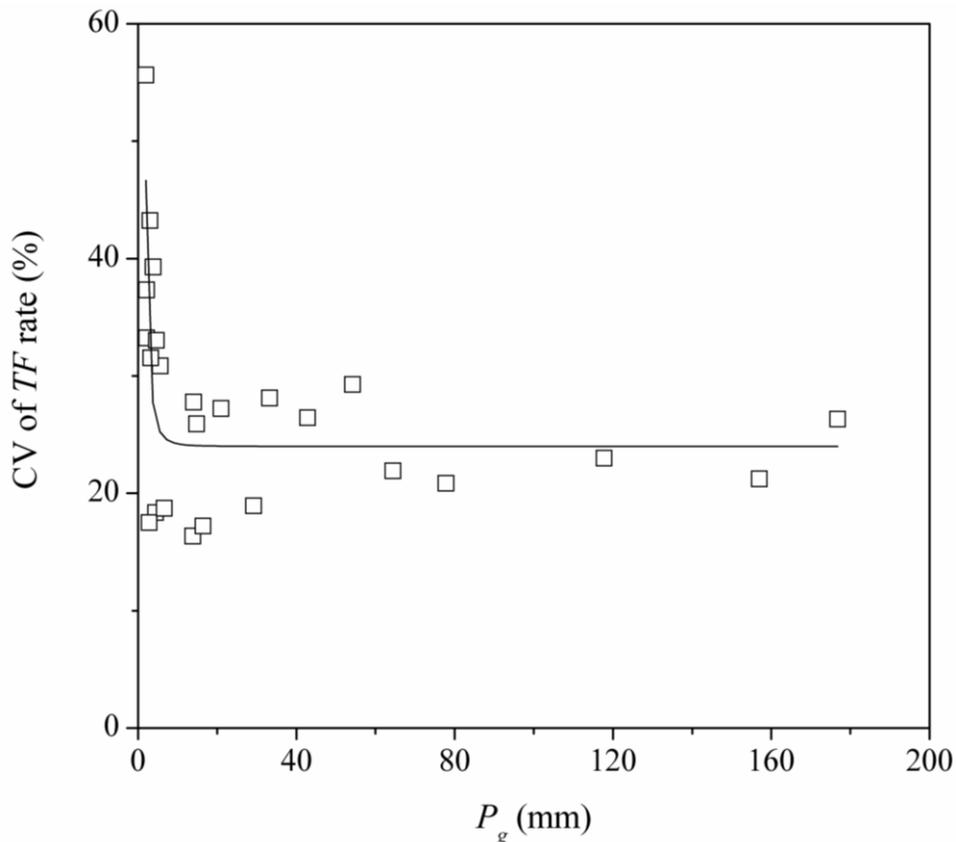
Fig. 3-2 Coefficient of variability (CV) of throughfall (TF) rate versus gross precipitation (P_g), using 29 event-based data.
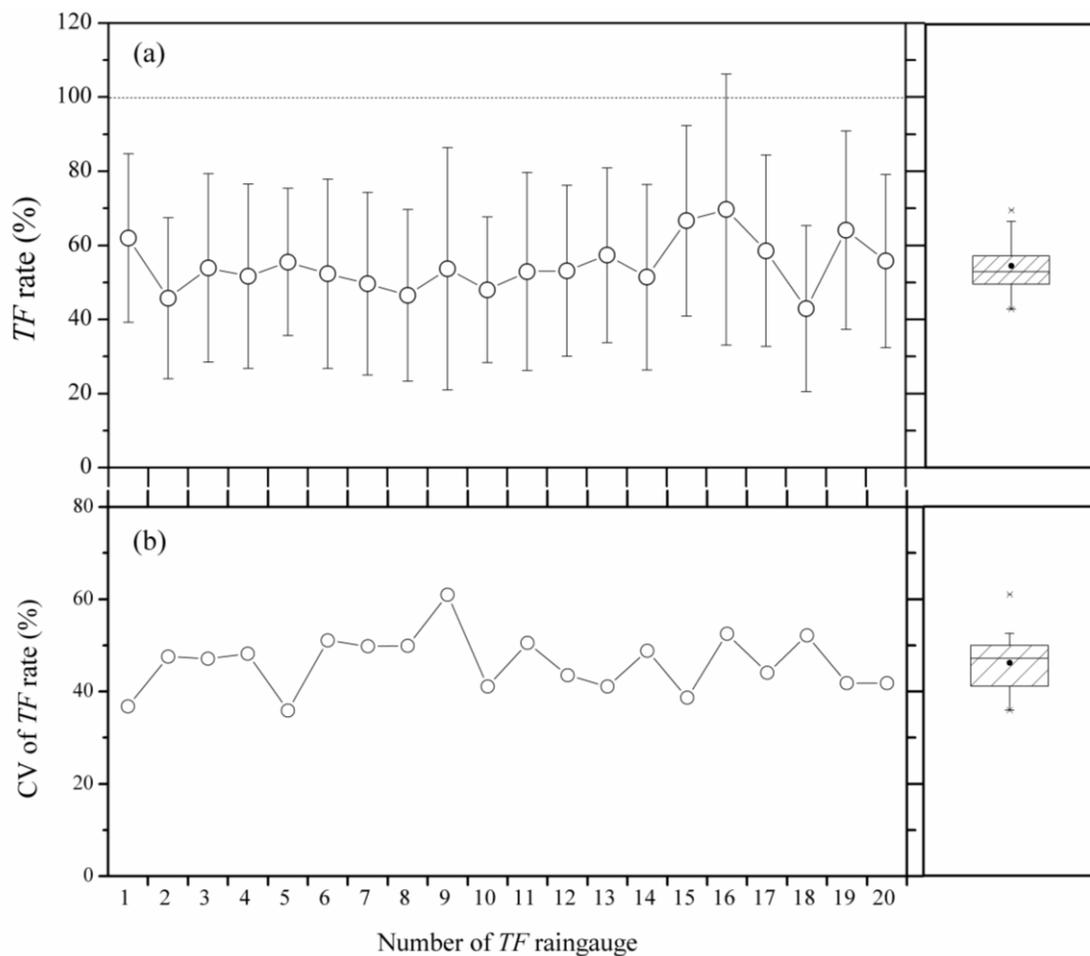
Fig. 3-3 Variation of throughfall (*TF*) among rain gauges. (a) Mean *TF* rate for rainfall events. (b) Coefficient of variability (CV) of *TF* rate for the events. The *boxplots* are drawn from data from 20 rain gauges. *Error bars* indicate standard deviation.

Canopy cover above the *TF* rain gauges was 93–98%, with mean 97%. The CV of *TF* rate at each rain gauge versus corresponding canopy cover is presented in Fig. 3-4a. The CV was not significantly correlated with canopy cover, according to Pearson correlation coefficients (r=0.152, p=0.521, n=20).

The distance from the *TF* rain gauges to the nearest trunk was 0.4–2.2 m, with mean 1.0 m. The CV of *TF* rate at each rain gauge versus distance to the nearest trunk is depicted in Fig. 3-4b. The CV was again not significantly correlated with distance to the nearest trunk, according to the Pearson coefficients (r=0.196, p=0.408, n=20).
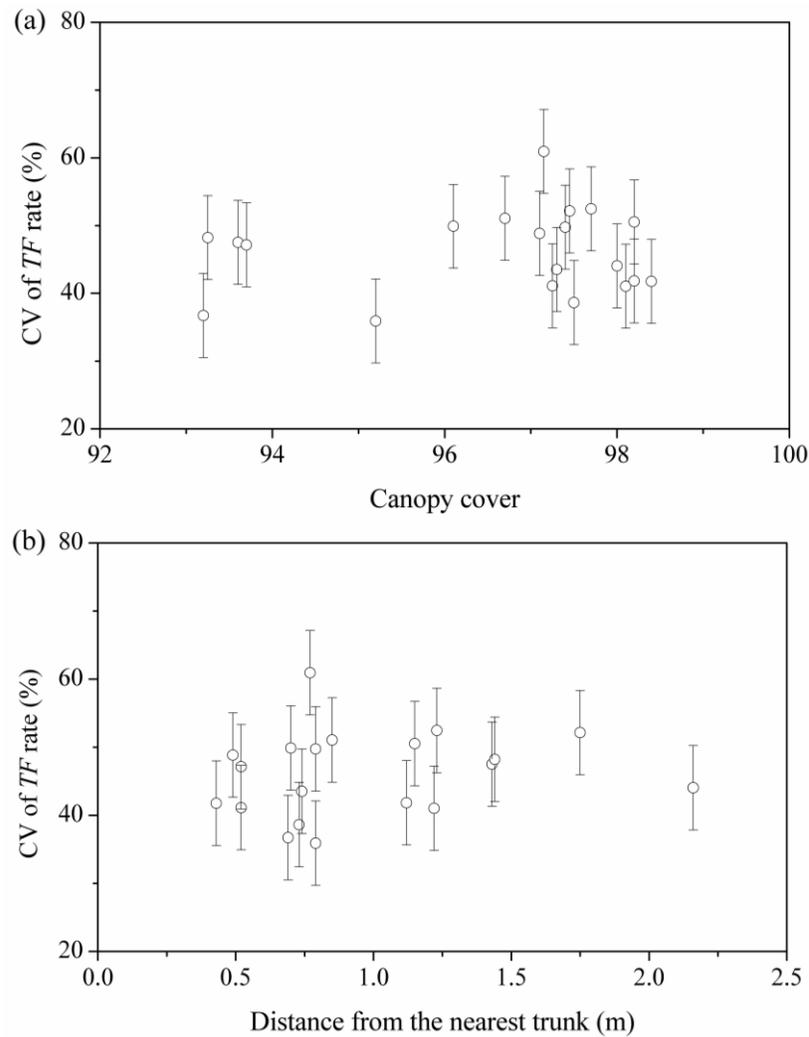
Fig. 3-4 Coefficient of variability (CV) of throughfall (*TF*) for rain gauges: versus canopy cover (a), and distance from nearest trunk (b).

In this study, the CV of *TF* rate was not significantly correlated with canopy cover ($r=0.152$, $p=0.521$, $n=20$) and distance from the nearest trunk ($r=0.196$, $p=0.408$, $n=20$) (Fig. 3-4). The CV of *TF* rate was 16–56%, with median 26% (Fig. 3-2). This median value was greater than that reported from other temperate forests: 14-22%, summarized by Staelens et al. (2006). Furthermore, the median CV obtained in this study was also higher than that of a mixed white oak forest (11.8%; Silva and Okumura, 1996), and a broad-leaved secondary forest (17.2%; Deguchi et al., 2006). It has been suggested that abandoned Japanese cypress forests represent the most difficult forest type to measure E_i, because of the high spatial variability of *TF*.

The spatial variability of *TF* is affected by both meteorological factors (e.g., rainfall intensity and wind speed) and canopy factors (e.g., canopy storage capacity and canopy species) (Levia and Frost, 2006). For example, Keim et al. (2005) showed that the relationship between *TF* amount and the radial distance from the trunk varied by canopy species and tree age. Estimation of *TF* thus is notoriously difficulty due to the spatial and temporal variability of *TF* (Keim et al., 2005; Staelens et al., 2006). Zimmermann et al. (2010) reported that the relative error of mean *TF* became stable and better as the number of sample sizes increase. This implies that large number of sample sizes would be required to estimate *TF*.

For determining the approximate number of *TF* collectors that would be required within the Japanese cypress forests, the acceptable standard error ε (%) was calculated using the following equation (Kimmins, 1973; Kostelnik et al., 1989; Price and Carlyle-Moses, 2003; Shinohara et al., 2010):

$$\varepsilon = \frac{t_{(\alpha,n-1)}CV}{\sqrt{n}}$$
(3.7)

where *n* is the number of collectors; CV is the CV of *TF* rate; and $t_{(\alpha,n-1)}$ is the Student's *t*-value for a desired confidence interval α and (*n*-1) degrees of freedom (d.f.). Our sampling design using 20 rain gauges per P_g event was found to estimate the cumulative study-period *TF* flux within acceptable error limits (12.2% at the 95% confidence level). This agrees with the range from 7.0% with 25 rain gauges to 15.0% with 5 rain gauges (at the 95% confidence level) reported by (Shinohara et al., 2010).

3-1-3 Validation of revised Gash analytical model

Event-basis interception loss was calculated, applying the revised Gash model with parameters shown in Table 3-3. Table 3-4 shows E_i components for the study period, as predicted by the model. Simulated E_i was 209.3 mm (accounting for 23.8% of P_g), underestimating measured E_i by 5.7%. In this model analysis, most interception loss (62.9%) evaporated during rainfall, with

evaporation after rainfall cessation contributing 26.8% and canopy wetting 2.5%. For weaker storms insufficient to saturate the canopy, evaporation represented 4.4%. Evaporation from trunks accounted for 3.4% of E_i. Comparison between observed and simulated E_i per event is shown in Fig. 3-5. It reveals that E_i is slightly overestimated for some weaker rainfall events, and greatly underestimated for heavier events. For some weaker events, the simulated E_i is nearly identical to observed.

Table 3-3 Values of parameters in revised Gash model in this study

Parameters	Values
Canopy cover, c	0.97
Canopy storage capacity, S (mm)	2.40
Canopy storage capacity by canopy cover, $S_c = S/c$ (mm)	2.47
Free throughfall coefficient, p	0.13
Trunk storage capacity, S_t (mm)	0.39
Proportion of rain diverted to stemflow, p_t	0.12
Mean evaporation rate during rainfall, $\overline{E}$ (mm h^{-1})	0.38
Mean evaporation rate scaling by canopy cover during rainfall, $\overline{E_c} = \overline{E}/c$ (mm h^{-1})	0.39
Mean rainfall rate, $\overline{R}$ (mm h^{-1})	2.37
$\overline{E_c}/\overline{R}$	0.17
Amount of rain to saturate the canopy, P_G' (mm)	2.70
Amount of rain to saturate the trunks, P_t' (mm)	3.17

Table 3-4 Components of simulated interception in this study

Components	The revised Gash model (mm)	Proportion of E_i (%)	Estimated error (%)
For storms $P_g < P_G'$			
Evaporation from canopy	9.1	4.4	
For storms $P_g \geq P_G'$			
Wetting up the canopy	5.1	2.5	
Wet canopy evaporation during the storms	129.7	62.9	
Evaporation after storms cease	55.2	26.8	
Evaporation from trunks	10.1	3.4	
Simulated interception	209.3	100	5.7
Observed interception	221.8	-	
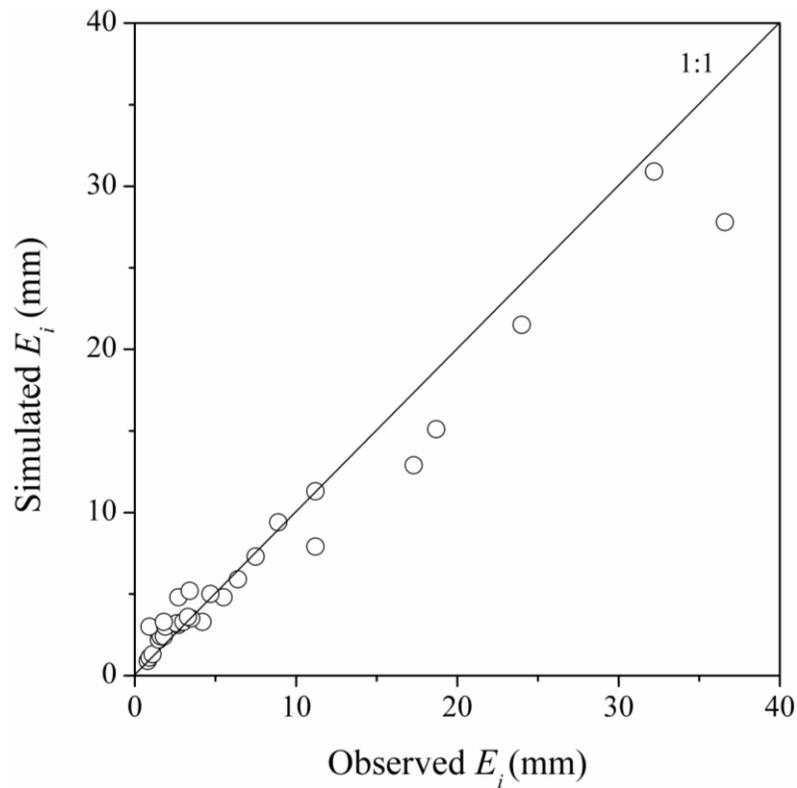
Fig. 3-5 Observed versus simulated interception loss (E_i) (mm) using revised Gash model; each point represents a rainfall event.

Fig. 3-6 shows the sensitivity of the canopy parameters and climatic variables to E_i. Sensitivity analysis for the six main parameters of the revised Gash model indicate that changes to S_t and p_t are not significant, whereas those to $\overline{E}$, S and c produce linear changes in predicted losses. Changes in $\overline{R}$ are nonlinear, and show opposite signs to those in $\overline{E}$, S and c. If values of $\overline{E}$, S, c, S_t and p_t decrease by 30%, E_i is reduced by 20%, 7%, 3%, 1%, and 0.6%. If $\overline{R}$ is also decreased by 30%, E_i increases at a rate of 28%. These results indicate that the revised Gash analytical model is very sensitive to changes of forest structural parameters S and c, and climatic variables $\overline{R}$ and $\overline{E}$. However, it is not sensitive to the stem parameters S_t and p_t, since these have only a small effect on E_i.
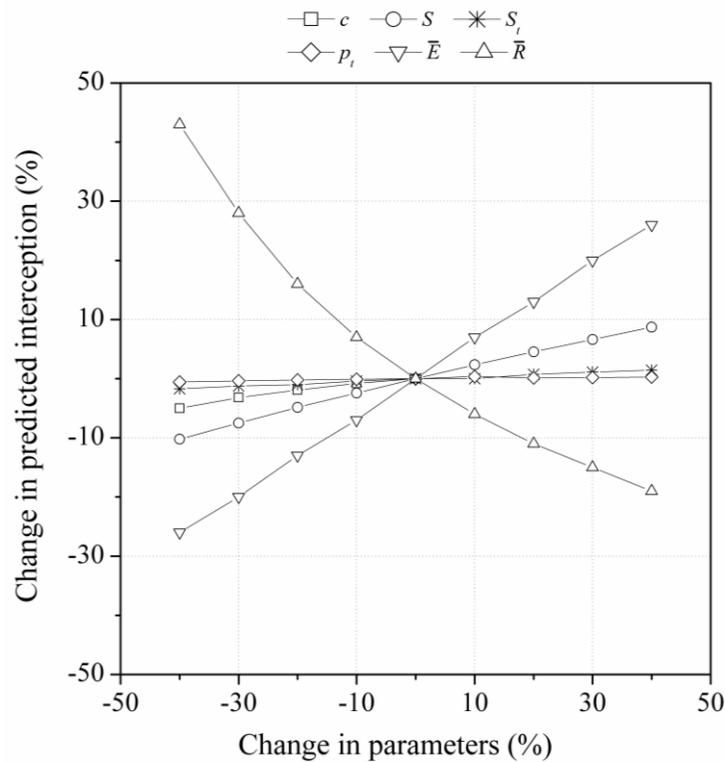
Fig. 3-6 Sensitivity analysis of revised Gash analytical model. Note that canopy cover fraction (c) was 0.974 in this study. The change in c was calculated only by decreasing 10%, 20%, 30% and 40% because its positive change does not meet the practical situation (i.e. c becomes >1.0).

The revised Gash analytical model produced good agreement between observed and simulated E_i, and we validated it in the environment of its application. The model assesses estimates of E_i components and identifies the most appropriate version for the abandoned Japanese cypress forests. Over the study period, the greater part of E_i (89.7%) was from evaporation of a saturated canopy, during the storms and after they ceased (Table 3-4). This agrees with earlier studies of broadleaf forest (90.0%; Deguchi et al., 2006), coniferous forests (76.7%; Loustau et al., 1992; 83.0%; Llorens, 1997; 94.7%; Shi et al., 2010), cultural cropping system (91.6%; van Dijk and Bruijnzeel, 2001), and agroforestry system (84.0%; Jackson, 2000). Evaporation from the trunk is a very small component of interception loss, as reported for rainforest (9.0%; Lloyd et al., 1988) and coniferous forest (1.7%; Llorens, 1997). This evaporation was ignored for broadleaf forest by Price and Carlyle-Moses (2003) and Deguchi et al. (2006).

The model tends to underestimate E_i, within a range of 5.7%. This error mainly occurs for heavy rainfall events, whereas E_i for weaker events tends to be slightly overestimated (Fig. 3-5). As the sensitivity analysis showed in Fig. 3-6, the model is highly sensitive to the parameters S, $\overline{E}$, and $\overline{R}$. The error in the prediction was dominated by these three key controlling variables, which were assumed to be consistent value for each parameter during the study period (Gash et al., 1995; Wallace and McJannet, 2006). The prediction error for the studied coniferous forest in the temperate maritime climate is within the range as those obtained from other kinds of forests of climate. For example, Gash et al. (1995) found 5.4% underestimation of measured E_i for coniferous forests in a maritime climate. Llorens et al. (1997) reported 4.3% underestimation of observed E_i in coniferous forests in a Mediterranean climate. Dykes (1997) underestimated observed E_i by 1.2% for rainforest in a tropical climate. Despite these errors in E_i estimation for different climates, the revised Gash analytical model is sufficiently robust and reliable to generally estimate that loss for the abandoned coniferous forests of Japanese cypress plantation in a maritime climate.

3-1-4 Summary

These results indicate that within the partitioning of P_g, *TF* has the largest proportion (64.2%), followed by E_i (25.2%) and *SF* (10.6%). Compared with earlier literatures, the *TF* rate was much lower but the *SF* rate much higher than values from other coniferous forests. E_i parameters such as *p*, drainage from the canopy, and *S* were found to improve understanding of the interception process and test generalized models. The CV of *TF* rate was higher than other temperate forests, implying that abandoned Japanese cypress forests are one of the most difficult forest types to measure E_i. The revised Gash analytical model produced good agreement between observed and simulated E_i, with underestimation of 5.7%, and was demonstrated to be sufficiently robust and reliable to apply to coniferous forest plantations in a maritime climate. The present study may

improve understanding of water resources of forested watersheds, and provide a basis for future studies of forest management (e.g., thinning) and rainfall partitioning interaction.

3-2 Tree transpiration and canopy conductance

3-2-1 Tree transpiration

Daily variations in stand E_t related to mean daily daytime VPD measured from April 28 to October 10, 2011 are shown in Fig. 3-7a. Daily E_t increased with increasing VPD, and had a mean of 1.29 ± 0.60 mm d^{-1} and range of $0.07 - 2.53$ mm d^{-1} during the measuring period. The cumulative E_t was 214.9 mm, accounting for 18.3% of P_g. Fluctuations in the daily E_t were directly related to rainfall events and daily E_t decreased quickly during rainfall events (Fig. 3-7b). On rainy days, daily E_t had a mean of 0.97 ± 057 mm d^{-1} and range of $0.07 - 2.27$ mm d^{-1}, with total E_t of 75.4 mm. On dry days, daily E_t mean was 1.59 ± 0.46 mm d^{-1}, with range of $0.36 - 2.53$ mm d^{-1} and total E_t of 141.2 mm. Daily E_t was 64.1% greater on dry compared to rainy days. In fact, rainfall events effectively reduced the solar radiation and vapor pressure deficit (VPD).

Average daily E_t was found to be 1.29 ± 0.60 mm d^{-1}, consistent with other coniferous forests in Japan. Komatsu et al. (2010) summarized stand transpiration of coniferous forests compared with a Moso bamboo forest, and showed that it was in the range of $0.5 - 1.6$ mm d^{-1} during the rainy season. The main error sources for E_t estimates are within-tree radial and tree-tree variations in F_d compared with circumferential variations in F_d (Kume et al., 2011). The within-tree variations in F_d can be ignored because F_d was measured at a depth of $0 - 20$ and $20 - 40$ mm to cover all the sapwood. Therefore, tree-tree variations in F_d are main source of error for E_t estimates, and the coefficient of variability (CV) with a sample size for ten measured individual trees was around 10% (Kumagai et al., 2007).
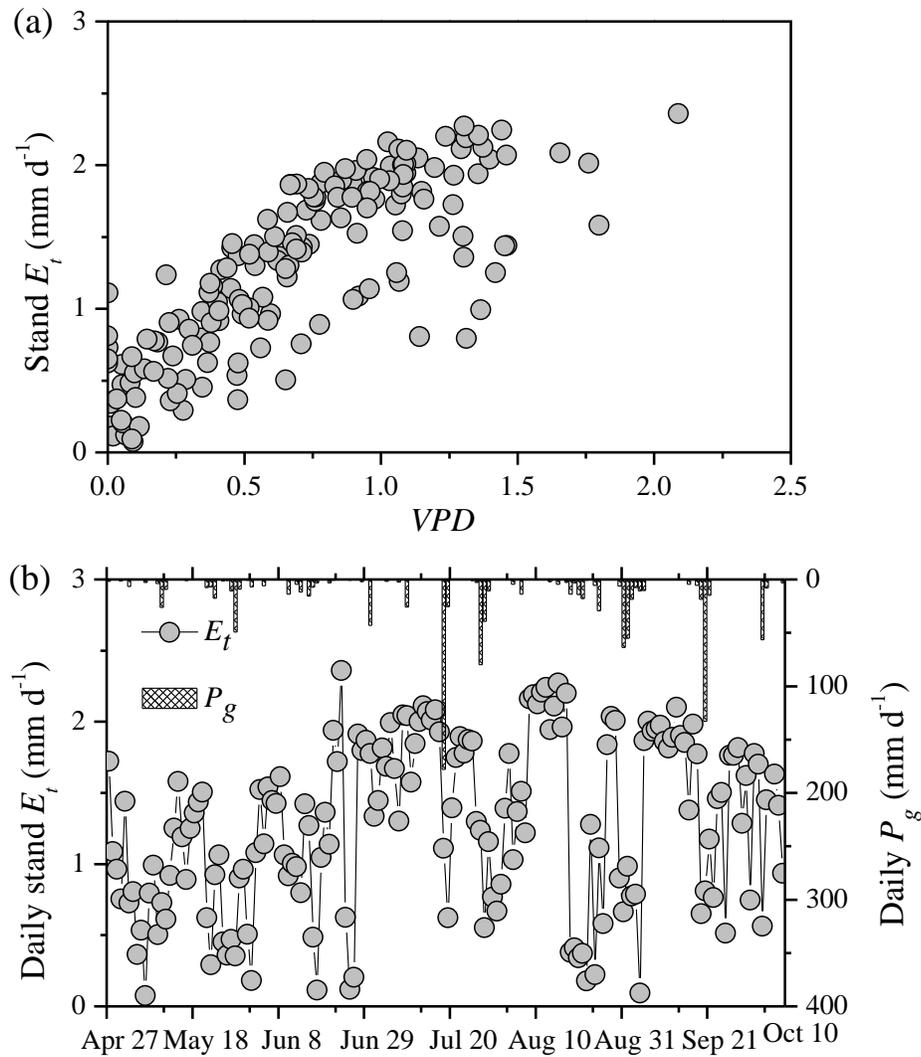
Fig. 3-7 (a) Daily stand transpiration (E_t) response to mean daily daytime vapor pressure deficit (*VPD*), and (b) time series of E_t and gross precipitation (P_g) measured from April 28 to October 10, 2011.

3-2-2 Relationship between tree transpiration and soil water content

The variations in E_t reflected the changes in soil moisture at different depths, shown by the correlation between E_t and soil water content at different depths (Table 3-5). Pearson correlation analysis showed that E_t was correlated with soil moisture at the depth of 5 − 15 cm (correlation coefficient 0.343 − 0.377; $P < 0.05$).

Table 3-5 Correlation analysis between tree transpiration (E_t), forest floor evaporation (E_f) and soil water content at different soil depths.

Soil depth	E_t		E_f	
	Correlation coefficient	p-Value	Correlation coefficient	p-Value
5	**0.377**	<0.05	**0.385**	<0.05
10	**0.343**	<0.05	0.163	0.262
15	**0.362**	<0.05	0.316	0.088
30	0.228	0.114	0.105	0.473
50	0.167	0.251	0.039	0.79
80	0.164	0.259	0.006	0.966

Unit of soil depth: cm.

Significant correlations at the 95% confidence level are marked in bold.

Numbers of days used for the correlation analysis: tree transpiration (E_t), 49; forest floor evaporation (E_f), 29.

These results suggest that E_t was correlated with soil water content in the fine root zone at the depth of 5 – 15 cm for this site (Table 3-5). Raz-Yaseef et al. (2012) reported that E_t was related to soil moisture at a depth of 10 – 20 cm in a pine forest ecosystem with shallow (20 – 40 cm) Aeolian-origin loess with clay–loam texture overlying chalk and limestone bedrock. Cavanaugh et al. (2011) reported that E_t was related to soil moisture at depths of 37.5 and 75 cm in creosote bush ecosystems with sandy loam and high gravel content. In contrast to these previous studies, E_t was correlated with soil moisture at a depth of 5 cm. This may be caused by the exposure of tree roots on the top of soil surface, which indicates that tree roots uptake water from shallow soil at a depth of 0 – 5 cm.

3-2-3 Canopy conductance

Fig. 3-8 shows the relations between the mean daily daytime VPD and G_c for the Japanese cypress forest from April 28 to October 10, 2011. G_c was 0.0031 ± 0.0035 m s^{-1} during the measuring period. We observed significant ($P<0.01$) negative correlation; thus, the G_c values for the study period was modeled as

$$G_c = 0.0021 - 0.001 \ln(VPD) \qquad R^2 = 0.51 \qquad (3.8)$$
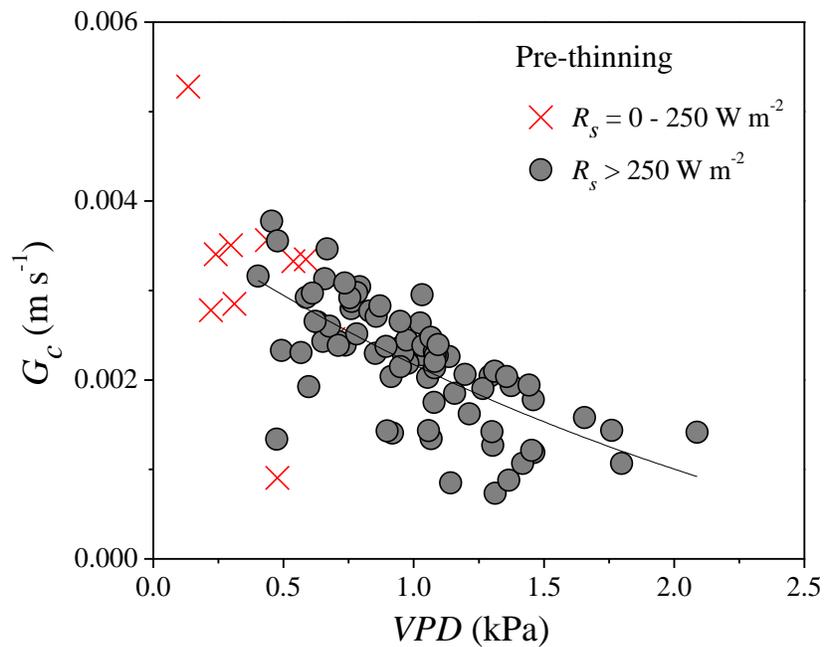
Fig. 3-8 Relationship between mean daily daytime vapor pressure deficit (VPD) and canopy conductance (G_c) for Japanese cypress forests from April 28 to October 10, 2011. Data are classified according to solar radiation (R_s). The solid line is the regression line, determined by the least-squares method for all data representing the pre-thinning period.

On the basis of G_c model (eq. 3.8), $E_{t-stand}$ during the measuring period from April 28 to October 10, 2011 was predicted as shown in Fig. 3-9a. The estimated $E_{t-stand}$ corresponded to the measured values. The correlation between estimated and measured $E_{t-stand}$ was significant ($P<0.01$: a two-tailed Pearson correlation test, $R=0.807$). Thus, the G_c model was robust in estimating daily $E_{t-stand}$ and could be used to extend the $E_{t-stand}$ time scale in the Japanese cypress plantation, although the estimated values were slightly higher than actual values observed at beginning of May 2011.

Fig. 3-9b shows the time series of the daily $E_{t-stand}$ estimated using the G_c model for the pre-thinning period from the November 1, 2010 to October 31, 2011. The daily $E_{t-stand}$ at annual scale was 1.23 ± 0.48 mm d^{-1} in the pre-thinning period. Annual stand E_t were 441.0 mm, accounting for 30.5% of P_g or 49.3% of PET.
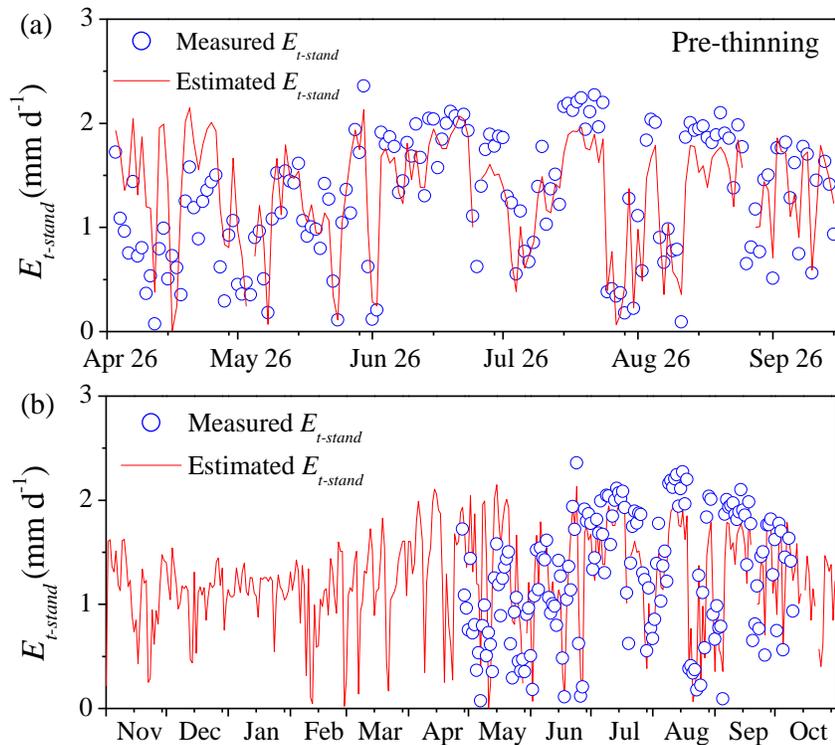
Fig. 3-9 Time series of stand transpiration ($E_{t-stand}$), measured by Granier method (circle) and estimated using the G_c model (solid line) for the pre-thinning period from November 1, 2010 to October 31, 2011 (b), and detailed for the period from April 28 to October 10, 2011 (a).

G_c was calculated by the simplified Penman-Monteith equation, assuming the complete coupling of the canopy with the atmosphere. Specifically, the G_c calculations assume that $E_{t-stand}$ is independent of the radiation term of the Penman-Monteith equation (Jarvis and McNaughton, 1986; Komatsu et al., 2006, 2012; McNaughton and Black, 1973). Thus, the use of the simplified Penman-

Monteith equation is invalid when this equation is applied to canopies decoupled with the atmosphere.

The relations between *VPD* and G_c for Japanese cypress forests during the measuring period is shown in Fig. 3-8. There is a significant ($P<0.01$) negative correlation, and the coefficient of determination (R^2) was 0.51 in the pre-thinning period. This result suggests that *VPD* was the primary factor controlling G_c in the Japanese cypress forests, which agrees with previous studies examining controlling factors affecting G_c in forests during growing seasons without a severe soil water deficit (Granier et al., 1996c; Komatsu et al., 2006; Komatsu et al., 2012). The data for different R_s classes are located along the regression line, which was determined using all data (Fig. 3-8). When R_s was > 250 W m^{-2} (i.e., light-saturated conditions) (Komatsu et al., 2012), the correlation was not particularly strong, and R^2 was 0.46. Thus, these results validate our assumption of a less-considerable contribution of the radiation term of the Penman-Monteith equation.
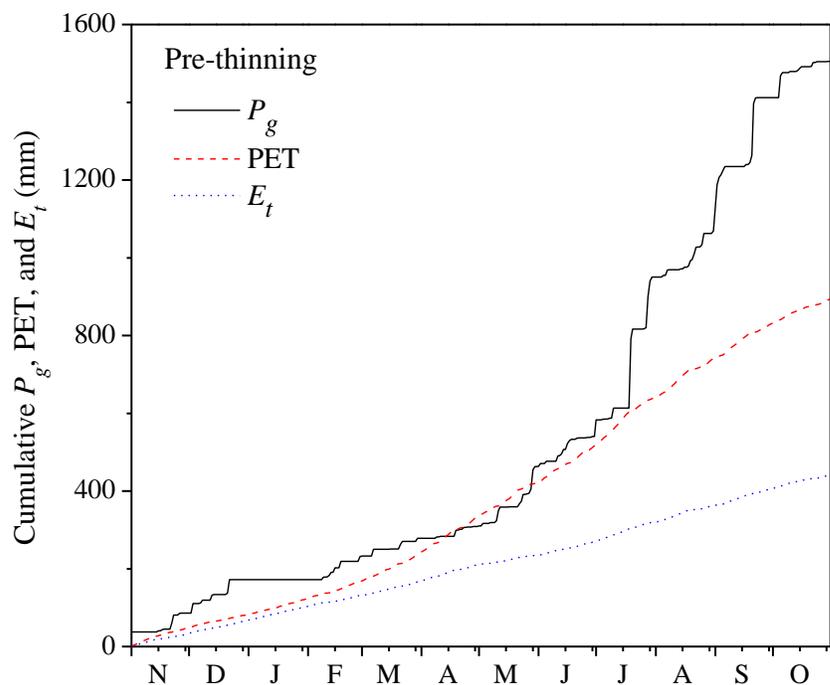
Fig. 3-10 Cumulative daily values of gross precipitation (P_g), potential evapotranspiration (PET), and stand transpiration (E_t) in the pre-thinning period from November, 2010 to October, 2011.

The predicted $E_{t\text{-}stand}$ from the G_c model had a significant correlation ($P<0.01$: a two-tailed Pearson correlation test, $R=0.807$) and a good performance with the measured values during the growing season in the pre-thinning (Fig. 3-9a). Komatsu et al. (2012) also reported that the estimated $E_{t\text{-}stand}$ using G_c model corresponded to the observed $E_{t\text{-}stand}$ and that the correlation coefficient ($R=0.878$) between these values was significant ($P< 0.01$) for the Japanese cypress forests during the growing season. The G_c was related to a range of environmental variables, including VPD, R_s, and soil water deficit (Granier et al., 2000a; Granier et al., 2000b). In this study, the estimated $E_{t\text{-}stand}$ values were slightly higher than those values observed at beginning of growing season of 2011 (Fig. 3-9a). This observation may be caused by the limiting soil water deficit. During the study period, the cumulative P_g was lower than the cumulative PET from late April to May 2011 (Fig. 3-10). The shortage of soil-water storage may restrain water uptake and limit $E_{t\text{-}stand}$. However, the soil water deficit was not severe from November 2010 to mid-April 2011 because the cumulative P_g was higher than PET (Fig. 3-10). Thus, the time series of estimated $E_{t\text{-}stand}$ can be well explained by the response of G_c to VPD in the pre-thinning period, without considering the response of G_c to the soil water deficit.

3-2-4 Summary

This section elucidated $E_{t\text{-}stand}$ and G_c model for an abandoned Japanese cypress plantation. The average daily $E_{t\text{-}stand}$ was 1.29 ± 0.60 mm d^{-1} measured from April 28 to October 10, 2011. It was well correlated with soil moisture at a depth of 5-15 cm. Contrast to previous studies, $E_{t\text{-}stand}$ was correlated with soil moisture at a depth of 5 cm. This reflected the abandoned Japanese cypress forest properties, i.e. tree roots were exposed on the forest floor, and tree roots also uptake water from shallow. Gc was calculated on the basis of $E_{t\text{-}stand}$, and primarily related to VPD, similar to the results obtained for other temperate forests. The estimated $E_{t\text{-}stand}$ using G_c model corresponded to the measured values. The correlation between estimated and measured $E_{t\text{-}stand}$ was significant ($P<0.01$). Thus G_c model was robust in estimating daily $E_{t\text{-}stand}$ and can be used to extend the $E_{t\text{-}stand}$

time scale in the Japanese cypress plantation. Daily $E_{t\text{-}stand}$ at annual scale was 1.23 ± 0.48 mm d^{-1} in the pre-thinning period. Annual $E_{t\text{-}stand}$ were 441.0 mm, accounting for 30.5% of P_g or 49.3% of PET. These results reported here would be useful for understanding the interaction between soil moisture and $E_{t\text{-}stand}$, and also simulating changes in terrestrial water and carbon cycles using ecosystem models due to thinning practice in the abandoned Japanese cypress plantations.

3-3 Forest floor evaporation

3-3-1 Measurement and estimation of forest floor evaporation

The validation of daily observations of E_f using lysimeters and that estimated from the modified Penman-Monteith equation for 12 September to 10 October 2011 is shown in Fig. 3-11a. The computed E_f had a mean of 0.38 ± 0.17 mm d^{-1} and range of $0.03 - 0.67$ mm d^{-1} for a total of 10.86 mm. The observed E_f had a mean of 0.40 ± 0.33 mm d^{-1} and range of $0.00 - 1.07$ mm d^{-1}. The cumulative daily observed E_f was 11.55 mm. The computed E_f had a similar trend and fitted very well with observed E_f (Fig. 3-11a); it was reasonably consistent with the results directly measured using weighing lysimeters, with an underestimation of 5.9%. Therefore, the modified Penman-Monteith equation was robust in estimating E_f and extending the time scale of E_f in this Japanese cypress stand.

Fig. 3-11b shows the daily E_f estimated by the modified Penman-Monteith equation in the pre-thinning period from November 2010 to October 2011. Daily E_f had an average of 0.34 ± 0.23 mm d^{-1} and range of $0.02 - 1.01$ mm d^{-1}. The cumulative values of E_f in the whole study period were 124.0 mm, accounting for 8.6% of P_g. Daily E_f was also affected by rainfall events and decreased quickly during rainfall events. On rainy days, daily E_f had a mean of 0.29 ± 0.20 mm d^{-1} and range of $0.02 - 0.82$ mm d^{-1}, with total E_f of 37.8 mm. On dry days, daily E_f had a mean of 0.37 ± 0.24 mm d^{-1} and range of $0.05 - 1.01$ mm d^{-1}, with total E_f of 86.2 mm. Daily E_f increased by 26.5% on dry compared to rainy days. Similarly to E_t, low E_f values are explained by lower solar radiation and VPD conditions during rainfall.
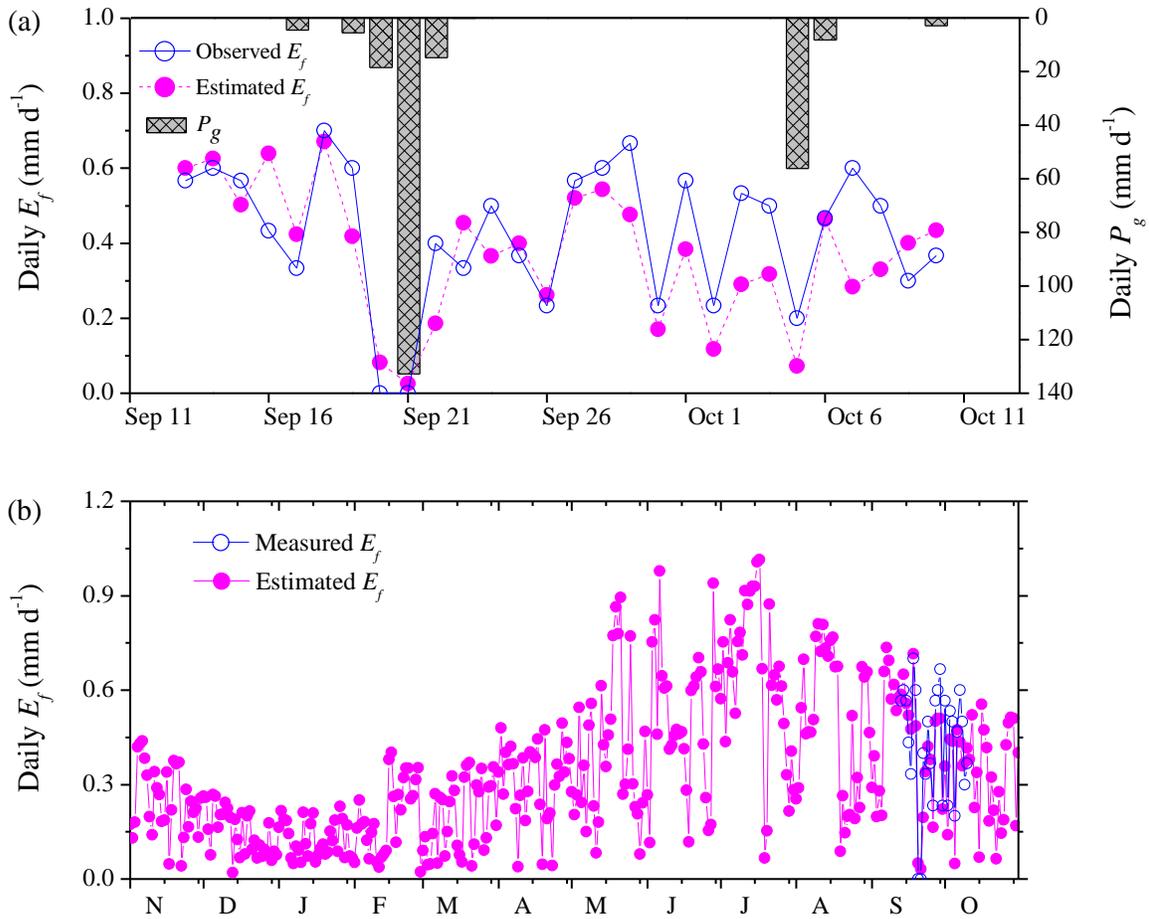
Fig. 3-11 Daily values of forest floor evaporation (E_f), measured by lysimeters (soil line and triangles) and estimated using the modified Penman–Monteith equation (dashed line and triangles) from November 1, 2010 to October 31, 2011 (b), and detail for the period 12 September to 10 October, 2011 (a).

Average daily E_f was found to be 0.34 ± 0.23 mm d^{-1} and was similar to the value of 0.39 d^{-1} in a 31-year-old Japanese cypress stand reported by Hattori (1983). The ratio of E_f to P_g in this study was also consistent with the range of 7.1 to 20.3% in Japanese coniferous plantations summarized by Hattori (1983). The variation of average daily E_f in three lysimeters ranged from 0.40 to 0.44 mm d^{-1} with a mean of 0.41 ± 0.02 mm d^{-1} during the measurement period. The CV of the results for these three lysimeters was 5.6%. The E_f value was higher compared to similar forest conditions

(e.g., stand density, understory vegetation cover). For instance, Schaap and Bouten (1997) reported that E_f was 0.23 mm d^{-1}, with range of 0.19 – 0.3 mm d^{-1} in a dense Douglas fir stand with no understory vegetation in the central Netherlands. In their study, soil water content had a mean of 0.12 m^3 m^{-3} and range of 0.05 – 0.21 m^3 m^{-3}, with total rainfall amount of 51 mm during 44 d. In the present study, soil water content had a mean of 0.18 m^3 m^{-3} and a range of 0.14 – 0.22 m^3 m^{-3}, with total rainfall of 938.8 mm. This abundant rainfall would be expected to maintain a high soil water content. The surface soil was the dominant reservoir for evaporation flux from the forest floor (Table 3-5), and this reservoir was constantly filled by abundant rainfall, the E_f found here could be large compared to other studies.

3-3-2 Relationship between forest floor evaporation and soil water content

The daily variations in E_f also reflected the changes in soil moisture at different depths. Pearson correlation analysis showed that the best correlation was between E_f and soil moisture at the depth of 5 cm (correlation coefficient 0.385; $P < 0.05$), while there was no significant correlation with the soil moisture at other depths (Table 3-5).

Table 3-5 suggests that E_f was correlated with soil water content of the topsoil. Averaged soil water content was consistently high throughout the rainy season and could support high E_f fluxes when energy was available. The results are consistent with those for a coniferous forest by Raz-Yaseef et al. (2012), who reported that E_f was best correlated with soil moisture in the topsoil (5 cm depth). The results also agree with those for grassland and shrubland ecosystems showing that soil evaporation was strongly correlated with surface soil moisture but poorly correlated with water content at greater depths throughout the entire root zone of both sites (Kurc and Small, 2004).

A simple ET-soil moisture relationship can be used to investigate soil moisture dynamics (e.g., Laio et al., 2001; Rodriguez-Iturbe, 2000) and the resulting impacts on plant productivity, species interactions, and nutrient cycling (Porporato et al., 2001). Combined with the findings in the Section 3-2-2, we identified the depth at which moisture was best correlated with E_t and E_f. This

relationship can help in understanding the interactions between soil moisture and evaporation fluxes, and also allows more accurate prediction of ET than when estimates of ET are based only on averaged soil moisture in the root zone (Guswa et al., 2002).

3-3-3 Summary

This section validated the daily variation of E_f using lysimeters and that estimated from the modified Penman-Monteith equation in the abandoned Japanese cypress plantation. The observed E_f had a mean of 0.40 ± 0.33 mm d^{-1} and the computed E_f had a mean of 0.38 ± 0.17 mm d^{-1} for the period from 12 September to 10 October 2011. The computed E_f had a similar trend and fitted very well with observed E_f with an underestimation of 5.9%. The modified Penman-Monteith equation was robust in estimating E_f and extending the time scale of E_f in the abandoned Japanese cypress stand. In the pre-thinning period, annual daily E_f had an average of 0.34 ± 0.23 mm d^{-1}. The cumulative values of E_f were 124.0 mm, accounting for 8.6% of P_g. This was consistent with the range for coniferous forests in Japan. Daily E_f was best correlated with soil moisture in the upper 5 cm of soil. Combined with the findings shown in Section 3-2-2, these relationships can help researchers understand the interactions between soil moisture and evaporation fluxes (E_t and E_f) and also allow increased accuracy in the prediction of ET than that based only on root zone average soil moisture. In addition, the surface soil was the dominant reservoir for evaporation flux from the forest floor, and this reservoir was constantly filled by abundant rainfall during the rainy season. The E_f could be large when energy was available. These results highlight a strong pressing to clarify the effect of thinning on E_f due to the increase in solar radiation penetrated into the forest, although E_f was a small component of forest water cycle in the abandoned Japanese cypress plantations.

3-4 Partitioning of the total evapotranspiration for an abandoned Japanese cypress stand during the growing season

3-4-1 Environmental conditions

Meteorological conditions during the growing season from July to October, 2011 are plotted in Fig. 3-12. The rainy season typically starts in July, with large storm events, and rain ceases in October. Total P_g during the growing season was 938.8 mm, and was consistent with the range of 407 – 1,196 mm and mean of 684 mm for the last 20 years. The measuring period included three storm events: 177.6, 81.0 and 132.6 mm d^{-1} on 19 July, 28 July and 21 September, respectively. During the observation period, there were 43 rainy days representing 42.2% of total days. The longest rain period was 8 d. The longest interval between rainfall events was 11 d. Soil water content had a mean of 0.18 m^3 m^{-3} and range of 0.14 – 0.22 m^3 m^{-3}. The high soil moisture conditions persisted throughout the rainy season. Other meteorological variables are also shown in Fig. 3-12. Mean daily solar radiation was 12.8 MJ m^{-2} d^{-1} with range of 1.0–22.4 MJ m^{-2} d^{-1}, with the relative peak values recorded during 11:00 – 15:00. The prevailing gust wind direction was southeast, with a mean of 0.33 m s^{-1}. Mean vapor pressure deficit (*VPD*) was 0.46 kPa with range of 0.00 – 3.61 kPa. Mean air temperature was 23.7°C with range of 9.3 – 37.9°C, and was consistent with the mean temperature of 22.3 ± 1.0°C for the last 20 years. The mean relative humidity was 87.1% (range 32.0 – 100%).
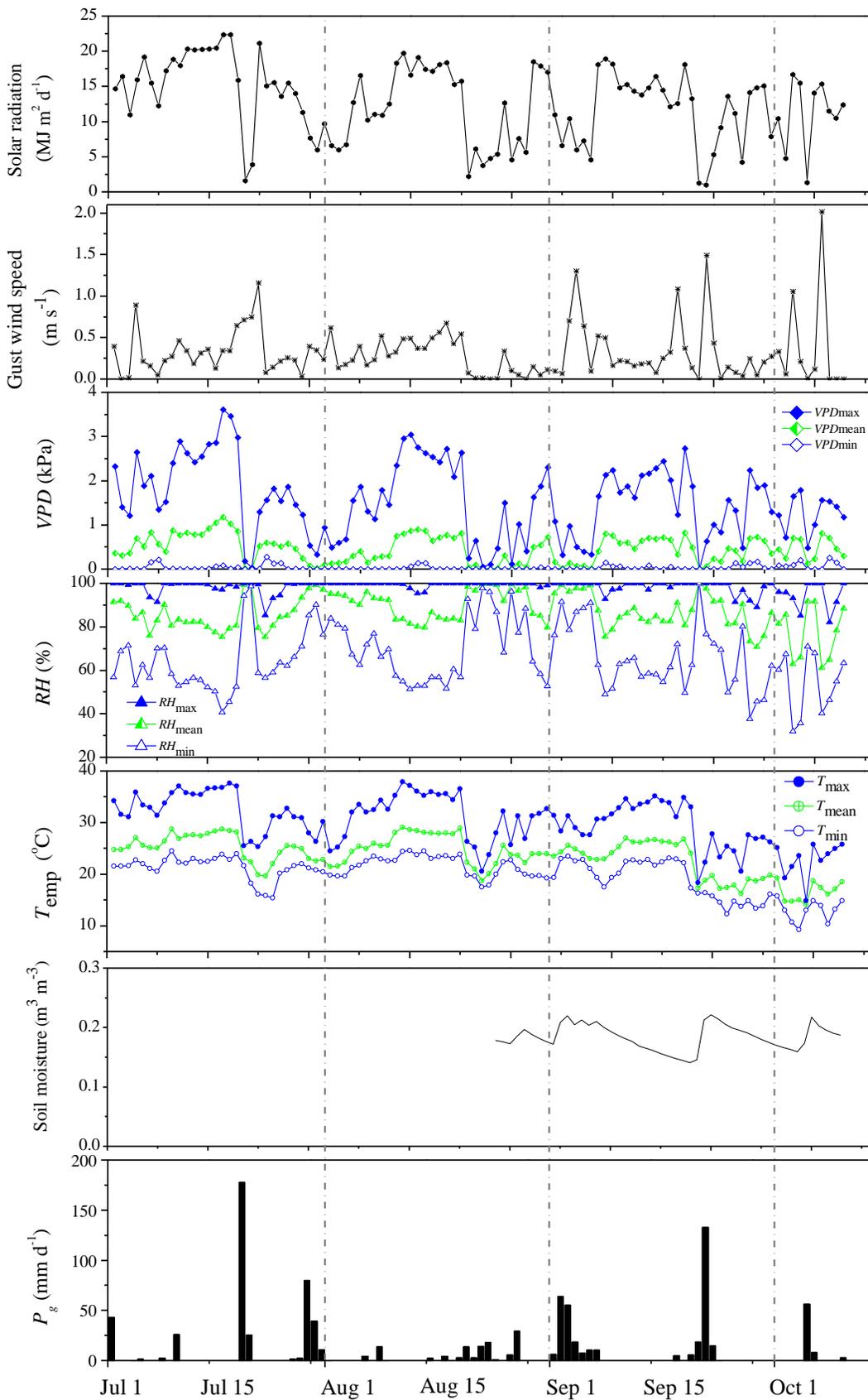
Fig. 3-12 Daily values from 1 July to 10 October 2011 of solar radiation; wind gust speed; maximum, mean and minimum vapor pressure deficit (VPD_{max}, VPD_{mean} and VPD_{min}, respectively); maximum, mean and minimum relative humidity (RH_{max}, RH_{mean} and RH_{min}, respectively); maximum, mean and minimum temperature (T_{max}, T_{mean} and T_{min}, respectively); soil water content averaged for depth of 0–80 cm and open gross precipitation (P_g) amount.

3-4-2 Partitioning of evapotranspiration during the growing season

Detailed monthly P_g, ET and its three sub-components in the Japanese cypress forest during the 2011 growing season are summarized in Table 3-6. For the whole growing season, E_i, E_t and E_f accounted for 53.6, 33.7 and 12.7% of total ET, respectively. Total ET was 446.3 mm, accounting for 47.5% of total P_g − this corresponds to almost half of the P_g being stored in the forested watershed or discharged by streams. The cumulative daily value of P_g, ET and its three sub-components is illustrated in Fig. 3-13a. ET was less than precipitation throughout the rainy season. ET was only close to P_g at the beginning of the rainy season, and afterward was much less than P_g.

Table 3-6 Monthly precipitation (P_g) and evapotranspiration (ET) and its three sub-components: canopy interception (E_i), tree transpiration (E_t) and forest floor evaporation (E_f) during the growing season, 2011.

	Jul	Aug	Sep	Oct[*]	Total	Ratio of P_g	Ratio of ET
			mm				%
E_i	90.1	44.8	85.2	19.1	239.2	25.5	53.6
E_t	50.0	42.9	43.1	14.4	150.4	16.0	33.7
E_f	21.4	18.4	13.4	3.5	56.7	6.0	12.7
ET	161.5	106.1	141.7	37.0	446.3	47.5	-
P	410.4	118.4	342.6	67.4	938.8	-	-

* Only for 1–10 October.
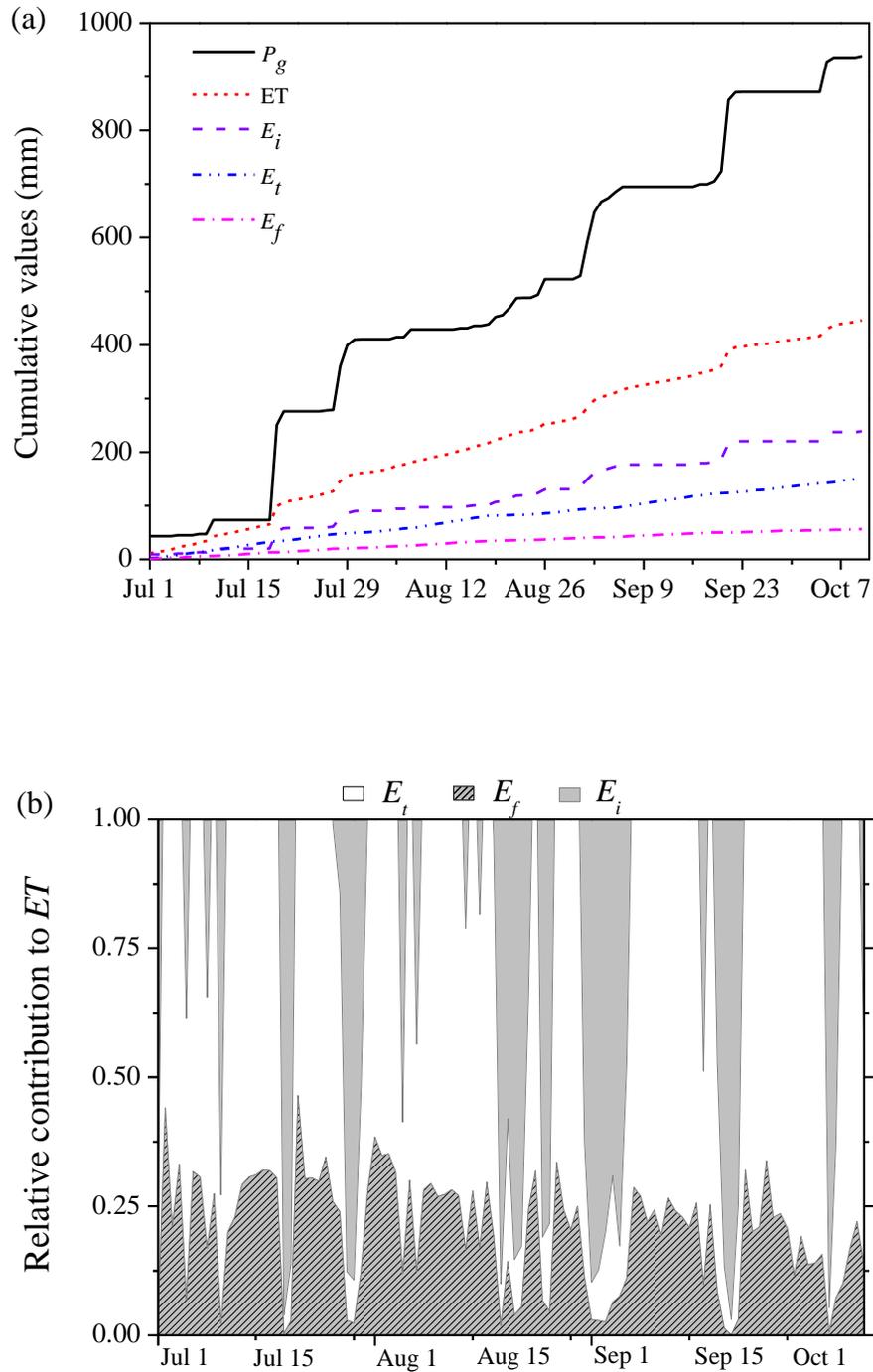
Fig. 3-13 (a) Cumulative daily values of gross precipitation (P_g), evapotranspiration (ET) ET = E_i + E_t + E_f, canopy interception (E_i), tree transpiration (E_t), and forest floor evaporation (E_f) in the Japanese cypress forest during the growing season. (b) Relative contribution of each flux (E_i, E_t and E_f) to total ET in the Japanese cypress forest during the growing season (1 July to 10 October 2011).

The daily relative contribution of each sub-component flux to ET varied greatly between rainy and dry days. On rainy days, the relative contribution of E_i was high, with a range of 10.1 – 97.1% and mean of 64.3 ± 27.7% of ET; this was particularly pronounced for rainfall events > 15 mm, with a mean E_i of 88.5 ± 6.4% and range of 75.1 – 97.1%. The relative contribution of E_f was the smallest, with range of 0.1 – 33.1% and mean of 11.1 ± 9.7%. The relative contribution from E_t was moderate, with range of 2.1 – 66.9% and mean of 24.6 ± 19.0% of ET. On dry days, there was obviously no E_i. The relative contribution of E_t was the dominant evaporation flux to ET, with range of 53.5 – 89.9% and mean of 73.6 ± 7.1%. Moreover, the contribution from E_f was a smaller component than E_t on a daily scale, with range of 10.1 – 46.5% and a mean of 26.4 ± 7.1% of ET.

E_i and subsequent evaporation loss from forest was the largest proportion (53.6%) of ET in the Japanese cypress stand during the growing season (Table 3-6). Literature concerning ET for coniferous forests shows that E_i loss from coniferous forests are in the range of 11.4 – 75.0% of total ET, depending on climate and forest structure parameters (Table 3-7). The ratio of E_i to ET in this study was relatively higher than found in other sites for coniferous forests. For instance, Tian et al. (2011) reported that interception loss from *Picea crassifolia* Kom. forest accounted for 32.2% of total ET in the growing periods in China. Jansson et al. (1999) found that E_i loss of a pine-spruce mixed forests (*Picea abies* L. and *Pinus sylvestris* L.) stand represented 22.3% of total ET during the growing season in Sweden. Shimizu et al. (2003) reported the mean annual E_i rate represented 40.0% of annual ET in coniferous forests of western Japan. E_i loss increases with the amount of P_g and forest stand density (Komatsu et al., 2008b). Compared with previous studies, values in our study probably reflect the relatively large number of storm events (three typhoon events) and the dense stand density. E_i was the largest component of total ET, an accurate estimation of the water balance in watersheds requires a precise quantification of this interception, at the event scale as well as at the yearly scale.

Table 3-7 Bibliographical summary of evapotranspiration (ET) in coniferous forests

Reference	Location	Species	Duration	Methodology	P_g	ET	E_i	E_r	E_f	ET/P_g	E_i/ET	E_r/ET	E_f/ET
					mm					%			
This study	Karasawa mountain, Japan	*Chamaecyparis obtusa*	Jul - Oct 2011	E_i:throughfall and stemflow measurements. E_r: Granier method. E_f: lysimeter.	939	446	239	150	57	47.5	53.6	33.7	12.7
Lin *et al.*, 2012	Gongga Mountain, Qinghai-Tibet Plateau, China.	*Abies fabri*	Apr - Oct 2009	E_i: throughfall and stemflow measurements. E_r:sapflow method. E_f: stable isotope.	1199	736	552	140	44	61.4	75.0	19.0	6.0
Tian *et al.*, 2011	Qilian mountain, China	*Picea crassifolia*	May-Sep 2008	ET: eddy covariance system. Modified Penman-Monteith equation.	379	314	101	161	52	82.7	32.2	51.3	32.3
Jansson *et al.*, 1999	Norunda forest, sweden	*Picea abies* (66%), *Pinus sylvestris* (33%)	May-Oct 1994	ET: eddy covariance measurements. Penman-Monteith equation.	-	314	70	181	63	-	22.3	57.6	20.1
Kosugi and Katsuyama, 2007	Kiryu Experimental watershed, Japan	*Chamaecyparis obtusa*	2001 - 2003	ET: eddy covariance system and water budget method	1438	720	-	-	-	50.1	-	-	-
				ET: eddy covariance system.	1646 ± 281ᵃ	749 ± 69ᵃ	-	-	-	45.5	-	-	-
					1971	750	-	-	-	38.1	-	-	-
					1179	735	-	-	-	62.3	-	-	-
Raz - Yaseef *et al.*, 2012	Yatir Forest, Israel	*Pinus halepensis*	2003 - 2007	ET: eddy covariance system. E_i: interception and precipitation relation. E_r: sapflow measurements. E_f: chamber and microlysimeter.	231	235	27	134	99	101.7	11.5	57.0	42.1
					377	343	39	156	112	91.0	11.4	45.5	32.7
					224	227	26	111	93	101.3	11.5	48.9	41.0
					308	263	33	115	106	85.4	12.5	43.7	40.3
Shimizu *et al.*, 2003	Kahoku experiment watershed, Japan	*Chamaecyparis obtusa* / *Chamaecyparis japonica*	1996 - 1998	ET: eddy covariance system and water budget method. E_i: interception and precipitation relation.	2373	889	356	-	-	37.5	40.0	-	-
					2166ᵃ	923	-	-	-	42.6	-	-	-
Waterloo *et al.*, 1999	Nabou forest estate, Viti Levu	*Pinus caribaea*	Nov 1989 - Nov 1990	ET: Penman-Monteith equation. E_i: throughfall and stemflow measurements.	2054	1926	382	1394	155	93.8	19.8	72.4	8.0
					2054	1717	371	1198	153	83.6	21.6	69.8	8.9

a: Annual data based on water budget method.

In the present study, $E_{t\text{-}stand}$ accounted for 33.7% of total ET although the value was smaller than for some areas with similar climates, where $E_{t\text{-}stand}$ is the dominant component of ET. For instance, in a *P. caribaea* forest on the Fiji islands, $E_{t\text{-}stand}$ accounted for > 70% of annual ET (Waterloo et al., 1999). The E_t/ET ratio is crucial to predicting ecosystem survival and productivity, especially in water limited regions. For instance, if this ratio is high, the tree components of the ecosystem uptake more water from the ground and transpire more to the atmosphere than when it is low. This implies that it creates an imbalance in the water use between trees and other components of the ecosystem that could affect proper ecosystem function. In light of this, it is possible to expect that knowing the value of this ratio can help land managers to manage abandoned dense plantations.

Total ET was 446.3 mm summed from three sub-components and accounted for 47.5% of total P_g. Because of the uncertainty of estimations of each component, further measurements should be applied to validate the total ET. For example, an eddy covariance system coupled with meteorological data allows analysis of the factors controlling ET for short/long-term periods. By contrast, the water balance approach cannot allow researchers to determine the factors controlling ET or their influences on the characteristics of ET; so, a long-term period of time is needed to evaluate ET. Therefore, an eddy covariance system would be a suitable method for evaluating total ET.

For the entire growing season, the ET/P_g ratio agreed well with that found for other Japanese cypress sites. For instance, our result for ET/P_g (47.5%) was within the measured range of 38.1 – 62.3% for Japanese cypress forest recorded by Kosugi and Katsuyama (2007), and 37.5 – 42.6% for a coniferous forest including Japanese cypress and Japanese cedar found by Shimizu et al. (2003) (Table 3-7). However, it was smaller than for other coniferous forests in dry climates. For example, the ET/P_g ratio was > 80% or sometimes > 100%, and E_t was the dominant evaporation flux due to dry climates (Raz-Yaseef et al., 2012). ET is the dominant component in the water balance at watershed-scale. The dynamics of ET partitioning can improve the understanding of water resources

of forested watersheds and can also help in predicting or modeling a forest stand water budget.

3-4-3 Summary

This study quantified partitioning of ET into E_i, E_t and E_f in a Japanese cypress plantation during the growing season. ET was the main component in the water balance and accounted for 47.5% of the total P_g (938.8 mm). E_i (53.6% of ET) was the dominant evaporation flux followed by E_t (33.7% of ET) and E_f (12.7% of ET). These findings can increase the understanding of water balances of forested watersheds, and help in predicting or modeling water budgets (e.g., ET partitioning and runoff) in forest ecosystems. Forest management practices (e.g., thinning) can alter the cover and structure of the forest canopy, and change the hydrological processes of forest. Japanese coniferous plantations are currently subjected to thinning treatments because of their overstocked stand densities and volumes. Hence, researchers need a clear understanding of the impacts of forest/vegetation on processes connected with ET. Thus, future ecohydrological studies should focus on quantifying the ET partitioning response to land use change in forested watersheds which in turn will help to improve the development of sound forestry techniques and resolve complex forest-water conflicts.

Chapter 4 The effect of strip thinning on partitioning of evapotranspiration in a Japanese cypress plantation

4-1 Meteorological characteristics in pre- and post-thinning

It is of important to understand the characteristics of meteorological conditions in pre- and post-thinning period. The time series of meteorological factors in the pre- and post-thinning periods are shown in Fig. 4-1. The meteorological variables (e.g., relative humidity (RH), temperature (T), PET and VPD) show clear seasonal trends and reached higher values during the growing season (May - October) in both periods. Maximum T reached more than 37 ℃ between later June and early August, and minimum T were below 0 ℃ mainly between January and February in both periods. The day-to-day variations in R_s generally corresponded to P_g and were low during the regular rainy season from mid-June to mid-July in Japan. The day-to-day variations in the VPD generally corresponded to those changes in T and RH. The P_g frequently occurred for both periods. The total P_g values were 1444.6 and 1266.8 mm, respectively. The P_g values during the growing season were 1139.8 mm and 869.0 mm, respectively. The total PET was 894.3 mm with a mean of 2.45 ± 1.43 mm d^{-1}, and 945.1 mm with a mean of 2.59 ± 1.60 mm d^{-1} in pre- and post-thinning, respectively. The PET values during the growing season were 533.9 mm and 605.4 mm, respectively. The P_g values were higher than PET in the annual and growing season scales, respectively.
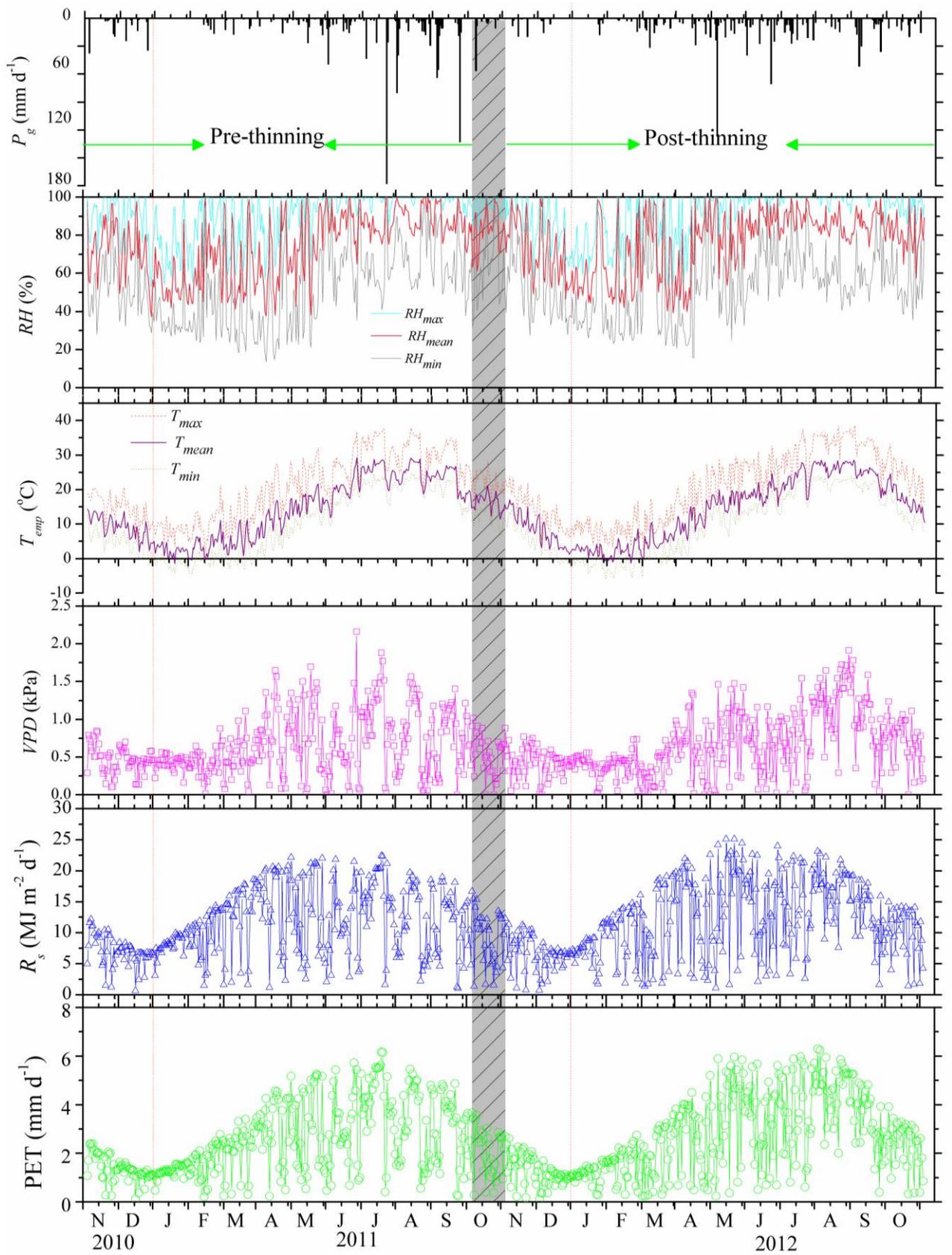
Fig. 4-1 Daily climatic values in the pre-thinning period (November 2010 – October 2011) and the post-thinning period (November 2011 – October 2012). Reading from the top: daily precipitation (P_g), maximum, mean and minimum relative humidity (RH_{max}, RH_{mean} and RH_{min}, respectively); maximum, mean and minimum temperature (T_{max}, T_{mean} and T_{min}, respectively); vapor pressure deficit (VPD); daily total solar radiation (R_s); and daily potential evapotranspiration (PET).

Rainfall characteristics in pre- and post-thinning were summarized in Table 4-1. Total gross rainfall was 1444.6 mm and 1266.8 mm in pre- and post-thinning, respectively. Less rainfall events but more precipitation was observed in the pre-thinning period than in the post-thinning period. Event-based gross rainfall ranged from 0.8 – 176.8 mm with a mean of 13.0 mm in the pre-thinning period and from 0.8 – 150.0 mm with a mean of 17.4 mm in the post-thinning period. Rainfall intensity ranged from 0.2 – 12.9 mm h^{-1} with a mean of 1.6 mm h^{-1} in the pre-thinning period and ranged from 0.1 – 16.5 mm h^{-1} with a mean of 1.5 mm h^{-1} in the post-thinning. No significance difference existed about rainfall between the pre-thinning and post-thinning periods ($p > 0.05$, Wilcoxon-Man-Whitney test). The characteristics of rainfall were similar in both periods.

Table 4-1 Rainfall characteristics in the pre- and post-thinning periods.

Rainfall conditions	Pre-thinning Nov 2010 - Oct 2011	Post-thinning Nov 2011 - Oct 2012
Number of storm events (mm)	83	98
Total rainfall (mm)	1444.6	1266.8
Max storm event rainfall (mm)	176.8	150.0
Mean storm event rainfall (mm)	13.0	17.4
Max duration (h)	51	40
Mean duration (h)	10	10
Max time since previous event (h)	1179	1008
Mean time since previous event (h)	89	77
Max rainfall intensity (mm/h)	12.9	16.5
Mean rainfall intensity (mm/h)	1.6	1.5

In addition, Fig. 4-2 showed frequency distribution of rainfall event classification in pre- and post-thinning period. Most rainfall events, 75 and 93 rainfall events in pre- and post-thinning period, respectively, were less than 40 mm. For the class between 40 and 100 mm, the number of rainfall events was similar, 5 and 4 rainfall events were collected in pre- and post-thinning period. But for classification of rainfall event more than 100 mm, 3 and 1 rainfall events was observed in pre- and post-thinning period. Overall, the frequency distribution of each rainfall event classification was uniform in both periods.
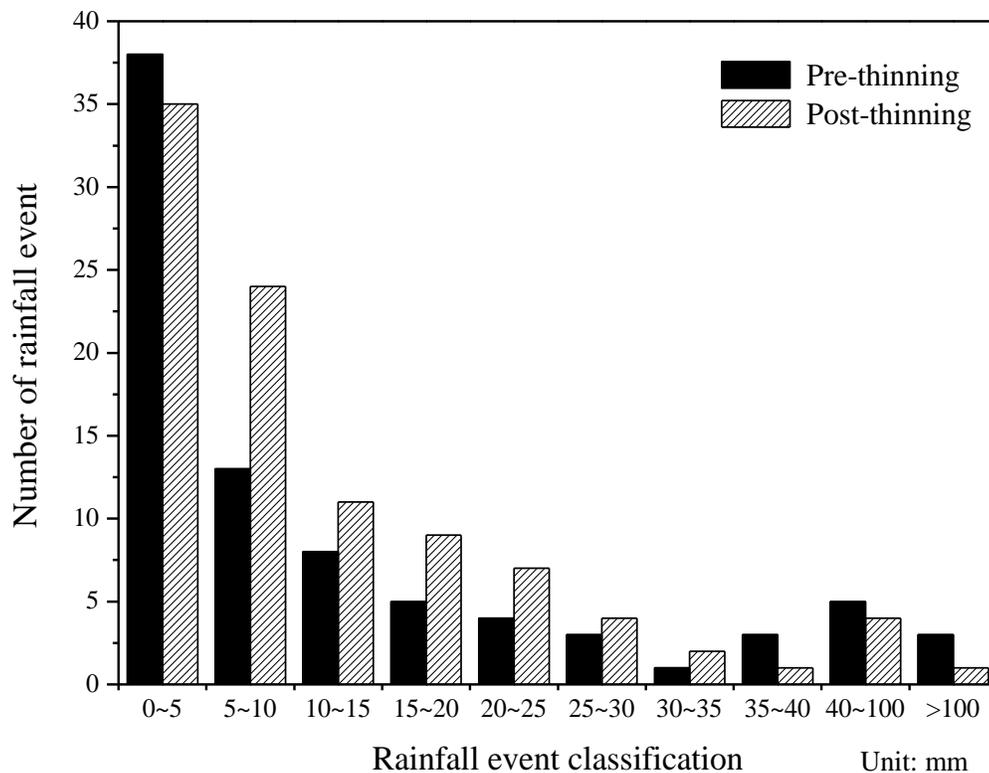
Fig. 4-2 Frequency distribution of rainfall event classification (grouped into 5 mm intervals) in the pre- and post-thinning periods.

4-2 The effect of strip thinning on canopy interception

4-2-1 Changes in rainfall partitioning

Annual-based scale: The annual canopy water balance for pre- and post-thinning periods is summarized in Table 4-2 and Fig. 4-3. Total *TF* was 887.7 mm (61.4% of P_g) and 925.0 mm (73.0% of P_g) in the pre- and post-thinning periods, respectively. More *TF* amount and a higher *TF* rate were observed in the post-thinning period, although less precipitation amount was observed. Total *SF* was 142.1 mm (9.8% of P_g) and 77.7 mm (6.1% of P_g), and total E_i was 414.8 mm (28.7% of P_g) and 263.0 mm (20.8% of P_g) in the pre- and post-thinning periods. Both *SF* and E_i decreased in the post-thinning period due to the thinning treatment ($p < 0.05$, Wilcoxon-Man-Whitney test).

Table 4-2 Annual and seasonal gross precipitation (P_g), canopy water balance (throughfall, *TF*; stemflow, *SF*; canopy interception, E_i) expressed as depth (mm) and as a percentage of P_g (%) in the pre- and post-thinning periods. Dry season is composed of spring and winter, and rainy season is composed of summer and autumn.

Year/season	Pre-thinning								Post-thinning							
	P_g	*TF*		*SF*		E_i			P_g	*TF*		*SF*		E_i		
	mm	mm	%	mm	%	mm	%		mm	mm	%	mm	%	mm	%	
Spring	229.8	129.0	56.1	19.8	8.6	81.0	35.3		473.2	355.7	75.2	29.2	6.2	87.1	18.4	
Summer	574.6	363.5	63.3	53.9	9.4	157.1	27.3		389.8	282.3	72.4	25.9	6.7	81.6	20.9	
Autumn	495.2	309.6	62.5	55.3	11.2	130.3	26.3		299.4	219.0	73.1	17.6	5.9	62.8	21.0	
Winter	145.0	85.6	59.0	13.1	9.0	46.3	32.0		104.4	68.0	65.2	4.9	4.7	31.5	30.2	
Dry	374.8	214.6	57.3	32.8	8.8	127.4	34.0		577.6	423.7	73.4	34.1	5.9	118.7	20.5	
Rainy	1069.8	673.1	62.9	109.3	10.2	287.4	26.9		689.2	501.3	72.7	43.6	6.3	144.4	20.9	
Annual	1444.6	887.7	61.4	142.1	9.8	414.8	28.7		1266.8	925.0	73.0	77.7	6.1	263.0	20.8	
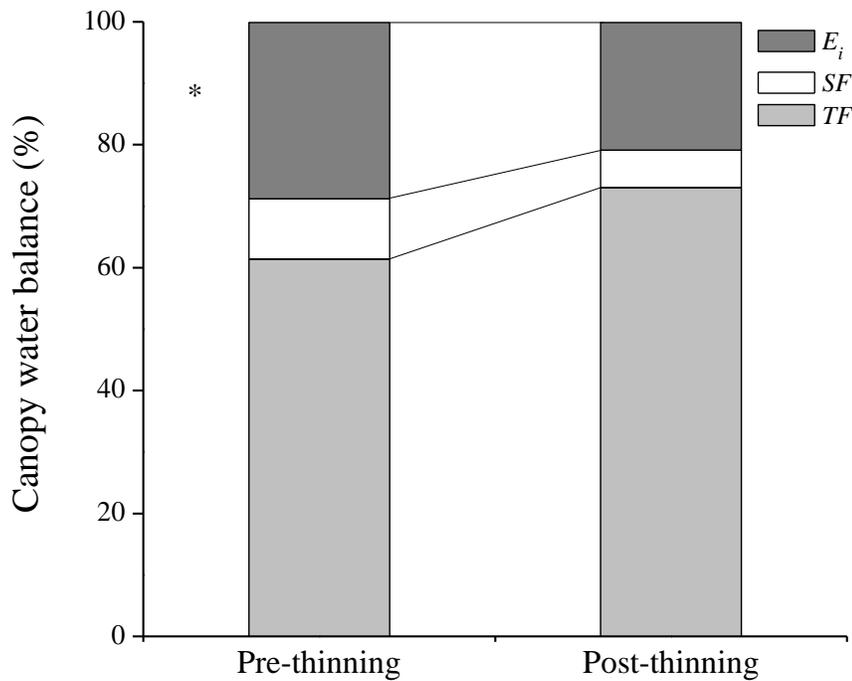
Fig. 4-3 Annual canopy water balance ratio (%) in the pre- and post-thinning periods. Significance differences are indicated by * ($p < 0.05$) by U-test.

Season-based scale: The seasonal canopy water balance in both periods is also shown in Table 4-2 and Fig. 4-4. The largest P_g amount was observed in summer and spring in the pre- and post-thinning period, respectively. The lowest P_g amount was observed in winter in both periods. *TF* rate ranged from 56.1-63.3% in the pre-thinning period and from 65.2-75.2% in the post-thinning period. *SF* rate ranged from 8.6-11.2% in the pre-thinning period and from 4.7-6.7% in the post-thinning period. E_i rate ranged from 26.3-35.3% in the pre-thinning period and from 18.4-30.2% in the post-thinning period (Table 4-2). After thinning, net precipitation (*TF* and *SF*) rate increased by 11.1% from 71.3 to 79.2%, of which it increased from 66.0-79.3% in dry season and from 73.1-79.1% in rainy season.
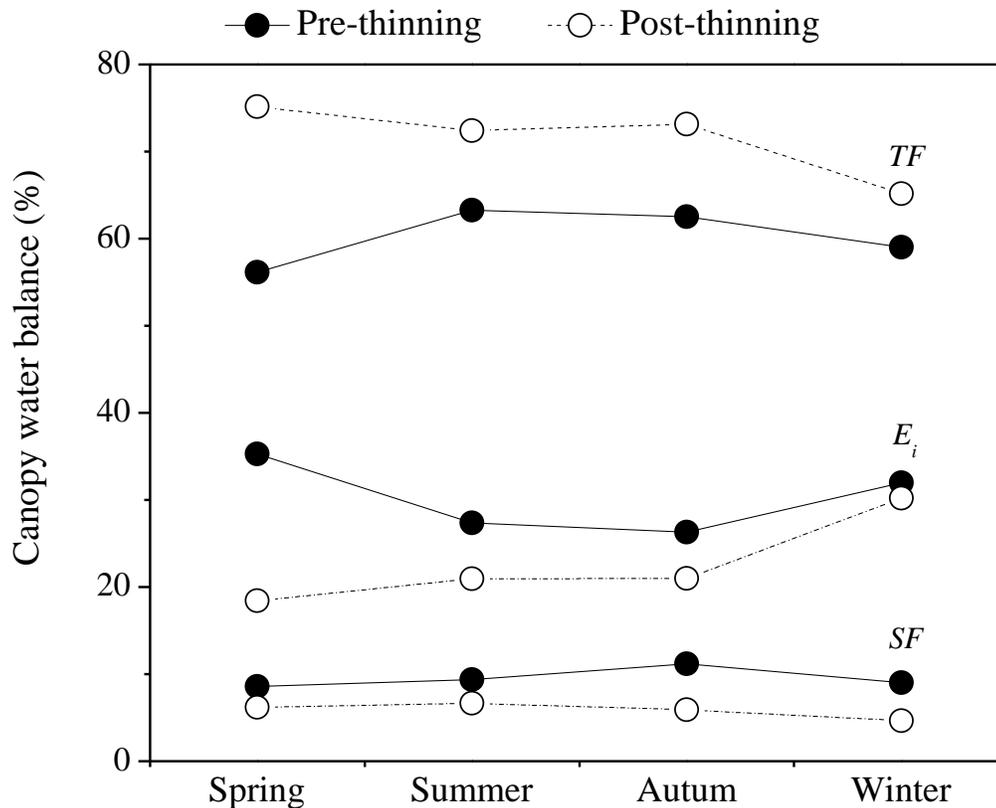
Fig. 4-4 Seasonal canopy water balance ratio (%) in the pre- and post-thinning periods.

Month-based scale: The monthly variation of canopy water balance in the pre- and post-thinning periods are shown in Fig. 4-5. Month-based P_g ranged from 0.0-383.4 mm with a mean of 120.4±120.2 mm in the pre-thinning period and from 26.1-281.2 mm with a mean of 105.6±80.9 mm in the post-thinning period. Monthly P_g was highest in July and May and lowest in January and December in pre- and post-thinning periods, respectively. Month-based *TF* ranged from 0.0-259.9 mm with a mean of 74.0±80.8 mm (0-67.8% of P_g) in the pre-thinning period and from 16.0-217.7 mm with a mean of 77.1±62.5 mm (60.2-77.4% of P_g) in the post-thinning period. Month-based *SF* ranged from 0.0-40.4 mm with a mean of 11.8±13.8 mm (0.0-11.8% of P_g) in the pre-thinning period and from 1.6-17.9 mm with a mean of 6.5±5.5 mm (3.5-7.7% of P_g) in the post-thinning period. Month-based E_i ranged from 0.0-85.1 mm with a mean of 34.6±26.5 mm (0.0-52.6% of P_g) in the pre-thinning period and from 8.9-45.6 mm with a mean of 21.9±13.3 mm (16.2-33.5% of P_g)

in the post-thinning period. In summary, monthly *TF* rate was significant higher whereas *SF* and E_i rate were lower after thinning treatment ($p < 0.05$, Wilcoxon-Man-Whitney test).
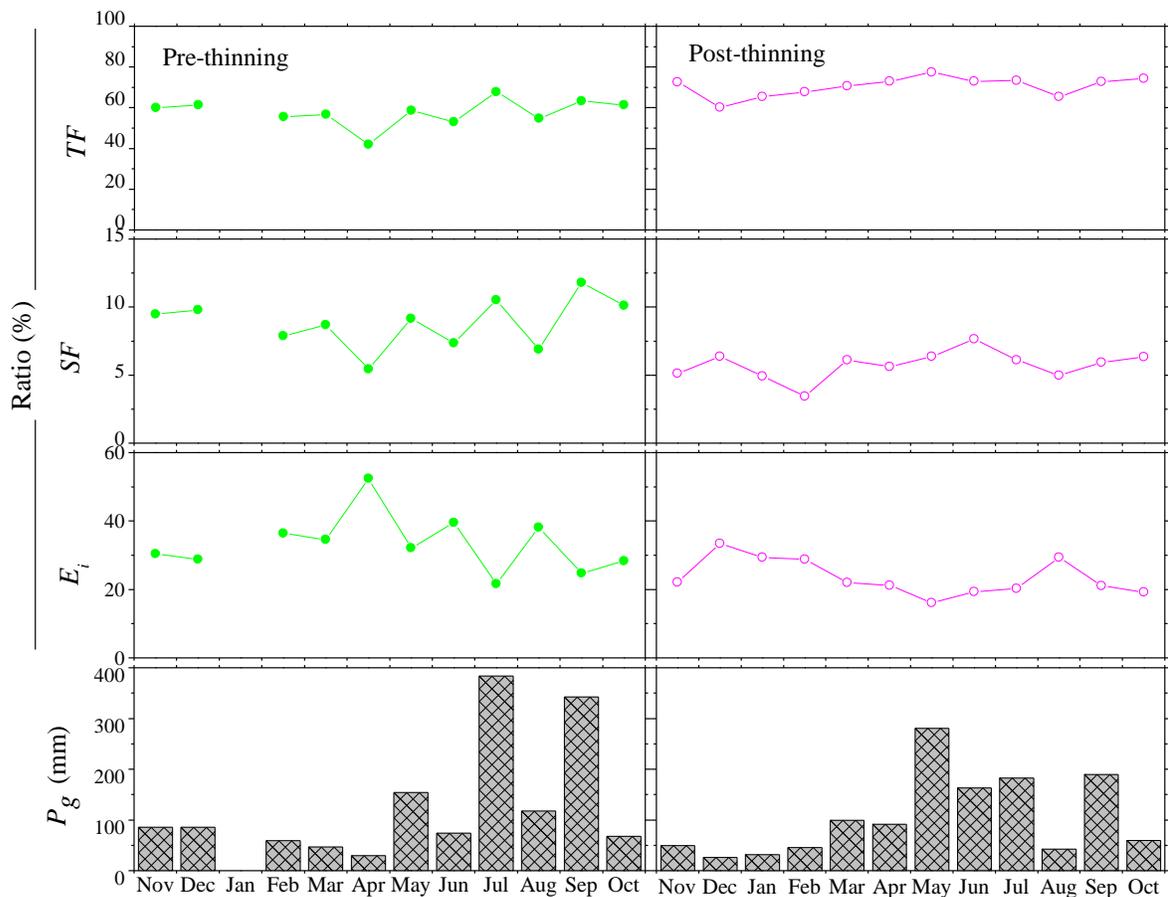
Fig. 4-5 Relationship between gross precipitation (P_g) and canopy water balance (throughfall, *TF*; stemflow, *SF*; canopy interception, E_i) using the month-based rainfall data: pre-thinning period (solid cycles), and post-thinning period (hollow cycles).

Event-based scale: The relationships between event-based P_g and canopy water balance are shown in Fig. 4-6. Event-based P_g ranged from 0.8-176.8 mm with a mean of 17.4±30.6 mm in the pre-thinning period, and from 1.0-150.0 mm with a mean of 12.0±18.8 mm in the post-thinning period. Event-based *TF* ranged from 0.0-125.8 mm with a mean of 10.7±20.9 mm (0.0-76.5% of P_g) in the pre-thinning period, and from 0.0-124.1 mm with a mean of 9.4±15.6 mm (0.0-85.2% of P_g) in the post-thinning period. Event-based *SF* ranged from 0.0-19.7 mm with a mean of 1.7±3.6 mm (0.0-13.1% of P_g) in the pre-thinning period, and from 0.0-13.2 mm with a mean of 0.8±1.7 mm (0.0-10.7% of P_g) in the post-thinning period. Event-based E_i ranged from 0.8-36.6 mm with a mean of 5.0±6.2 mm (18.2-100% of P_g) in the pre-thinning period, and from 0.4-12.7 mm with a mean of 2.7±1.7 mm (8.4-100% of P_g) in the post-thinning period.

Based-event canopy water balance (*TF*, *SF*, and E_i) increased linearly with P_g (Fig. 4-6 a, c, e). The following equations were determined for the linear regressions:

$$TF_{pre} = 0.68P_g - 1.19 \quad (R^2 > 0.99) \quad (4.1)$$

$$TF_{post} = 0.83\,P_g - 1.29 \quad (R^2 > 0.99) \quad (4.2)$$

$$SF_{pre} = 0.12\,P_g - 0.34 \quad (R^2 = 0.99) \quad (4.3)$$

$$SF_{post} = 0.09\,P_g - 0.34 \quad (R^2 = 0.97) \quad (4.4)$$

$$E_{i\,pre} = 0.20\,P_g + 1.52 \quad (R^2 = 0.98) \quad (4.5)$$

$$E_{i\,post} = 0.08\,P_g + 1.61 \quad (R^2 = 0.85) \quad (4.6)$$

where TF_{pre}, SF_{pre}, and $E_{i\,pre}$ represent *TF*, *SF*, and E_i in the pre-thinning period, and TF_{post}, SF_{post}, and $E_{i\,post}$ represent *TF*, *SF*, and E_i in the post-thinning period.
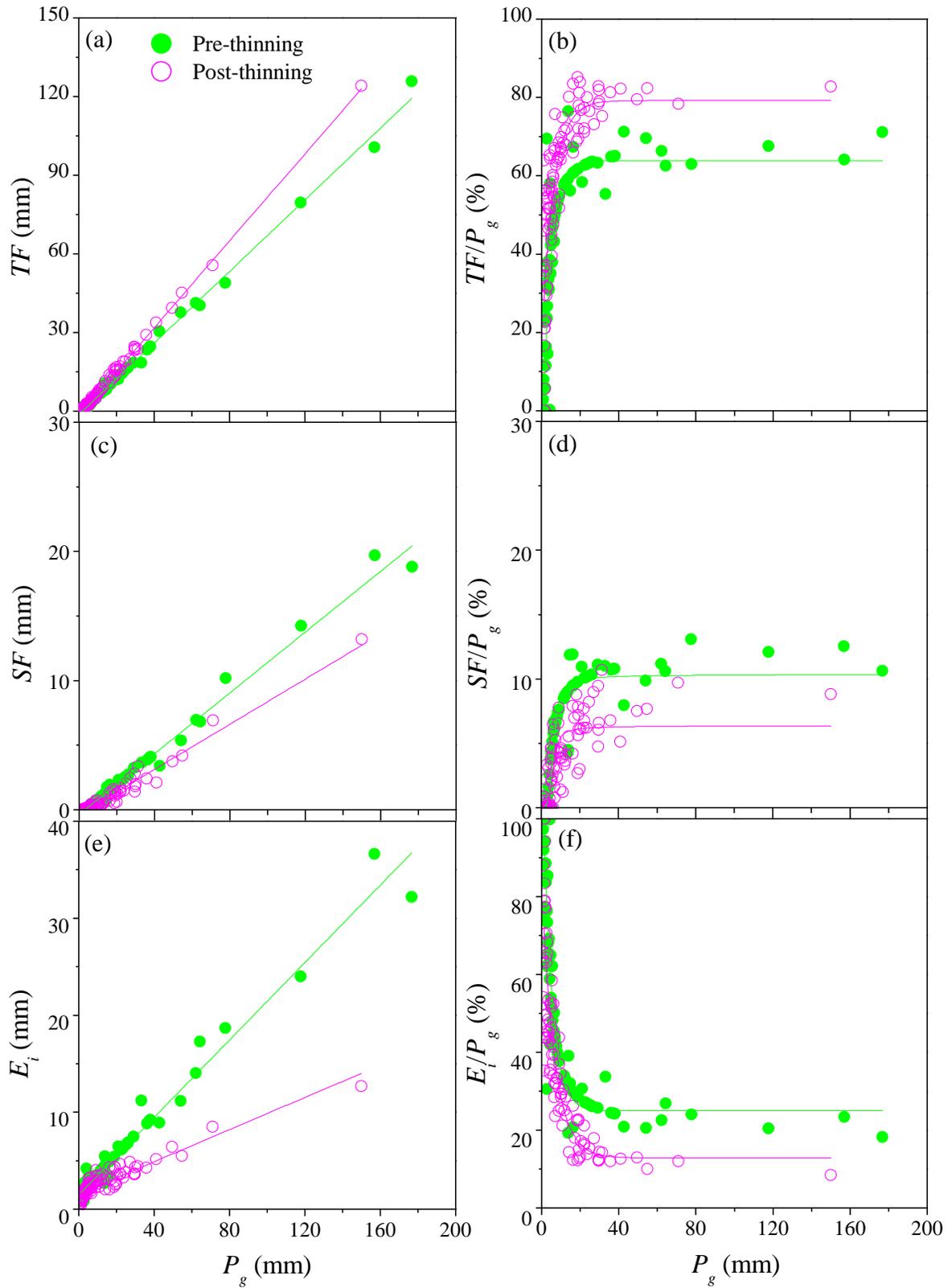
Fig. 4-6 Relationship between gross rainfall (P_g) and canopy water balance using the rainfall event data: pre-thinning period (solid circles), post-thinning period (hollow circles). (a) throughfall (*TF*) amount, (b) ratio of *TF* to P_g, (c) stemflow amount (*SF*), (d) raito of *SF* to P_g, (e) canopy interception amount (E_i), and (f) ratio of E_i to P_g.

The percentages of canopy water balance stabilized with increasing P_g in both periods (Fig. 4-6b, d, f). Table 4-3 shows that mean percentage of canopy water balance to corresponding mean P_g class using event-based data in both periods. The percentages of canopy water balance changed significantly after rainfall depth greater about 10 mm after thinning treatment, and were relatively stable for larger magnitude events with rainfall depth greater than 40 mm in both periods (Fig. 4-7).

Table 4-3 Mean ratio of canopy water balance (throughfall, *TF*; stemflow, *SF*, and canopy interception, E_i) and standard deviation (SD) corresponding to mean gross precipitation (P_g) classified into 14 classes using event-based data in the pre-thinning period and post-thinning periods. Entries indicate that there is no rainfall event in that classification.

No.	Rainfall class	Pre-thinning										Post-thinning								
		Rainfall event	Pg (mm)		*TF/Pg* (%)		*SF/Pg* (%)		E_i/Pg (%)		Rainfall event	Pg (mm)		*TF/Pg* (%)		*SF/Pg* (%)		E_i/Pg (%)	
			Mean	SD	Mean	SD	Mean	SD	Mean	SD		Mean	SD	Mean	SD	Mean	SD	Mean	SD
1	0~2	14	1.2	0.3	1.6	3.7	0.0	0.0	98.4	3.7	15	1.4	0.3	29.0	20.6	0.2	0.3	70.9	20.6
2	2~4	19	2.8	0.6	25.1	13.9	0.2	0.4	74.7	14.0	15	2.7	0.6	41.7	12.0	0.6	1.2	57.7	12.3
3	4~6	8	4.9	0.6	37.9	16.8	2.0	2.2	60.1	17.7	13	4.9	0.6	52.5	7.8	1.9	1.8	45.6	7.0
4	6~8	7	6.9	0.4	49.4	2.9	6.3	0.4	44.3	2.9	11	6.7	0.6	60.4	7.9	3.4	2.1	36.2	8.0
5	8~10	3	8.7	0.5	54.0	0.8	7.4	0.3	38.7	1.1	5	8.9	0.4	60.9	7.0	5.1	2.1	34.0	7.0
6	10~15	8	13.2	1.1	60.1	6.7	8.0	2.5	31.9	5.6	11	11.3	1.4	69.9	4.6	3.7	1.3	26.4	5.4
7	15~20	5	17.0	1.1	62.3	2.9	10.0	1.1	27.7	3.9	9	18.3	1.3	75.4	6.9	6.4	1.9	18.2	5.4
8	20~25	4	22.8	1.4	61.8	2.3	10.3	0.4	27.8	1.9	7	22.1	1.7	76.8	4.4	6.3	1.7	16.2	2.6
9	25~30	2	27.8	2.0	63.4	0.2	10.7	0.5	25.9	0.3	4	29.1	1.2	79.1	4.4	7.3	2.3	13.6	2.8
10	30~40	4	36.3	2.2	62.5	4.8	10.8	0.1	26.6	4.7	3	32.4	3.0	78.5	3.1	8.0	2.3	13.5	1.4
11	40~60	2	48.5	8.1	70.4	1.2	8.9	1.4	20.7	0.2	3	48.5	7.0	81.4	1.6	6.8	1.4	11.9	1.6
12	60~100	3	68.1	8.4	63.9	2.0	11.6	1.3	24.4	2.2	1	71.0	0.0	78.3	0.0	9.7	0.0	12.0	0.0
13	100~150	1	117.8	0.0	67.5	0.0	12.1	0.0	20.4	0.0	-	-	0.0	-	0.0	-	0.0	-	0.0
14	150~200	2	166.9	14.0	67.6	5.0	11.6	1.3	20.8	3.6	1	150.0	0.0	82.8	0.0	8.8	0.0	8.4	0.0
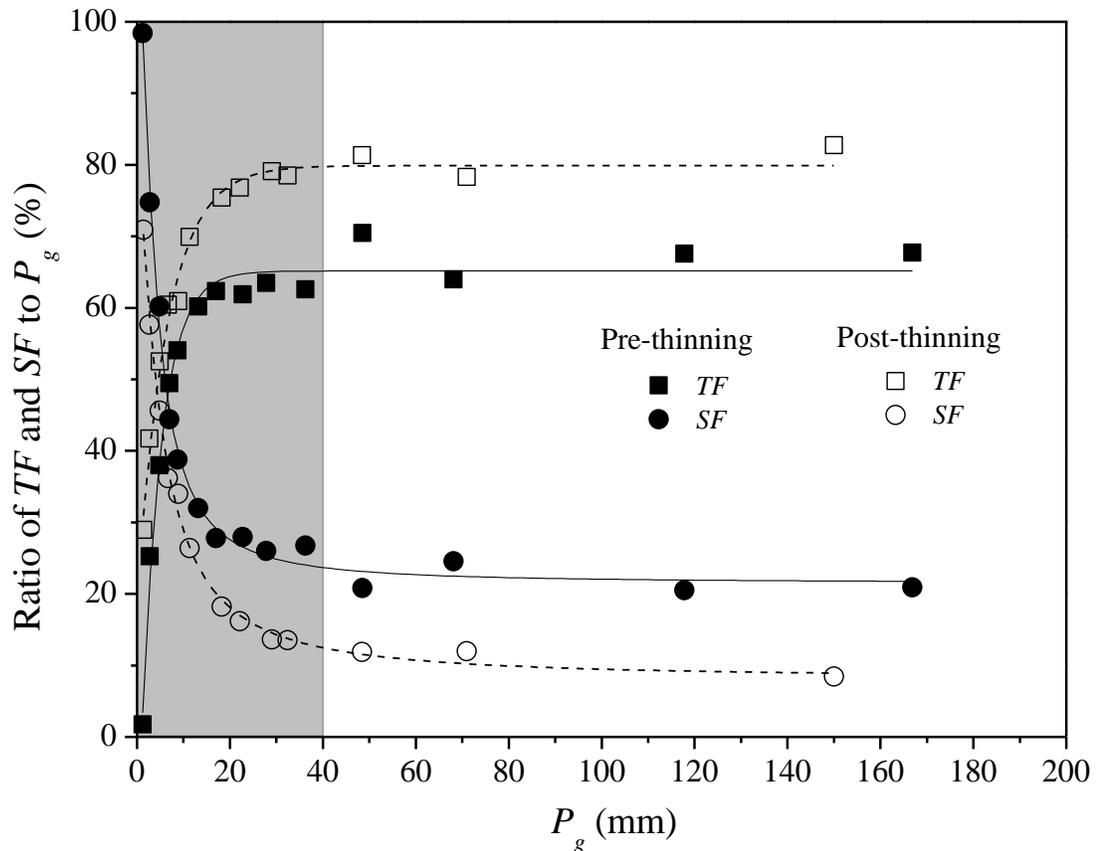
Fig. 4-7 Mean ratio of canopy water balance (throughfall, *TF* and stemflow, *SF*) to corresponding mean gross precipitation (P_g) classified into 14 classes using event-based data in pre-thinning period (solid symbol) and post-thinning period (hollow symbol). P_g was grouped into 14 intervals: 0~2 mm; 2~4 mm; 4~6 mm; 6~8 mm; 8~10 mm; 10~15 mm; 15~20 mm; 20~25 mm; 25~30 mm; 30~40 mm; 40~60 mm; 60~100 mm; 100~150 mm; 150~200 mm. Data were from Table 4-3.

This study elucidated the changes in canopy water balance after heavy strip thinning in a dense and matured stand of Japanese cypress plantation. The thinning experiment (removing 50% of trees) resulted in an increase in *TF* rate and decreases in *SF* rate and E_i rate. For example, at annual-based scale, *TF* rate increased from 61.4-73.0% whereas *SF* decreased from 9.8-6.1%, and E_i decreased from 28.7-20.8% after thinning treatment (Table 4-2, Fig. 4-3). These results support the hypothesis that thinning reduces canopy interception and increases net precipitation (*TF* and *SF*) on the soil surface.

For the abandoned Japanese cypress plantation (i.e., before thinning), the *TF* rate was in the down range (60.1-85%) while the *SF* rate was in the up range (0.3-12.1%) compared with other coniferous forests (Table 3-2). Both *TF* and *SF* were affected by the characteristics of forest structure. For example, *TF* rate is affected by forest cover and branch architecture (Staelens et al., 2006) and decreased with increasing canopy cover (Molina and del Campo, 2012). *SF* rate is greater in denser stands (Huber and Iroume, 2001) and smaller values for horizontal branches (Crockford and Richardson, 2000). Rainfall partitioning by forests plays a crucial role in canopy water balance and thereby on water resources in forested watershed (Crockford and Richardson, 2000; Llorens and Domingo, 2007). The thinning of forest stands alters the forest structures (e.g., canopy cover and basal area), and can be an important and immediate tool to exhibit a strong hydrological function on regulating the redistribution of water resources.

In the present study, thinning caused an increase in water availability in the soil matrix, especially in dry season (Table 4-2). Dung et al. (2012) examined runoff responses to forest thinning (removing 58.3% of trees) at plot and catchment scales in a Japanese cypress plantation. They reported that annual catchment runoff increased significantly (mean: 240.7 mm), yet increases in hillslope plot runoff were not significant. That implies that after thinning, the increased net precipitation directly infiltrated the soil and increased base flow or recharged groundwater. The changes in forest water cycles by thinning contribute to increase low flow discharge in the drought periods and recharge groundwater in the rainy season. Examining changes in various components of the forest water cycle (e.g., E_i, tree transpiration, and runoff) due to forest practices are of important to improve the understanding of processes underling changes in water yield in forested watersheds.

4-2-2 Strip thinning and selective thinning effects on canopy interception

In the present study, the change in E_i rate caused by strip thinning agrees with the simple relationship between stand density and E_i rate in Japanese coniferous forests developed by Komatsu et al. (2007) (Fig. 4-8). The equation is determined based on a summary of 16 earlier observational

E_i studies, and is a useful tool for predicting the influence of forest management on E_i rate in Japanese coniferous plantations. Furthermore, the reduction in E_i rate (27.5%) by strip thinning tended to be smaller than that by selective thinning reported by Nanko et al. (2013), although the thinning of magnitude was similar (Table 4-4, Fig. 4-8). They reported that selective thinning by removing 46% of the trees in a Japanese cypress plantation in Kochi, Japan, resulted in a 208.4 mm decrease in E_i or a 58.2% reduction in E_i rate from 29.9-12.5% (Table 4-4, Fig. 4-8). The reduction in E_i rate caused by selective thinning is approximately twice as that by strip thinning.
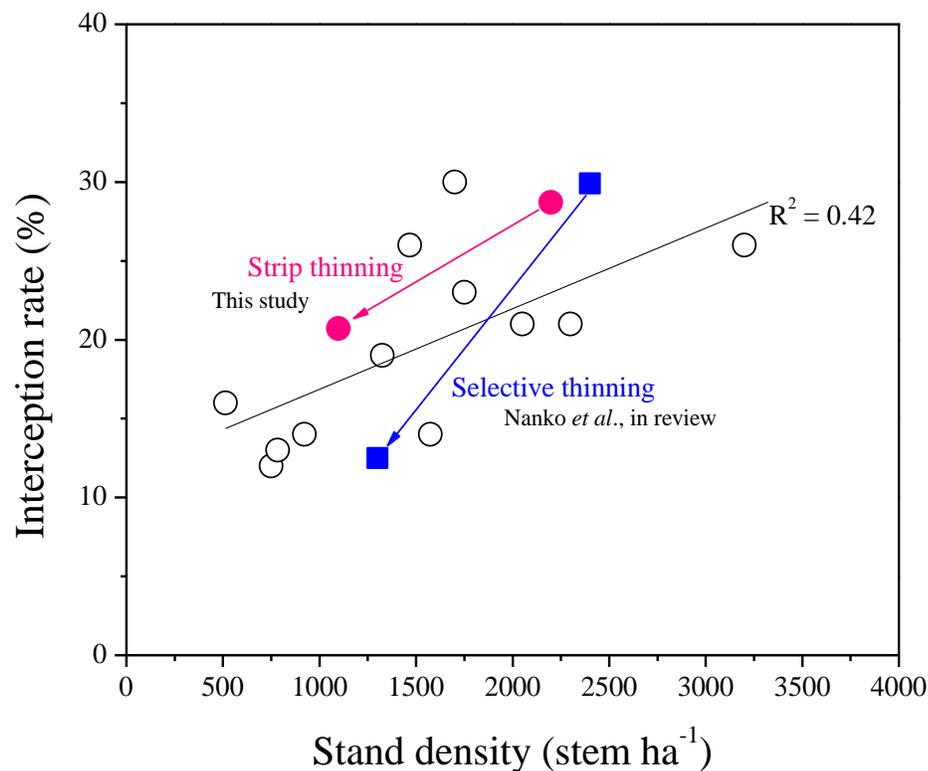
Fig. 4-8 Comparison of strip thinning and selective thinning with a simple relationship between stand density (D, stem ha^{-1}) and interception rate (E_i, %) in coniferous forests in Japan developed by Komatsu et al. (2007). The linear equation was expressed as: E_i (%) = 0.00498 D + 12 (500<D<3000), R^2 = 0.42.

The differences between strip thinning and selective thinning may be related to the changes in forest canopy cover. Although both thinning ways removed about 50% of trees in a catchment, selective thinning caused a 30.2% decrease in canopy cover from 85.5-59.7% (Nanko et al., 2013) while strip thinning caused a 22.2% decrease in canopy cover from 97.4-75.8% (Table 2-1, Fig. 4-8). The decrease in canopy cover caused by strip thinning is smaller than that by selective thinning. The E_i is determined by forest structural parameters (forest density, canopy structure, and leaf area index) (Deguchi et al., 2006; Komatsu et al., 2007). The two thinning methods caused different changes in forest structures. Strip thinning only caused the canopy cover at corridors change while selective thinning resulted in the whole canopy cover of forest stand change. Therefore, the resultant changes in E_i rate may differ between strip thinning and selective thinning. This study is one of case studies on the influence of strip thinning on E_i. In the future, it is important to accumulate data related to changes in canopy water balance caused by thinning, especially strip thinning, to require an integrated understanding of the effects of management practices in forest watersheds.

4-2-3 Interception response to thinning ratio and gross precipitation

The reduction in E_i rate (27.5%) obtained in this study also agrees with previous literatures on thinning effects on E_i (Table 4-4). For example, Limousin et al. (2008) reported a 34.6% reduction in E_i after 47% thinning in *Quercus ilex* forest in southern France. (Whitehead and Kelliher, 1991) reported a 27.2% reduction in E_i after 56% thinning in *Pinus radiate* forest in New Zealand. The degree of decline in E_i loss/rate after thinning may be related to gross precipitation and ratio of thinning (Fig. 4-9a, b). The decrease in E_i loss with gross precipitation > 1000 mm was significantly larger than that with gross precipitation < 1000 mm (Fig. 4-9a). For example, Breda et al. (1995) reported a 45.5 mm decrease of E_i after 23% thinning for 650 mm of annual P_g while for 1245 mm of annual P_g, Sado and Kurita (2004) observed a 83.4 mm decrease in annual E_i after 21% of the stems removal. This pattern suggested that areas with more annual precipitation appear to have greater decrease in E_i after thinning treatment compared to areas with less precipitation.
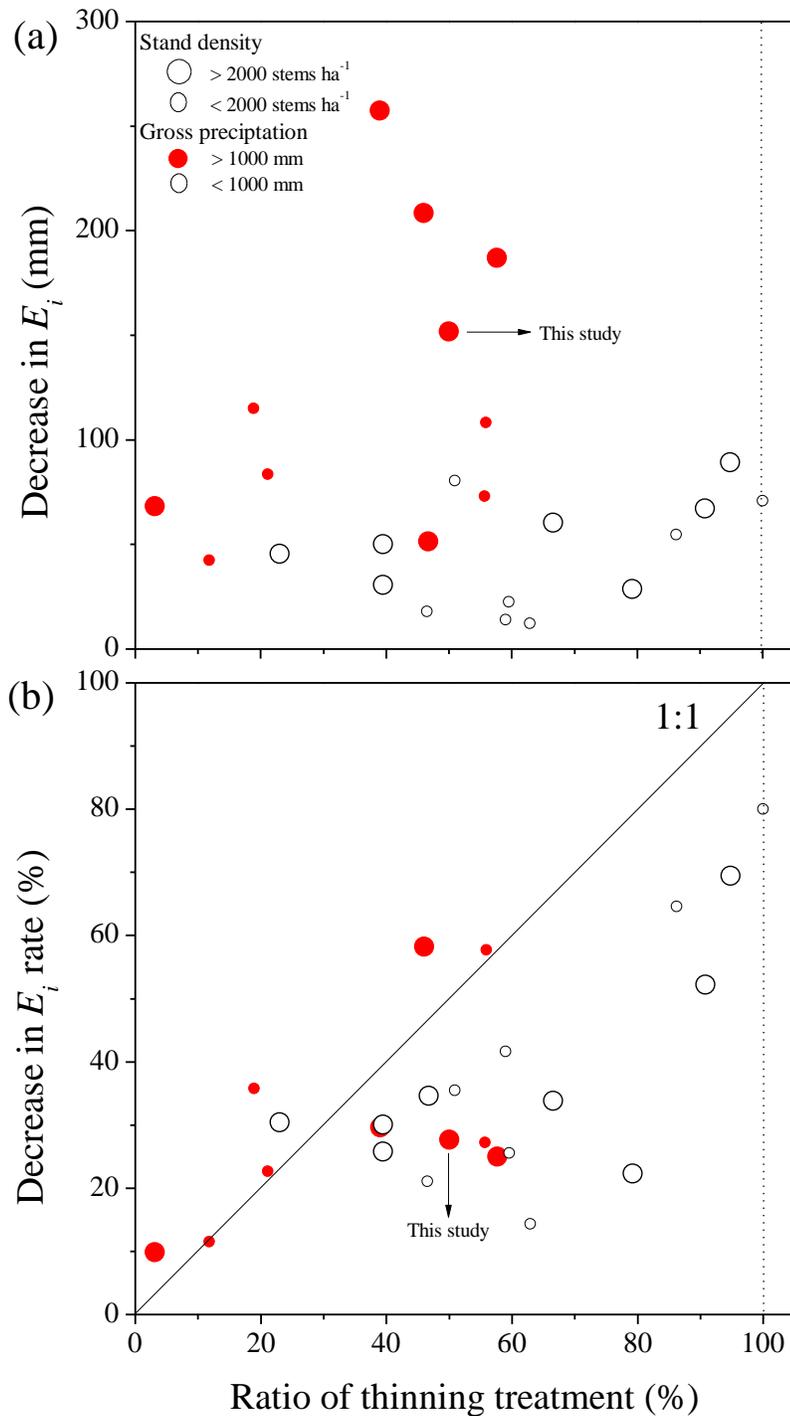
Fig. 4-9 The relationship between (a) ratio of thinning treatment and canopy interception (E_i) decrease (mm) and (b) ratio of thinning treatment and decrease in E_i rate in the present study and previous studies (data were from Table 4-4). Ratio of thinning treatment was selected based on ratio of stem removal because basal area cannot be found in some previous studies.

In addition, the degree of decline in E_i rate may be also related to the amount of biomass removed (Table 4-4, Fig. 4-9b). For thinning ratio < 30%, the decrease in E_i rate is proportional or more than the removal of biomass. For example, Sado and Kurita (2004) reported that the observed reduction in E_i rate (11.5% and 22.6%, respectively) was proportional to the removal of the stems (12% and 21%, respectively) (corresponding to 29.3% and 27.8% of the basal area, respectively) in a *Chamaecyparis obtusa* forest in Japan. In addition, the observed reduction in E_i rate (35.8%) was larger than the removal of the stems (19%) in a *Pinus densiflora* forest in Japan (Hattori and Chikaarashi, 1988). However, for thinning ratio > 30%, the decrease in E_i rate was usually lower than the removal of the stems. For instant, after removing 67% of the stems (corresponding to 42.5% of the basal area) with respect to control-plot value in a *Pinus densiflora* forest in Japan, the observed decline in E_i rate was 33.8% (Murai, 1970). In a *Pinus radiata* forest in Yass catchment, Australia, removing 59% of the stems (corresponding to 50.4% of the basal area) with respect to pre-thinning value resulted in a 41.6% decrease in E_i (Crockford and Richardson, 1990).

The changes in E_i are affected by thinning ratio/method and P_g. Thus there should be an optimum value of reduction of the stems (or the basal area) to attain a significant decrease in E_i and increase in water yield. The results with summarizing from previous studies can be used for researchers to get a general understanding to manage and implement hydrology-based silviculture. This study only examined the changes in canopy water balance after one-year thinning. Thinning will increase the growth of remained individual trees due to apportion a higher availability of site resources (e.g., soil water and solar radiation). The canopy closure fraction will also increase each year into to the future and this will lead to the changes in rainfall partitioning. In the future, temporal changes in canopy water balance after thinning are required to evaluate the effects of forest management on water resources of forested watersheds.

Table 4- 4 Literatures about thinning effects on canopy interception

Reference	Location	Species	Treatment	Ratio of thinning (%)	Stand density (Stem ha⁻¹)	Basal area (m² ha⁻¹)	Height (m)	DBH (cm)	LAI	P_g (mm)	E_i (mm)	E_i/P_g (%)	Decrease in E_i (mm)	Decrease ratio in E_i (%)
This study	Tochi, Japan	*Chamaecyparis obtusa*	Unthinned		2198	50.4	16	19	-	1445	414.8	28.7		
			Strip thinned	50	1099	26.2	16	19	-	1267	263.0	20.8	151.8	27.7
Nanko et al., under review	Kochi, Japan	*Chamaecyparis obtusa*	Unthinned		2400	-	18	25	-	1007	301.0	29.9		
			Thinned	46	1300	-	-	25	-	741	92.6	12.5	208.4	58.2
Hattori and Chikaarashi, 1988	Ibaraki, Japan	*Chamaecyparis obtusa*	Unthinned 1st Yr		1750	-	14	18	5.7	1543	328.9	21.3		
			Unthinned 2st Yr		1750	-	14	18	5.7	1336	312.9	23.4		
			Thinned	19	1325	-	-	-	-	1087	205.9	18.9	115[a]	35.8[a]
Sado and Kurita, 2004	Yamaguchi, Japan	*Chamaecyparis obtusa*	Control		1836	79.2	19	23	-	1245	368.6	29.6		
			Thinned Plot 1	12	1440	56.0	17	22	-	1245	326.3	26.2	42.3	11.5
			Thinned Plot 2	21	1487	57.2	17	22	-	1245	285.2	22.9	83.4	22.6
Linousin et al., 2008	Puechabon state forest, France	*Quercus ilex*	Unthinned		5564	-	-	-	3.1	909	280.9	30.9		
			Thinned	47	2964	-	-	-	1.6	1136	229.5	20.2	51.4	34.6
Teklehaimanot et al., 1991	Cloich, Edinburgh	*Picea sitchensis*	Unthinned (spaced 2m)		3000	53.9	10	15	-	442	128.6	29.1		
			Tree spacing 4m	79	625	11.7	10	15	-	442	99.8	22.6	28.7	22.3
			Tree spacing 6m	91	277	5.0	10	15	-	442	61.4	13.9	67.2	52.2
			Tree spacing 8m	95	156	3.1	10	15	-	442	39.3	8.9	89.2	69.4
Molina and del Campo, 2012	Valencia Province, Spain	*Pinus halepensis*	Control		1289	35.6	-	-	2.6	179	84.8	47.4		
			Low thinned	47	689	26.3	-	-	1.9	179	66.9	37.4	17.9	21.1
			Moderate thinned	63	478	20.9	-	-	1.5	179	72.7	40.6	12.2	14.3
			Heavy thinned	86	178	8.3	-	-	0.5	179	30.1	16.8	54.8	64.6
Mazza et al., 2011	Castel Fusano pinewood, Italy	*Pinus pinea*	Control		483	38.3	18	-	5.1	1030	187.5	18.2		
			Thinned	56	213	21.2	18	-	1.9	1030	79.3	7.7	108.2[b]	57.7[b]
Crockford and Richardson, 1990	Yass catchment, Australia	*Pinus radiata*	Control		560	40.8	18	-	5.4	855	226.6	26.5		
			Thinned	51	275	23.3	18	-	3.0	855	146.2	17.1	80.4[c]	35.5[c]
			Unthinned		1708	35.1	10	16	-	164	34.3	20.9		
			Thinned	59	700	17.4	-	-	-	166	20.3	12.2	14.0	41.6
Whitehead and Kelliher, 1991	Longmile, New Zealand	*Pinus radiata*	Unthinned		754	-	17	-	4.9	1623	268.0[a]	16.5		
			Thinned	56	334	-	-	21	2.9	1623	195.0[a]	12.0	73.0	27.2

Table 4-4 (continued)

Murai and Kumagai, 1989	Shizuoka, Japan	*Pinus densiflora*	Plot 1 Unthinned		3326	-	-	-	3116	691.8	22.2		
			Thinned	3	3222	-	-	-	2847	623.5	21.9	68.3	9.9
			Plot 2 Unthinned		3896	-	9	12	3116	869.4	27.9		
			Thinned	39	2376	64.9	9	15	2847	612.1	21.5	257.3	29.6
			Plot 3 Unthinned		3810	-	8	14	3116	747.8	24.0		
			Thinned	58	1614	59.4	8	11	2847	560.9	19.7	187.0	25.0
Murai, 1970	Iwate, Japan	*Pinus densiflora*	Control		2373	26.6	13	15	874	178.3	20.4		
			Thinned	67	793	15.3	10	11	874	118.0	13.5	60.3	33.8
Aussenac and Granier, 1988	Northeastern France	*Pseudotsuga menziessii*	Control		2392	39.3	-	-	384	166.4	43.3		
			Strip thinned	40	1447	19.9	-	-	384	116.5	30.3	50.0	30.0
	France		Control		2392	39.3	-	-	384	118.5	31.0		
			Strip thinned	40	1447	19.9	-	-	382	87.9	23.0	30.6[d]	25.8[d]
Breda et al., 1995	Champenous Forest, France	*Quercus petraea*	Unthinned		3998	27.3	-	9	650	149.5	23.0		
			Thinned	23	3077	17.6	-	8	650	104.0	16.0	45.5	30.4
Ganatsios et al., 2010	Taxiarhis university forest, Greece	*Quercus frainetto*	Control		1368	21.8	15	-	983	88.5	9.0		
			Thinned	60	553	14.8	15	-	983	65.9	6.7	22.6	25.6
			Clear-cutting	100	0	0.0	-	-	983	17.7	1.8	70.8	80.0

a Calculated as the mean value of E_i before thinning minus the value after thinning. b measured following thinning. c measured after 5-year thinning. d measured after 2-year thinning.

4-2-4 Summary

This section quantified the effect of strip thinning on gross precipitation (P_g) partitioning into throughfall (*TF*), stemflow (*SF*) and canopy interception (E_i) at various time scales (e.g., annual, season, month, and event) in a Japanese cypress plantation. The results indicated that (1) strip thinning caused annual *TF* rate to increase (from 61.4-73.0%) whereas annual *SF* rate (from 9.8-6.1%) and E_i rate (from 28.7-20.8%) to decrease; (2) strip thinning caused net precipitation (*TF* and *SF*) rate to increase by 11.1%, which increased the water availability in the soil matrix, especially in dry season; (3) the reduction in E_i rate (27.5%) by strip thinning tended to be smaller than that by selective thinning, which may be induced by the changes in forest canopy cover; (4) by summarizing the findings of previous studies, it appears that the degree of decline in E_i loss/rate caused by thinning was related to P_g and ratio of thinning. This work provides useful information for researchers to forecast the effects of land use and cover change on water resources in forested watersheds. These results with summarizing from previous studies can also be used for researchers to get a general understanding to manage and implement hydrology-based silviculture. In addition, it is important to collect data related to the changes in E_i under different thinning methods to achieve an integrated understanding of watershed water balance and best management practice.

4-3 The effect of strip thinning on tree transpiration

4-3-1 Sapwood area estimates in pre- and post-thinning

A_{s_stand} in the pre-thinning period was 26.1 m^2 ha^{-1} and decreased 46.4% after thinning (Table 2-1). The sapwood area at xylem bands of 0-20 and 20-40 mm before and after thinning are also shown in Table 2-1. Fig. 4-10 shows the relations between DBH and A_{S_tree} in the pre- and post-thinning periods (DBH and A_{S_tree} were measured in/around the observation plot, with 44 trees were selected before thinning, and 18 trees were left after thinning). The A_{S_tree} in the pre-thinning period ranged from 57.7 to 229.6 cm^2 with a mean of 150.8 cm^2, and ranged from 71.9 to 223.1 m^2 with a mean of 155.5 cm^2 in the post-thinning period. Power functions of DBH were fitted to A_{S_tree} using linear regression analysis. The R^2 values were 0.83 for both the pre- and post-thinning periods.

A_{s_stand} in this study decreased by 46.4% after 50% thinning (Table 2-1). The sapwood area at xylem bands of 0-20 and 20-40 mm also showed similar trends and declined by 47.5% and by 44.0%, respectively (Table 2-1). The decline of A_{s_stand} corresponded to the ratio to thinning. A linear relation between DBH and $A_{S\text{-}tree}$ was found for Japanese cypress plantations (Fig. 4-10). Although several studies estimated the $A_{s\text{-}tree}$ from a power function-based regression (Kumagai et al., 2007; Vertessy et al., 1995; Wullschleger and King, 2000), this regression did not drastically heighten the relation between DBH and A_{S_tree} because individuals with a DBH were larger than approximately 0.1 m in this study plot (Fig. 4-10). Kume et al. (2010) reported that there was no significant change between the measured and estimated A_{S_tree} using the linear relationship between DBH and A_{S_tree} from 58 Japanese cypress trees. A linear relationship was also produced from an allometric data set on 1226 Japanese cypress plantations (Kumagai et al., 2005c). These findings can be used to estimate A_{S_tree} according to the allometric data (DBH) and then to obtain A_{s_stand} for Japanese cypress plantations.
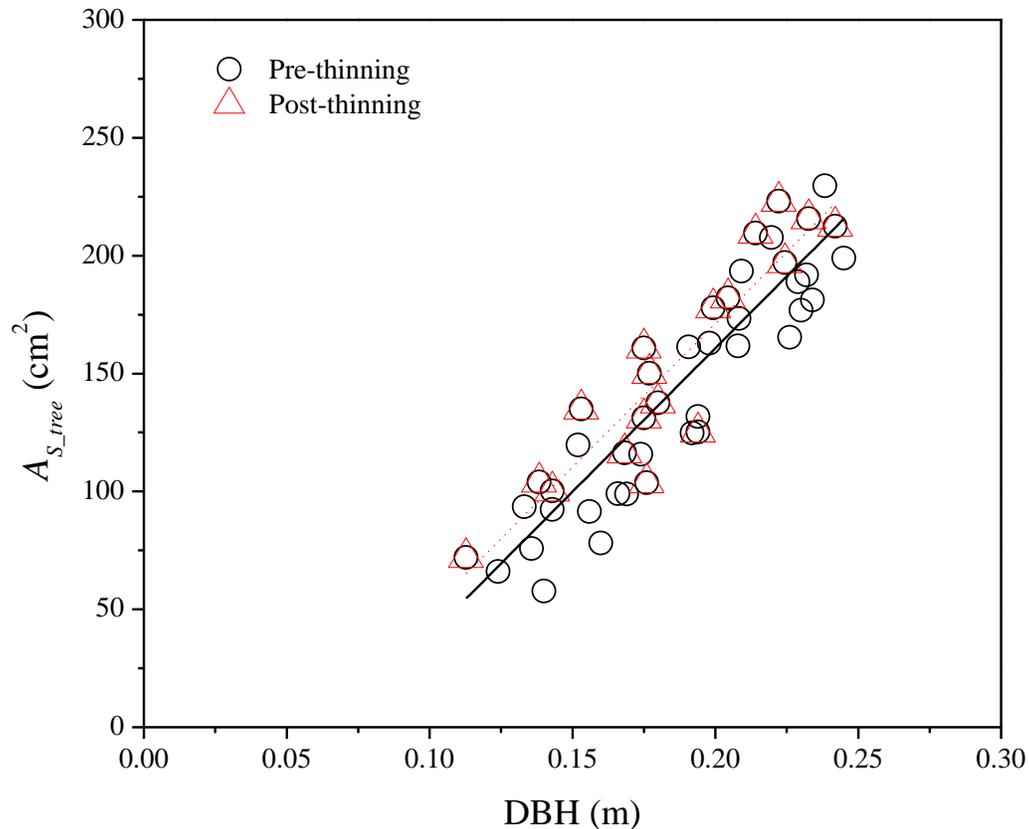
Fig. 4-10 Stem diameters at breast height (DBH) versus tree sapwood area (A_{S_tree}) for 44 Japanese cypress trees in the pre-thinning and 18 Japanese cypress trees in the post-thinning. The trees are selected in/around the study plot; the overlapped scatters indicate the trees were not felled after thinning. Black line represents regression equation derived in the pre-thinning ($y = 1218.4\ x - 82.9$ ($R^2 = 0.83$)). Dotted line represents regression equation generated after thinning ($y = 1215.5\ x - 72.0$ ($R^2 = 0.83$)).

4-3-2 Changes in sapflow density

Fig. 4-11 shows the diurnal courses in F_d at depths of 0-20 (outer xylem) and 20-40 mm (inner xylem) in the three tree classes (large, medium and small) (Table 4-5), with the R_s and *VPD* values on given days without rain (Aug 9, 2011 and Aug 9, 2012) representing the pre- and post-thinning days, respectively. The R_s values were 18.3 and 17.5 MJ m^{-2}, and *VPD* values were 1.2 and 1.3 kPa on August 9 in 2011 and 2012, respectively. There was a pronounced diurnal hysteresis

between R_s and VPD (2-3 h between the peaks). The climatic conditions are considered to be similar on these two days, with a moderate atmospheric evaporative demand. The dynamics of the F_d reflected R_s and VPD values; however, the F_d at the outer xylem was more sensitive to climatic conditions in the post-thinning day compared with the pre-thinning day. For example, the F_d decreased sharply when the VPD declined suddenly on August 9, 2012. However, the F_d slightly changed when the VPD decreased abruptly on August 9, 2011.

Furthermore, the F_d decreased with an increase in the measurement depth. In addition, the F_d at the outer xylem obviously increased in the three tree classes, particularly in the small tree class, whereas the F_d at the inner xylem did not significantly change after thinning (Fig. 4-11). The maximum F_d (outer xylem + inner xylem) of the three classes (large, medium and small) increased from 47.15 to 60.41 cm^3 m^{-2} s^{-1}, from 48.25 to 57.70 cm^3 m^{-2} s^{-1} and from 20.91 to 36.88 cm^3 m^{-2} s^{-1}, respectively. In addition, the daily F_d of the three classes increased by 20.2 ± 0.5%, reaching 1040.24 cm^3 m^{-2} d^{-1}, by 19.9 ± 0.4%, reaching 990.86 cm^3 m^{-2} d^{-1}, and by 92.2 ± 2.1%, reaching 610.37 cm^3 m^{-2} d^{-1}, respectively.

Table 4-5 Number (n) and mean diameter at 1.3 m aboveground (1 SE) of sampled Japanese cypress trees for each size class.

	Pre-thinning		Post-thinning	
Size class	n	DBH (mm)	n	DBH (mm)
Small	3	16.4 (0.5)	2	16.7 (0.3)
Medium	3	19.3 (0.7)	2	19.7 (0.5)
Large	4	22.1 (1.0)	2	21.7 (0.9)
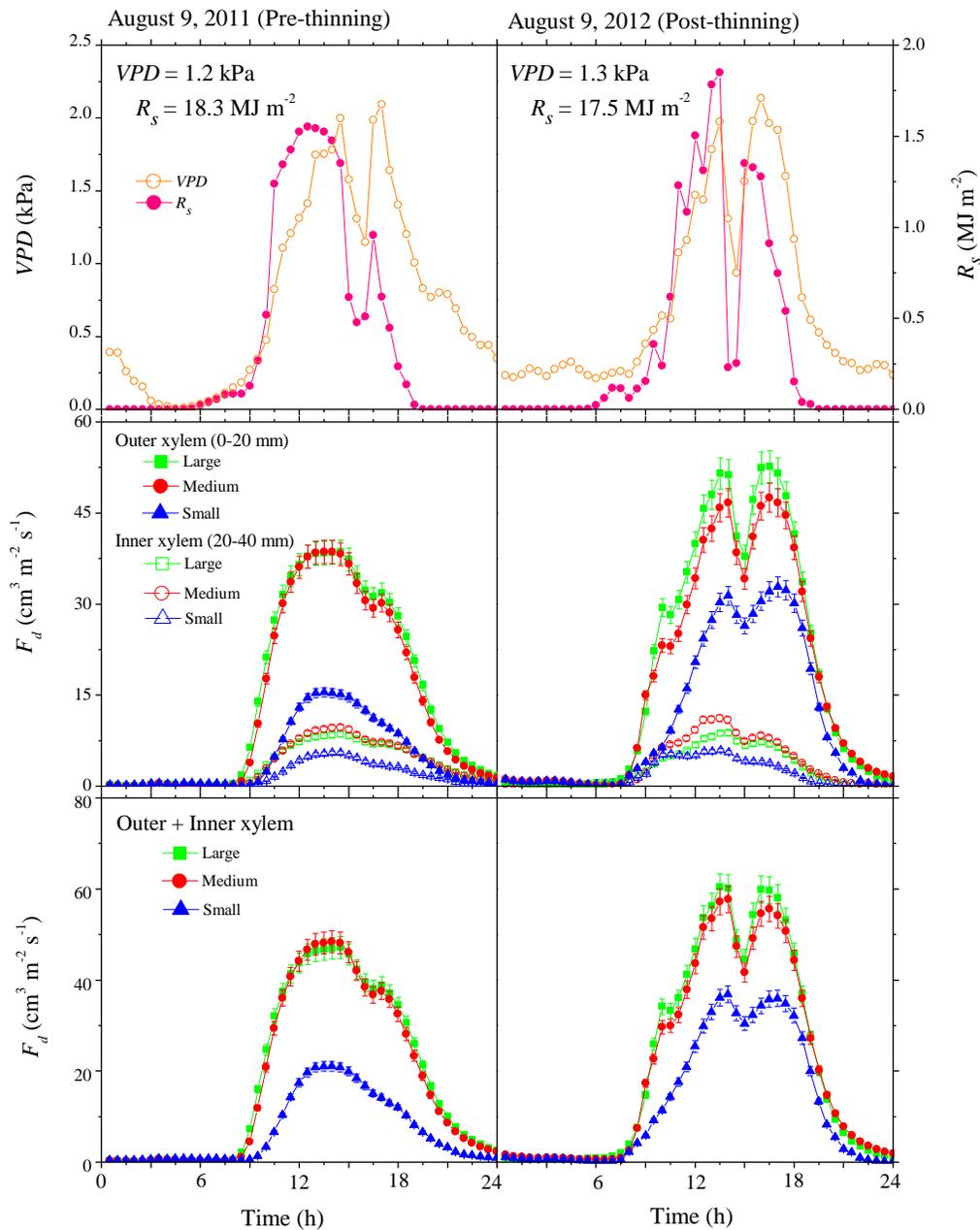
Fig. 4-11 Half-hourly patterns of sap flux density (F_d) in two depth categories (outer xylem: 0-20 mm, and inner xylem: 20-40 mm) and three tree size classes (large, medium and small) on August 9, 2011 (pre-thinning) and on August 9, 2012 (post-thinning). Climatic conditions (e.g., vapor pressure deficit (VPD) and solar radiation (R_s)) are also shown. Vertical bars represent standard deviation (SD). (see Table 4-5 for the number of each tree class).
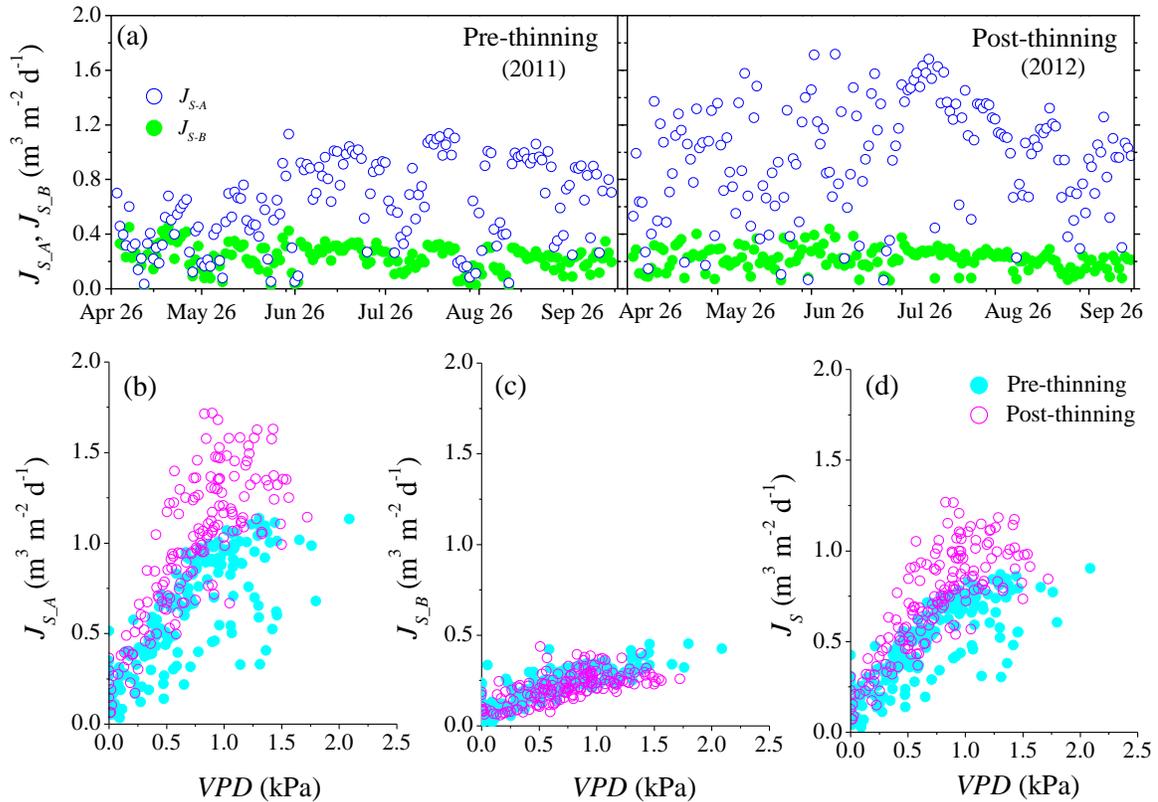
Fig. 4-12 (a)Time series of mean daily sap flux densities for xylem bands 0-20 (J_{S_A}) and 20-40 mm (J_{S_B}), (b) relation between mean daily daytime vapor pressure deficit (*VPD*) and J_{S_A}, J_{S_B} (c) for all measured Japanese cypress trees, and (d) stand sap flux density (J_S) during the growing season in the pre-thinning period (April 28 – October 10, 2011) and the post-thinning period (April 28 – October 10, 2012).

Daily J_{S_A} and J_{S_B} values with tree-to-tree variations in the pre- and post-thinning period during the growing season are shown in Fig. 4-12a. The mean stand F_d measured at radial depths of 0-20 and 20-40 mm consistently decreased with depth over both periods and varied with meteorological conditions (e.g., *VPD* and R_s). During the rainy period (e.g., May 22-29, 2011), the sap flow was appreciably reduced due to the low *VPD* and R_s.

The J_{S_A} values were higher in the post-thinning period than in the pre-thinning periods (*P*<0.01: Mann-Whitney U test), and the differences significantly increased with increasing *VPD* (Fig. 4-12b). The daily J_{S_A} values ranged from 0.03 to 1.26 m^3 m^{-2} d^{-1}, with a mean of 0.62 ± 0.31

m^3 m^{-2} d^{-1} in the pre-thinning period, and ranged from 0.06 to 1.72 m^3 m^{-2} d^{-1}, with a mean of 0.97 $\pm$

0.40 m^3 m^{-2} d^{-1}, in the post-thinning period. However, unlike the J_{S_A} values, the J_{S_B} values had no

significant differences between the two periods ($P>0.05$: Mann-Whitney U test) (Fig. 4-12c). The

daily J_{S_B} values ranged from 0.02 to 0.58 m^3 m^{-2} d^{-1}, with a mean of 0.23 $\pm$ 0.10 m^3 m^{-2} d^{-1} in the

pre-thinning period, and ranged from 0.06 to 0.44 m^3 m^{-2} d^{-1}, with a mean of 0.22 $\pm$ 0.08 m^3 m^{-2} d^{-1},

in the post-thinning period. The changes in J_S values reflected a similar trend compared with the J_{S_A}

values and were higher in the post-thinning period than in the pre-thinning period ($P<0.05$: Mann-

Whitney U test). The differences significantly increased with increasing VPD (Fig. 4-12d). The

daily J_S values averaged over the growing season were 0.50 $\pm$ 0.23 m^3 m^{-2} d^{-1}, ranging from 0.03 to

1.00 m^3 m^{-2} d^{-1}, in the pre-thinning period, whereas the daily J_S values were 0.71 $\pm$ 0.29 m^3 m^{-2} d^{-1},

ranging from 0.07 to 1.27 m^3 m^{-2} d^{-1}, in the post-thinning period.

Radial patterns in the F_d declined with depth (Fig. 4-11, 4-126a), which have often been

investigated in different species (e.g., Kumagai et al., 2005b; Oren et al., 1999; Phillips et al., 1996),

indicating that xylem conductivity decreases quickly with radial depth. The F_d at the outer xylem

significantly increased, whereas the F_d at the inner xylem did not significantly change after thinning

(Fig.4-11, 4-12b, c). This result indicates that thinning only enhanced the capacity of conducting

water at the outer xylem. Furthermore, the effect of tree classes (Large, medium and small) on the

F_d showed that the F_d for the three tree classes increased significantly after thinning, particularly for

the small class. The differences in the F_d between small trees and dominant trees were reduced due

to the thinning treatment (Fig. 4-11). The transpiration rate (i.e., the physical process of water

vaporization) is mostly determined by the amount of available solar radiation above the canopy

(Gebauer et al., 2011). For example, in a fully closed Norway canopy, the uppermost 10% of needle

biomass intercepted as much as 50% of the incoming solar radiation (Kucera et al., 2002). The

higher radiation interception in the upper canopy in turn results in higher transpiration (Moren et al.,

2000). Indeed, the F_d was related to the tree class, and co-dominant trees exhibited a lower F_d in

Eperua falcata forest (Granier et al., 1996c). In this study, the high stand density (2198 tree ha^{-1}) caused an almost fully closed canopy cover (canopy cover fraction: 0.974); thus, the small trees were partly shaded by dominant trees and experienced lower light before thinning. However, after 50% thinning, solar radiation can penetrate deeper into the lower crowns. Therefore, small trees were able to receive more irradiance, and F_d largely increased.

The dynamic of F_d was more sensitive to climatic variables (e.g., *VPD* and R_s) after thinning, and the differences in J_S were significantly higher with increasing *VPD* in the post-thinning (Fig. 4-11, 4-12d). This result suggests a higher influence of climatic factors on J_S after thinning. In this study, we did not consider the effect of soil water content on J_S because P_g was higher than PET during both periods, and thus, the soil-water competition among trees is not severe. This finding is similar to previous studies (Komatsu et al., 2006; Komatsu et al., 2012; Kumagai et al., 2008; Morikawa et al., 1986), who reported soil water deficit had little or no effect on the examination of E_t and evapotranspiration in Japan.

4-3-3 Canopy conductance response to thinning

Fig. 4-13 shows the relations between *VPD* and G_c for the Japanese cypress forest during the growing season in pre- and post-thinning period, respectively. the mean daily daytime *VPD* and G_c for the Japanese cypress forest during the growing season in pre- and post-thinning periods, respectively. The G_c was 0.0031 ± 0.0035 m s^{-1} in the pre-thinning period, whereas the G_c was 0.0021 ± 0.0017 m s^{-1} in the post-thinning period. We observed significantly ($P<0.01$) negative correlations in both periods; thus, the G_c values were modeled before and after thinning, respectively, as:

$$G_c = 0.0021 - 0.001\ln(VPD) \quad R^2 = 0.51 \qquad (4.7)$$

$$G_c = 0.0016 - 0.001\ln(VPD) \quad R^2 = 0.54 \qquad (4.8)$$
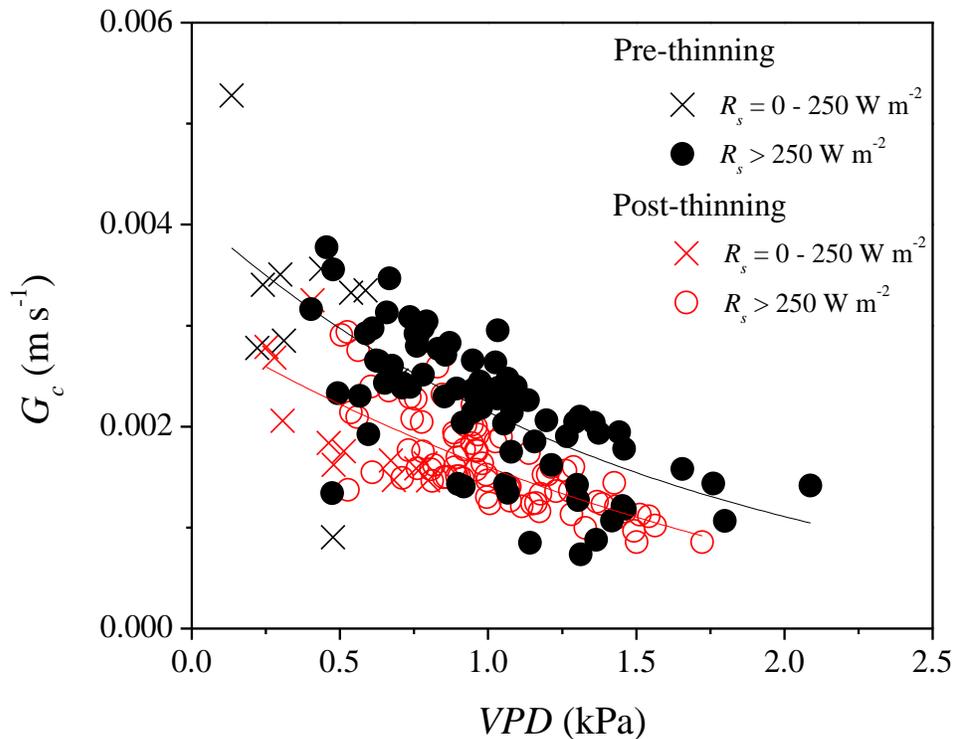
Fig. 4-13 Relations between the mean daily daytime vapor pressure deficit (VPD) and canopy conductance (G_c) for Japanese cypress forests during the growing season (April 28 – October 10) in the pre-thinning period (solid circle) and the post-thinning period (white circle). The data are classified according to solar radiation (R_s). The solid lines are the regression lines, which were determined by the least-squares method for all data, representing the pre- and post-thinning periods, respectively.

In this study, the G_c significantly decreased after thinning (Fig. 4-13). G_c expresses the physiological control of E_t (Kelliher et al., 1995; Raupach, 1995) and affects the transpiration rates of forest canopies (Jarvis and Mcnaughton, 1986; Kelliher et al., 1993; Komatsu, 2004). G_c also strongly correlates with canopy photosynthesis rates (Lai et al., 2000; Law et al., 2001b). Therefore, the low G_c after thinning implies lower E_t and photosynthesis, and thus, possible changes in terrestrial water and carbon cycles due to thinning treatment.

4-3-4 Changes in single tree transpiration
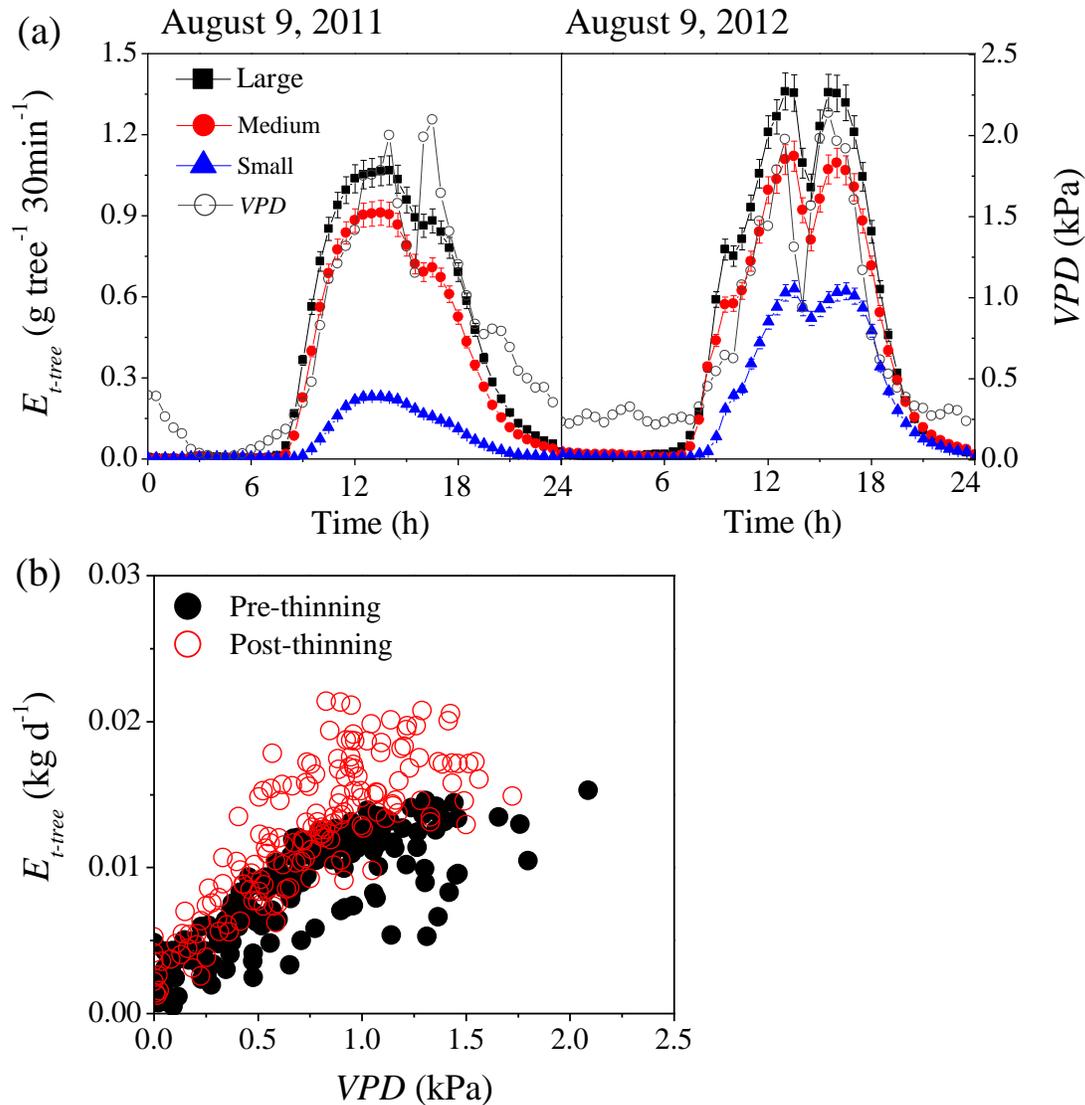
Fig. 4-14 (a) Half-hourly patterns of tree transpiration (E_{t-tree}) in three tree size classes (large, medium and small) and vapor pressure deficit (*VPD*) on August 9, 2011 (pre-thinning) and on August 9, 2012 (post-thinning). Vertical bars represent the standard deviation (SD). (see Table 4-5 for the number of each tree class). (b) Mean daily E_{t-tree} averaged by all measured Japanese cypress trees using the Granier method response to the mean daily daytime *VPD* in the pre- and post-thinning periods during the growing season (April 28 – October 10).

The diurnal courses in E_{t-tree} in the three tree classes (large, medium and small) under given similar climatic conditions without rain on Aug 9, 2011 and Aug 9, 2012 are shown in Fig. 4-14a. E_{t-tree} correlated with tree sizes and was smallest in the small tree class on both days. Furthermore, E_{t-tree} increased after thinning. The maximum half-hourly E_{t-tree} in the three classes increased from 1.0689 to 1.3605 g tree^{-1} 30 min^{-1}, from 0.9115 to 1.1212 g tree^{-1} 30 min^{-1}, and from 0.2312 to 0.6292 g tree^{-1} 30 min^{-1}, respectively. The daily E_{t-tree} in the three classes increased by 20.1%, reaching 0.023 kg d^{-1}, by 24.2%, reaching 0.019 kg d^{-1}, and by 195.1%, reaching 0.010 kg d^{-1}, respectively. In particularly, the daily E_{t-tree} in the small class significantly increased.

Fig. 4-14b shows the mean daily sampled E_{t-tree} response to the mean daily daytime *VPD* in the pre- and post-thinning periods during the growing season. The mean daily E_{t-tree} was 0.008 ± 0.004 kg d^{-1}, ranging from 0.001 to 0.016 kg d^{-1}, in the pre-thinning period, whereas the mean daily E_{t-tree} was 0.012 ± 0.005 kg d^{-1}, ranging from 0.001 to 0.021 kg d^{-1}, in the post-thinning period. The daily E_{t-tree} was significantly higher in the post-thinning period than in the pre-thinning period during the growing season (*P*<0.01: Mann-Whitney U test). Moreover, the difference in both periods became remarkable with increasing mean daily daytime *VPD*.

The daily E_{t-tree} in the present study increased after thinning (Fig. 4-14a, b). The increase in the daily E_{t-tree} may primarily be due to the increase in the F_d (Fig. 4-11) because the F_d increased significantly at the outer xylem (0-20 mm) after thinning (Fig. 4-11, 4-12b), and because the effect of the growth of the sapwood area of residual trees were assumed to be small after one-year thinning. Breda et al. (1995) also observed that there were no significant differences in the sapwood area in an oak forest. The results regarding the daily E_{t-tree} increased were consistent with previous studies (Lagergren and Lindroth, 2004; Medhurst et al., 2002; Morikawa et al., 1986; Reid et al.,

2006; Simonin et al., 2006). For example, Morikawa et al. (1986) reported that the daily E_{t-tree} was higher at a given level of R_s after 24% thinning in a 31-year-old Japanese cypress stand. Reid et al. (2006) found that individual trees in the thinned plot transpired more water in a lodgepole pine (*Pinus contorta*) forest in Alberta, Canada. However, several studies reported that E_{t-tree} had no clear differences when thinned. Gebauer et al. (2011) found that E_{t-tree} remained similar between thinned and control plots for a spruce forest in southeast Norway. These authors implied that sun-exposed needles were subjected to higher water shortage in the thinned plot.

The results also show that the daily E_{t-tree} for the small tree class increased by 195.1%, reaching 0.010 kg d^{-1} on given days after thinning (Fig. 4-14a). This result was contrary to the results of Morikawa et al. (1986), who reported that there was no significant difference in the daily E_{t-tree} on suppressed Japanese cypress before and after thinning. This conflict may be related to the deference of the stand density and the ratio of thinning. In their study, the ratio of thinning was 24% and stand density decreased from 1750 to 1325 trees ha^{-1}. The spacing for small tree class was not significantly changed. In the present study, the ratio of thinning was 50%, and the stand density decreased from 2198 to 1099 trees ha^{-1}. The openness of the crown declined significantly (22.2%) after thinning (Table 2-1). Solar radiation can penetrate deeper into the dense canopy by heavy thinning and, thus, result in remarkably increases in the F_d of small tree class. Therefore, the daily E_{t-tree} for the small class significantly increased after thinning in the present study.

4-3-5 Changes in stand transpiration

The daily variations in $E_{t-stand}$, which are related to the mean daily daytime *VPD* in the pre- and post-thinning periods during the growing season, are shown in Fig. 4-15. Although J_S values in the post-thinning period increased (Fig. 4-12d), the daily $E_{t-stand}$ was significantly lower in the post-thinning period than in the pre-thinning period (*P*<0.01: Mann-Whitney U test), because

$A_{S\text{-}stand}$ was reduced by 46.4% after 50% thinning (Table 2-1). The mean daily $E_{t\text{-}stand}$ was 1.29 ± 0.60 mm d^{-1}, ranging from 0.07 to 2.36 mm d^{-1}, in the pre-thinning period, whereas the mean daily $E_{t\text{-}stand}$ was 1.00 ± 0.40 mm d^{-1}, ranging from 0.10 to 1.77 mm d^{-1}, in the post-thinning period (Table 4-6, Fig. 4-15). The total $E_{t\text{-}stand}$ during the growing season was 214.9 mm, accounting for 18.9% of P_g or 40.3% of PET in the pre-thinning period. After thinning, the total $E_{t\text{-}stand}$ decreased by 23.0% and was 165.5 mm, accounting for 19.0% of P_g or 27.3% of PET after thinning (Table 4-6).
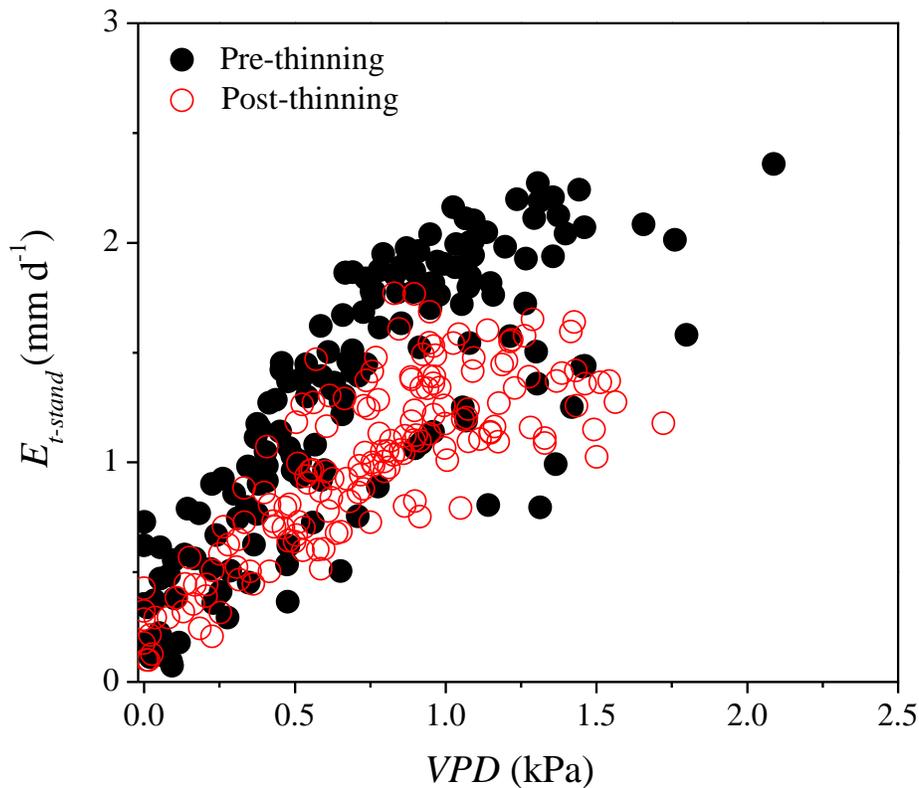
Fig. 4-15 Daily stand transpiration ($E_{t\text{-}stand}$) response to the mean daily daytime vapor pressure deficit (*VPD*) in the pre- and post-thinning periods during the growing season (April 28 – October 10).

Daily variations in $E_{t-stand}$ related to mean daily daytime *VPD* in the pre- and post-thinning periods at annual scale are shown in Fig. 4-16. The daily $E_{t-stand}$ was also significantly lower in the post-thinning period than in the pre-thinning period (*P*<0.01: Mann-Whitney U test) (Fig. 4-16a). The mean daily $E_{t-stand}$ decreased by 39.8%, from 1.23 ± 0.48 mm d^{-1} in the pre-thinning period to 0.74 ± 0.42 mm d^{-1} in the post-thinning period (Table 4-6; Fig. 4-16a). The annual $E_{t-stand}$ in the pre-thinning period was 441.0 mm, accounting for 30.5% of P_g or 49.3% of PET. After thinning, the annual $E_{t-stand}$ decreased by 38.3% and was 272.1 mm, accounting for 21.5% of P_g or 28.8% of PET (Table 4-6; Fig. 4-16b).
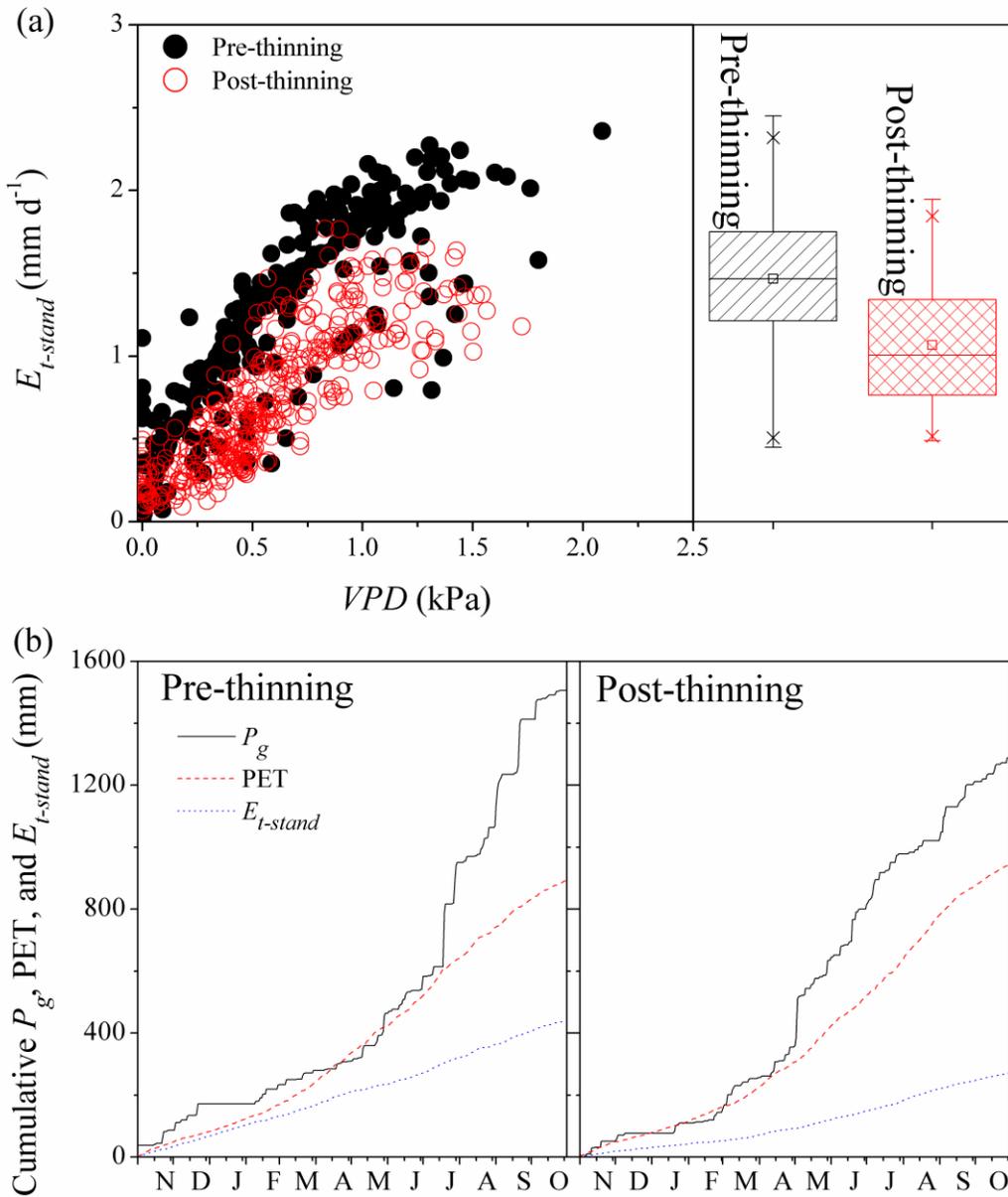
Fig. 4-16 Daily stand transpiration ($E_{t-stand}$) response to the mean daily daytime vapor pressure deficit (*VPD*) with boxplots drawn from the data; and (b) cumulative daily values of gross precipitation (P_g), potential evapotranspiration (PET), and $E_{t-stand}$ in the pre-thinning period (November 1, 2010 – October 31, 2011) and the post-thinning period (November 1, 2011 – October 31, 2012), respectively.

Table 4-6 Gross precipitation (P_g), potential evapotranspiration (PET), and stand transpiration (E_t) at the annual- and growing season-scale for the pre- and post-thinning periods, respectively.

Period	P_g			PET			E_t							
	Annual	Season	Daily	Annual	Season	Daily	Annual	Daily	E_t/P_g	E_t/PET	Season	Daily	E_t/P_g	E_t/PET
	mm	mm	mm d⁻¹	mm	mm	mm d⁻¹	mm	mm d⁻¹	%	%	mm	mm d⁻¹	%	%
Pre-thinning (Nov 2010 - Oct 2011)	1444.6	1139.8	2.45 ± 1.43	894.3	533.9	3.22 ± 1.52	441.0	1.23 ± 0.48	30.5	49.3	214.9	1.29 ± 0.60	18.9	40.3
Post-thinning (Nov 2011 - Oct 2012)	1266.8	869.0	2.59 ± 1.60	945.1	605.4	3.65 ± 1.53	272.1	0.74 ± 0.42	21.5	28.8	165.5	1.00 ± 0.40	19.0	27.3

Season means growing season from April 28 to October 10.

Contrary to the daily E_{t-tree} increased after thinning (Fig. 4-14b), the daily $E_{t-stand}$ decreased significantly after thinning (Fig. 4-11, 4-15a). This result was consistent with the lower G_c that was caused by thinning in this study (Fig. 4-13). The daily $E_{t-stand}$ was calculated from A_{S_stand}/A_G and J_S (Eq. (2.8)). Therefore, the decreases in the daily $E_{t-stand}$ were caused by the reduction in the sapwood area (46.4%) (Table 2-1), although there was an increase in J_S after thinning (Fig. 4-12d). The total $E_{t-stand}$ decreased by 23.0% during the growing season and by 38.3% at the annual scale after thinning. The results agree with previous studies (Breda et al., 1995; Lagergren et al., 2008; Morikawa et al., 1986; Simonin et al., 2007). For example, Morikawa et al. (1986) reported that $E_{t-stand}$ decreased by 21.2% after 24% thinning in a 31-year-old Japanese cypress forest. Lagergren et al. (2008) found that $E_{t-stand}$ for a thinned plot of a pine-spruce forest was lower by 40% than that for the control plot for the first year after removing 24% basal area.

However, the difference in $E_{t-stand}$ between the thinned and control plot may not be significantly reduced due to the drought period or temporal changes in $E_{t-stand}$ after thinning. Simonin et al. (2007) found considerable differences in $E_{t-stand}$ between the thinned and control plots when the soil water content was high in semi-arid *Pinus ponderosa* forests, whereas the difference was much less when the soil water content was low. Lagergren et al. (2008) reported that $E_{t-stand}$ in the thinned plot was rather higher than in the control plot during the drought period (July-September) when soil water content was low due to low precipitation. Additionally, $E_{t-stand}$ might gradually increase for several years after thinning and approach the total $E_{t-stand}$ value before thinning. Breda et al. (1995) reported that $E_{t-stand}$ was lower in the thinned plot of an oak forest for the first year after thinning. However, $E_{t-stand}$ was nearly the same between the thinned and control plots for the second year after thinning. Lagergren et al. (2008) also found that the

difference in $E_{t-stand}$ between the thinned and control plots diminished successively for the second year after thinning. Therefore, further studies were recommended to examine the variation in $E_{t-stand}$ for Japanese coniferous forests for the drought (low-precipitation) years, although the annual P_g is usually higher than PET, and the soil water deficit is not severe in Japan (Komatsu et al., 2006, 2012; Kumagai et al., 2008). Furthermore, measurement studies at a multi-year scale are also required to elucidate the temporal changes in $E_{t-stand}$ after thinning in Japanese coniferous forests.

In the present study, the decrease in the total $E_{t-stand}$ was less than that in A_{s_stand} after 50% strip thinning in a Japanese cypress plantation. The results were in contrast to those results observed by Komatsu et al. (2013). Recently, these authors conducted 45% selective thinning (from 1100 to 600 stem ha^{-1}) in a *Cryptomeria japonica* plantation in Japan and reported that the change in $E_{t-stand}$ was comparable to that in A_{s_stand} and that J_S did not increase due to thinning. The different results may be related to the stand characteristics and to the thinning method. In their studied stand, the stand density is relative sparse, which may cause water and environmental variables (light competition) to be less significant just after thinning. Additionally, the different thinning methods may be other possible factors. Different forestry practices (e.g., strip thinning and selective thinning) can result in different changes in stand structures and environmental variables. The resultant changes in stand/tree E_t under different forestry practices would be different. However, until now, data regarding the stand/tree E_t response to forest managements are so limited that it is difficult to obtain the single most important factor affecting tree water use. Therefore, further research should evaluate the responses of stand/tree E_t under different management plans (e.g., selective thinning and partial cutting) to identify those practices that are most optimized for water and forest management in forest watersheds.

4-3-6 Summary

This section elucidated the variations in E_t and G_c, in addition with tree-to-tree and radial F_d by 50% strip thinning in a Japanese cypress forest. The results showed that the F_d at the outer xylem (0-20 mm) increased remarkably, whereas the F_d at the inner xylem (20-40 mm) had no significant change in three tree classes (large, medium and small) after thinning. This result implies that thinning only enhanced the capacity of conducting water at the outer xylem. Correspondingly, the J_{S_A} values were higher in the post-thinning period, whereas the J_{S_B} values had no significant differences between the pre- and post-thinning periods. Similar to J_{S_A}, the J_S values were higher in the post-thinning period, and the differences significantly increased with increasing *VPD*. Furthermore, the daily E_{t-tree} increased in the three tree classes after thinning. Specially, the daily E_{t-tree} for the small class significantly increased, which may due to deeper solar radiation penetration into the canopy after heavy thinning, and then increased the transpiration of the lower crowns. Unlike the daily E_{t-tree}, the daily $E_{t-stand}$ decreased by 39.8%, from 1.23 ± 0.48 to 0.74 ± 0.42 mm d^{-1}, at the annual scale, which is due to the reduction in the sapwood area (46.4%) that is caused by thinning, although there was an increase in J_S. The annual $E_{t-stand}$ decreased by 38.3%, from 441.0 to 272.1 mm. The G_c values were significantly lower in the post-thinning period during the growing season. This result implies lower $E_{t-stand}$ and photosynthesis and would be useful for simulating possible changes in terrestrial water and carbon cycles due to the thinning treatment using ecosystem models. This study was conducted only one year after thinning, without soil water stress. Thus, further studies are recommended to examine the variation in E_t for drought (low-precipitation) years and the temporal changes in E_t at a multi-year scale by thinning. Further research should also evaluate the effects of different management practices on tree water use to identify those practices that are most appropriate for water and forest management in forest watersheds.

4-4 The effect of strip thinning on forest floor evaporation

4-4-1 Spatial variation of forest floor evaporation response to thinning

Daily variations in E_f of three lysimeters (L1, L2 and L3) located at different points at the forest floor in the pre- and post-thinning measuring periods are shown in Fig. 4-17. L1 and L2 were placed on the remained tree lines while L3 was placed on the thinned tree lines. In the pre-thinning measuring period (September 12 – October 10, 2011), daily E_f of the three lysimeters had a mean of 0.41±0.20, 0.45±0.18 and 0.40±0.19 mm d^{-1}, respectively. Total amount was 11.30, 12.70 and 11.10 mm, respectively. In the post-thinning measuring period (November 6 – October 31, 2012), daily E_f of the three lysimeters had a mean of 0.67±0.48, 0.72±0.0.50 and 0.64±0.0.46 mm d^{-1}, respectively. Total amount was 241.3, 260.7 and 233.4 mm, respectively. There are no significance differences on E_f among the three lysimeters in both periods. This indicates that spatial differences in E_f are not dependent on the location at the forest floor.
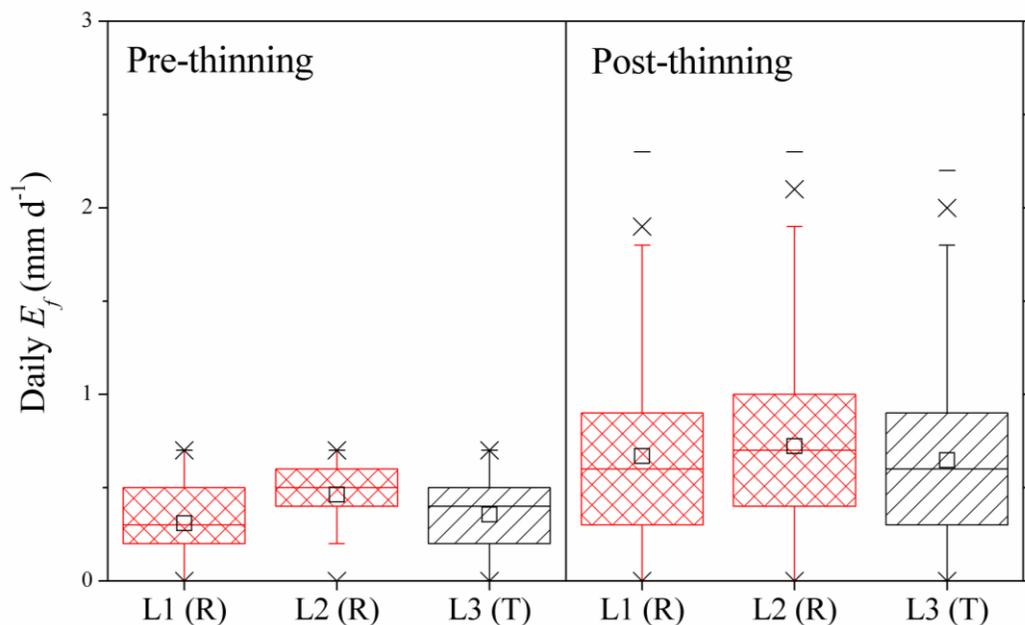
Fig. 4-17 Variations in daily forest floor evaporation (E_f) of three lysimeters located in the remained tree lines: L1(R) and L2 (R), and the thinned tree lines: L3(T) in the pre-thinning measuring period from September 12 to October 10, 2011, and post-thinning measuring period from November 6, 2011 to October 31, 2012, respectively.

Surface soil was the dominant reservoir for evaporation flux from forest floor, and could support high E_f flux when energy was available. Soil water deficit was not severe because annual P_g was larger than PET in both pre- and post-thinning periods (see Fig. 4-1; Table 4-7). Therefore, spatial variations in E_f are affected by photoenvironment (e.g., solar radiation) under the forest canopy. Before thinning, photoenvironment was considered to be constant under the dense canopy cover (canopy cover fraction: 0.974) caused by the high stand density. This was consistent with the result that there were no significant changes among the three lysimeters located at different points at the forest floor before thinning. After thinning, solar radiation penetrated increasedly into the forest. E_f increased largely among the three lysimeters while there were still no significant differences among them located at the remained tree lines and the thinned tree lines. Fig. 4-18 shows the variations in solar radiation at the forest floor measured at three different points: the remained tree lines, the thinned tree lines, and between one remained tree line and one thinned tree line after thinning. Daily solar radiation of the three points had a mean of 4.9±2.5, 4.8±2.7 and 4.7±2.1 MJ m^{-2}, respectively. There were also no significant differences among them located at different positions. The spatial variations in E_f corresponded to solar radiation at the forest floor. That may partially explain the homogeneity spatial variations in E_f after thinning.

The results showed that it is particularly important to understand the changes in spatial variations in E_f and solar radiation by thinning, and will be used to analyze and model the energy balance at the forest floor.
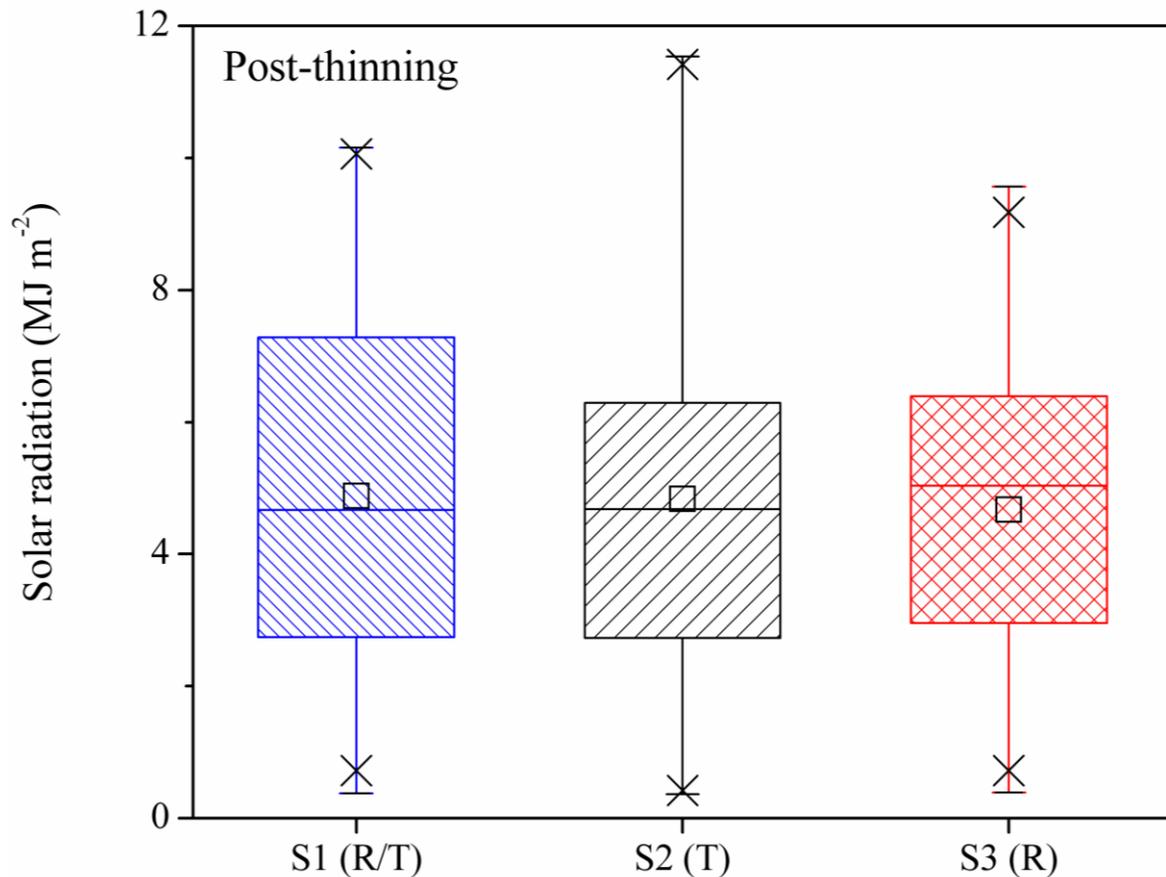
Fig. 4-18 Daily variations in solar radiation at the forest floor located in the remained tree lines: S(R); the thinned tree lines: S(T); and between one remained tree line and one thinned tree line: S(R/T) for the period of May 13 to October 24, 2013.

4-4-2 Changes in forest floor evaporation

Time series of daily E_f for the pre-thinning period from the November 1, 2010 to October 31, 2011 and for the post-thinning period from the November 1, 2011 to October 31, 2012 are shown in Fig. 4-19. Mean daily E_f was 0.34±0.23 mm d^{-1} ranging from 0.02 to 1.01 mm d-1 in the pre-thinning period (Fig. 4-19a) while it was 0.68±0.47 mm d^{-1} ranging from 0.00 to 2.10 mm d^{-1} in the post-thinning period (Fig. 4-19b). Mean daily E_f increased by 99.3% and was significantly larger in the post-thinning period than in the pre-thinning period ($P< 0.01$: Mann-Whitney U test).
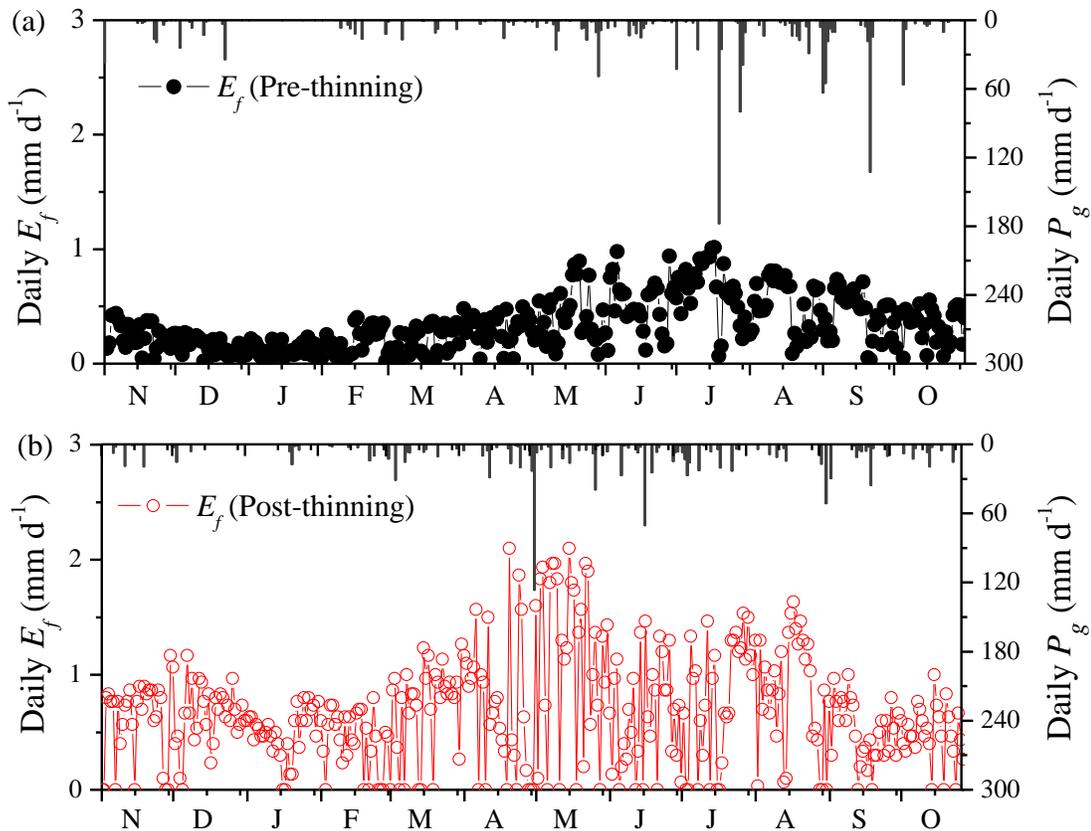
Fig. 4-19 (a) Time series of daily forest floor evaporation (E_f) responded to gross precipitation (P_g) in the pre- and (b) post-thinning periods, respectively.

Seasonal changes in monthly E_f in the pre- and post-thinning period are shown in Fig. 4-20. In the pre-thinning period, monthly E_f varied from 3.9 to 19.9 mm with a mean of 10.3±5.1 mm. Monthly E_f was highest in July and lowest in January. In the post-thinning period, monthly E_f varied from 13.9 to 33.9 mm with a mean of 20.4±6.3 mm. Monthly E_f was highest in May and lowest in September. In summary, monthly E_f was significant higher in the post-thinning period than in the pre-thinning period ($P < 0.01$: Mann-Whitney U test). Additionally, there are clear seasonal trends in both periods (Fig. 4-19 and 4-20). A similar seasonal tendency for E_f has been found in temperate deciduous forests (e.g., Daikoku et al., 2008; Deguchi et al., 2008). That said, the seasonal peak of E_f was found before leaf emergence, and the local maximal value of solar radiation beneath the forest canopy was also just observed because of the lack of leaves and the solar elevation angle in

those deciduous forests (Deguchi et al., 2008; Wilson et al., 2000). However, the seasonal tendency of E_f was also found in evergreen stands (e.g., Japanese cypress plantation). It is possible that it was influenced by energy allocation into latent and sensible heat fluxes (Moore et al., 1996).
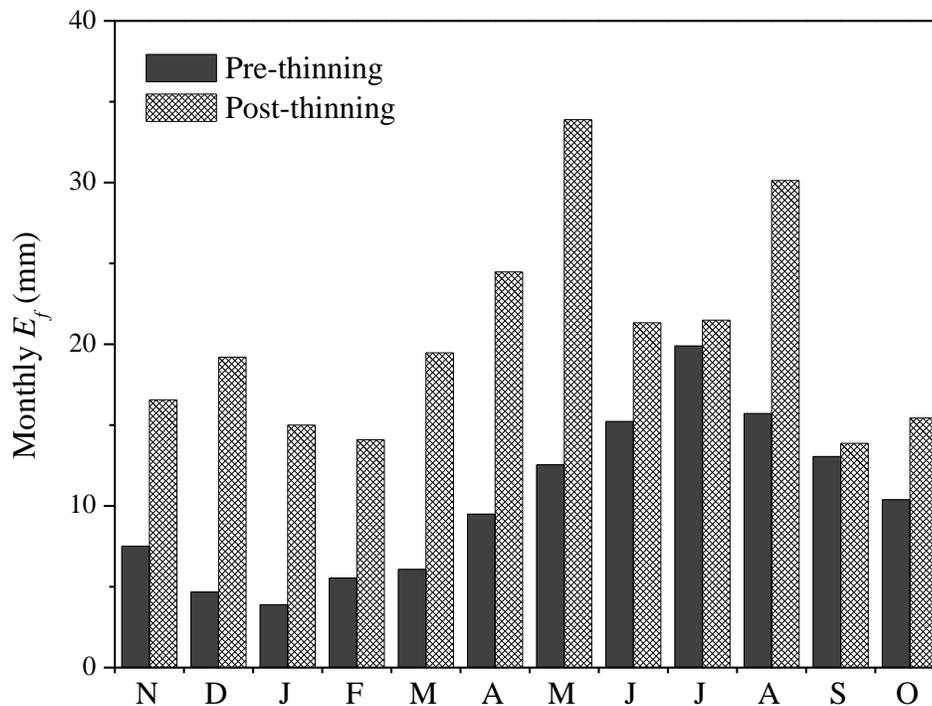
Fig. 4-20 Time series of monthly forest floor evaporation (E_f) in pre- and post-thinning periods, respectively.

Annual changes in E_f for the pre- and post-thinning periods are summarized in Table 4-7. Annual E_f in the pre-thinning period was 124.0 mm, accounting for 8.6% of P_g or 13.9% of PET. Annual E_f in the post-thinning period was 245.0 mm, accounting for 19.3% of P_g or 25.9% of PET. After thinning, annual E_f was significantly larger and increased by 97.6% due to the thinning treatment ($P < 0.01$: Mann-Whitney U test).

Table 4-7 Gross precipitation (P_g), potential evapotranspiration (PET), and forest floor evaporation (E_f) in the pre- and post-thinning periods, respectively.

Period	P_g Annual	PET Annual	PET Daily	E_f Annual	E_f Daily	E_f/P_g	E_f/PET
	mm	mm	mm d^{-1}	mm	mm d^{-1}	%	%
Pre-thinning (Nov 2010 - Oct 2011	1444.6	894.3	2.45 ± 1.43	124.0	0.34±0.23	8.6	13.9
Post-thinning (Nov 2011 - Oct 2012)	1266.8	945.1	2.59 ± 1.60	245.0	0.68±0.47	19.3	25.9

In this study, greater E_f was found in the post-thinning period compared to the pre-thinning period. Soil evaporation occurs in two stages: (1) the constant-rate stage controlled by energy input as influenced by light penetration through the canopy, atmospheric turbulence and soil albedo; and (2) the falling rate stage controlled by overall soil moisture and hydraulics (Suleiman and Ritchie, 2003). As such, the evaporation rate from a soil surface depends upon the radiation rate and the moisture condition of the forest surface (e.g., Suleiman and Ritchie, 2003; Tsujimura and Tanaka, 1998). Surface soil could constrain E_f, and E_f is higher in open sites because shade from overstory canopy and forest floor litter reduces light penetration and soil temperature. Because soil moisture is not severe in Japan, thus the increase in E_f was contributed to the higher solar radiation and increased net precipitation all of which contribute to greater potential soil evaporation after thinning treatment. These results support the hypothesis that E_f could be high when energy was available in the abandoned Japanese cypress plantations.

Canopy structure and leaf area index are known to affect below-canopy radiation characteristics (Kuuluvainen and Pukkala, 1989), which can potentially increase E_f and its spatial variability. Simonin et al. (2006) reported that after 82% basal area thinning (corresponding to 45% leaf area index reduced), understory evapotranspiration was greater in thinned compared with unthinned plots and increased during extreme drought when overstory transpiration was low due to

stomatal closure in a semi-arid ponderosa pine stand of the southwestern US. Previous studies have also examined the effects of tree shade on spatial variations in soil evaporation (Jackson and Wallace, 1999; Raz-Yaseef et al., 2010). For example, Raz-Yaseef et al. (2010) reported that evaporation fluxes measured in sun-exposed areas were on average double those in shaded areas, and solar radiation was 92% higher in exposed compared to shaded sites in a semi-arid pine forest in Southern Israel. Thus the quantitative E_f before and after thinning in the present study could improve the understanding of hydrological processes at the forest floor, and develop predictive and management tools to improve water use and water-use efficiency in forest ecosystems.

4-4-3 Summary

This section elucidated the changes in E_f by 50% strip thinning in a Japanese cypress plantation. Spatial distribution of E_f was examined in the pre- and post-thinning measuring periods, respectively. Daily variations in E_f of three lysimeters located at different points had no significant differences in both periods. The spatial variations in E_f in the post-thinning period corresponded to solar radiation measured at the forest floor. That indicates spatial differences in E_f are not dependent on the location and homogeneousness at the forest floor even after thinning treatment. These results provide useful information for understanding the changes in spatial variations in E_f and solar radiation by thinning, and will be used to analyze and model the energy balance at the forest floor. Besides, changes in E_f by thinning were quantified. Daily E_f increased by 99.3% from 0.34 ± 0.23 to 0.68 ± 0.47 mm d^{-1}, which was due to the increase in solar radiation. Annual E_f increased by 97.6% from 124.0 (8.6% of P_g) to 245.0 mm (19.3% of P_g). The quantification of changes in E_f by thinning could improve the understanding of hydrological processes at the forest floor, and develop predictive and management tools to improve water use and water-use efficiency in forest ecosystems.

4-5 The effect of strip thinning on partitioning of evapotranspiration

4-5-1 Changes in partitioning of evapotranspiration

Detailed monthly P_g, PET, ET and its three sub-components in the Japanese cypress forest in the pre-thinning period from November 2010 to October 2011and the post-thinning period from November 2011 to October 2012 are summarized in Table 4-8. In the pre-thinning period, monthly ET varied from 39.6 to 153.1 mm with a mean of 81.7±34.6 mm. Monthly ET was largest in July and lowest in January. In the post-thinning period, monthly ET varied from 36.2 to 107.0 mm with a mean of 65.0±23.4 mm. Monthly ET was largest in May and lowest in January. Annual ET was 980.2 mm, accounting for 67.9% of P_g or 109.6% of PET in the pre-thinning period. After thinning, annual ET was 780.1 mm, accounting for 61.6% of P_g or 82.5% of PET. Thinning resulted in annual ET decreased by 15.5% corresponding 200.1 mm. In summary, annual ET decreased significantly due to thinning treatment (*P*< 0.01: Mann-Whitney U test).

Table 4-8 Summary on gross precipitation (P_g), potential evapotranspiration (PET), evapotranspiration (ET), and its three sub-components: canopy interception (E_i), tree transpiration (E_t) and forest floor evaporation (E_f) in the pre-thinning period (November 2010 – October 2011) and post-thinning period (November 2011 – October 2012).

		N	D	J	F	M	A	M	J	J	A	S	O	Total	Ratio of P_g	Ratio of PET	Ratio of ET
							mm									%	
Pre-thinning	E_i	26.0	24.7	0.0	21.6	16.1	15.5	49.5	29.2	83.1	44.8	85.1	19.1	414.8	28.7	46.4	42.3
	E_t	32.5	34.3	35.7	28.4	36.3	42.5	25.5	34.6	50.0	42.9	43.1	35.5	441.4	30.6	49.4	45.0
	E_f	7.5	4.7	3.9	5.5	6.1	9.5	12.5	15.2	19.9	15.7	13.1	10.4	124.0	8.6	13.9	12.6
	ET	66.0	63.7	39.6	55.6	58.5	67.5	87.6	79.0	153.1	103.4	141.3	65.0	980.2	67.9	109.6	-
	PET	47.5	34.3	40.4	46.0	72.1	93.2	88.9	94.3	122.8	101.0	89.2	64.6	894.3	61.9	-	-
	P_g	85.4	85.8	0	59.2	46.6	29.4	153.8	73.8	383.4	117.4	342.4	67.4	1444.6	-	-	-
Post-thinning	E_i	11.1	8.9	9.5	13.1	22.0	19.6	45.6	31.7	37.3	12.6	40.2	11.5	263.0	20.8	27.8	33.7
	E_t	17.9	12.3	11.8	10.3	18.0	22.2	27.5	28.4	32.8	39.4	25.9	25.7	272.1	21.5	28.8	34.9
	E_f	16.6	19.2	15.0	14.1	19.5	24.5	33.9	21.3	21.5	30.1	13.9	15.4	245.0	19.3	25.9	31.4
	ET	45.5	40.4	36.2	37.5	59.5	66.2	107.0	81.4	91.6	82.2	80.0	52.6	780.1	61.6	82.5	-
	PET	48.3	29.8	37.0	45.1	62.5	82.8	114.3	99.5	116.5	143.2	94.5	71.5	945.1	74.6	-	-
	P_g	50	26.6	32.2	45.6	100	92	281.2	164	183.2	42.8	189.8	59.6	1266.8	-	-	-

The cumulative and annual values of P_g, PET, ET and its three subcomponents in the pre- and post-thinning periods are illustrated in Fig. 4-21 and 4-22. ET was less than P_g throughout the pre-thinning period expect period from March to May (i.e., before the beginning of rainy season). For the post-thinning period, ET was almost close to P_g from November 2011 to March 2012 and afterward was much less than P_g. Compared with PET, ET was consistently higher during the whole pre-thinning period. However, in the post-thinning period, ET was almost close to PET before June, and afterward was much less than PET. In the both periods, P_g was significantly larger in the pre-thinning period than that in the post-thinning period while PET in the pre-thinning was close to the post-thinning period (Table 4-8). Therefore, because the interannual variability of P_g was remarkable large, we assumed that the interannual variability of PET was insignificant and a constant parameter in the pre- and post-thinning periods.
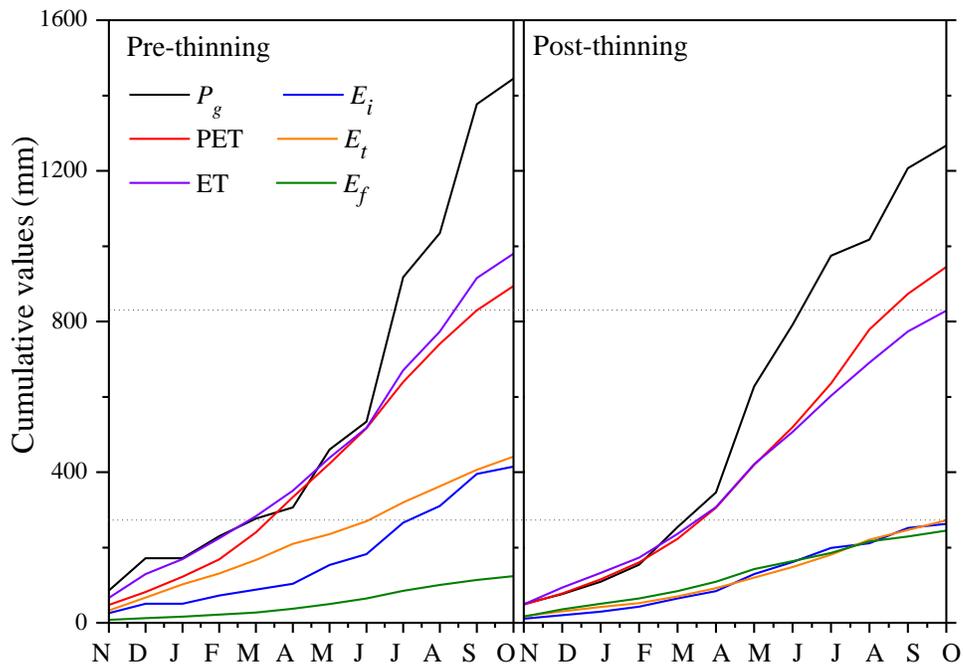
Fig. 4-21 Cumulative daily values of gross precipitation (P_g), potential evapotranspiration (PET), evapotranspiration (ET), canopy interception (E_i), tree transpiration (E_t) and forest floor evaporation (E_f) in the Japanese cypress stand in the pre- and post-thinning periods, respectively.

As shown in Fig. 4-21, cumulative values of E_t in the pre-thinning period was the dominant component of ET, and consistent higher than E_i and E_f. Moreover, the annual E_f was the smallest component. However, after thinning, although E_t was still the dominant component of ET, the relative contributions of the three components to ET were changed to be close. For example, before the beginning of rainy season (November 2011 - May 2012), the contribution from E_f was the main component of ET while E_i was the smallest component of ET. During the rainy season (June – July, 2012), the relative contribution of E_i instead of E_f and became the dominant component of ET. E_t was the smallest component of ET. After the rainy season (August – October, 2012), the relative contribution of E_t gradually increased and finally exceeded E_i, and was the dominant component of ET. The contribution from E_f was the smallest component of ET.
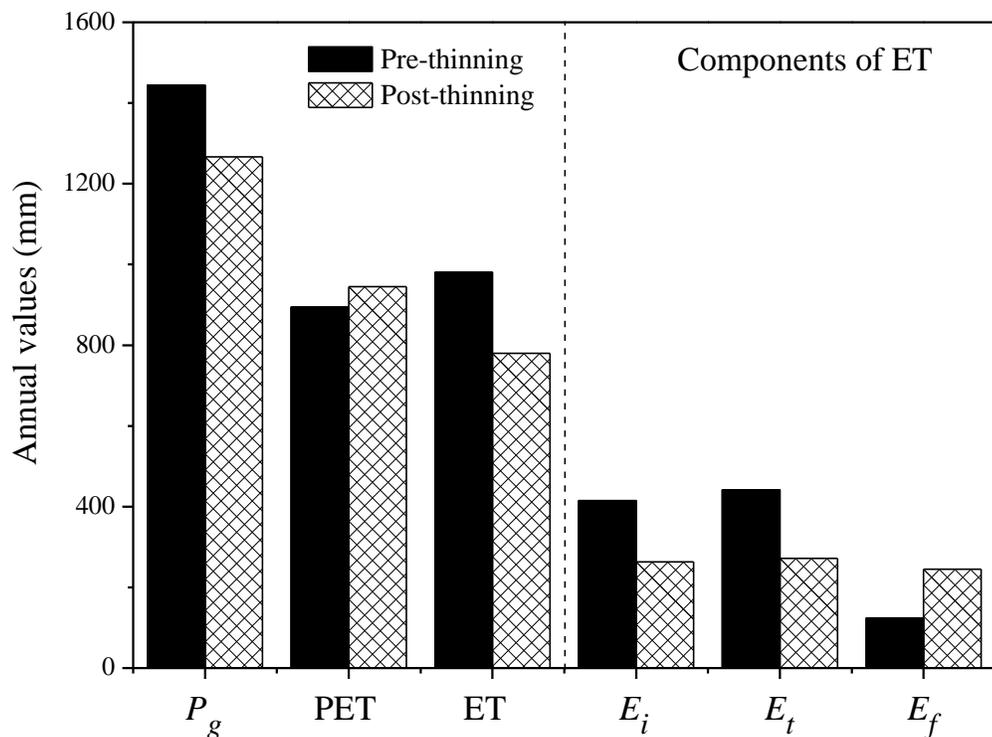
Fig. 4-22 Annual values of gross precipitation (P_g), potential evapotranspiration (PET), evapotranspiration (ET), canopy interception (E_i), tree transpiration (E_t) and forest floor evaporation (E_f) in the Japanese cypress stand in the pre- and post-thinning periods, respectively.

The changes in partitioning of ET by thinning were quantified. Fig. 4-23 shows the ratio of each evaporation flux (E_i, E_t and E_f) to total ET in pre- and post-thinning period. In the pre-thinning period, E_i, E_t and E_f was 414.8, 441.4 and 124.0 mm, accounting for 42.3%, 45.3% and 12.6% of total ET, or 46.4%, 49.4% and 13.9% of total PET, respectively (Table 4-8). After thinning, E_i, E_t and E_f was 263.0, 272.1 and 245.0 mm, accounting for 33.7%, 34.9% and 31.4% of total ET, or 27.8%, 28.8% and 25.9% of total PET, respectively (Table 4-8). Thinning altered the partitioning of ET and resulted in decreases in E_i and E_t, and an increase in E_f.
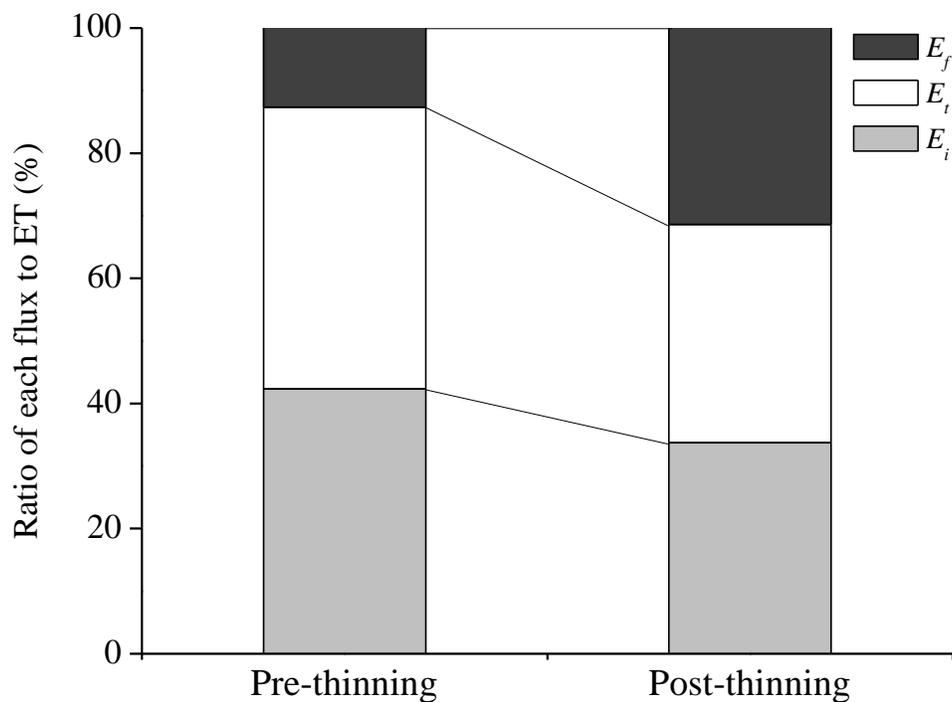
Fig. 4-23 Ratio of each flux (canopy interception, E_i; tree transpiration, E_t, and forest floor evaporation, E_f) to total evapotranspiration (ET) in the pre- and post-thinning periods, respectively.

In this study, the experimental treatment of 50% strip thinning caused a 15.5% decrease in annual ET corresponding 200.1 mm in the Japanese cypress plantation. In forest water cycle, ET is a hydrologic component of major importance in determining the water budget of forest areas, especially in the Japanese coniferous plantations (Kuraji, 2003). These results support the positive effect of thinning on water resources that thinning efficiently increased the water availability in the

forested watershed. The partitioning of ET by forests is a dominant control on climate and hydrology at local to global scales. For example, ET returning to the atmosphere may support future precipitation events and influence canopy gas exchange through a boundary layer feedback (Jarvis and Mcnaughton, 1986). Thinning of forests changed the relative contribution of individual flux components to total ET. Thus, the quantification of changes in partitioning of ET response to thinning could help to understand the thinning effects on forest stand water balance, and improve the development of sound forestry techniques and resolve complex forest-water conflicts.

4-5-2 Summary

This section elucidated the changes in partitioning of ET by thinning in a Japanese cypress plantation. The results showed that thinning caused the annual ET decreased by 15.5% (corresponding 200.1 mm) from 980.2 to 780.1 mm. The ratio of ET to PET decreased from 109.6% to 82.5%. Thinning efficiently increased the water availability, and highlighted the positive thinning effects on water resources in forested watersheds. Then the changes in partitioning of ET by thinning were quantified. ET partitioned into E_i, E_t and E_f was 42.3%, 45.3% and 12.4%, respectively, in the pre-thinning period. After thinning, ET partitioned into E_i, E_t and E_f was 33.7%, 34.9% and 31.4%, respectively. Thinning resulted in decreases in E_i and E_t, and an increase in E_f. Besides, thinning changed the relative contribution of individual flux components to total ET. Although E_t was the dominant component of ET in both periods, the relative contributions of the three components to ET were changed to be very close after thinning. The quantification of changes in partitioning of ET response to thinning could guide us for predicting the effect of thinning on forest stand water balance, and achieving an optimized water and forest management in forested watersheds.

Chapter 5 Over-all conclusions and future research

5-1 Over-all conclusions

Forest management (e.g., thinning) alters the cover and structure of forest and plays a great role in regulating the hydrological cycle at multiple temporal and spatial scales by altering ecosystem water balances. Moreover, different management practices could result in different effects on components of forest water cycle due to its effect on soil moisture available and environmental variables. Evapotranspiration (ET) is an important component in water balance and is used to evaluate forest hydrological functions. When evaluating the effects of ET by changes in stand conditions and understory vegetation, the quantification of changes in partitioning of ET response to thinning could help to understand the changes in forest stand water balance, and guide integrated forest and water management. Despite numerous studies on the relations between forest practices and the forest water, few studies attempt to elucidate the effect of strip thinning on partitioning of ET. Strip thinning requires less time and skill needed for tree selection compared with conventional selective thinning. It has been widely adopted in these abandoned Japanese coniferous plantations because of their overstocked stand densities and volumes. This study employed intensive field measurements to examine the effect of strip thinning on partitioning of ET in the Japanese cypress plantation. The followings are key conclusions drawn from this study.

5-1-1 Incident rainfall partitioning and canopy interception modeling for an abandoned Japanese cypress stand

Canopy interception (E_i) in forests has been studied widely. However, E_i parameters and modeling as well as spatial patterns of throughfall (TF) in abandoned Japanese cypress plantations remain poorly documented. Results indicate that P_g partitioning into TF, SF and E_i were, respectively, 64.2±3.6%, 10.6±0.6 % and 25.2±1.1% of the 880.8 mm cumulative P_g from 29 rainfall events. Direct throughfall proportion (p) and drainage from the canopy contributed about 14±7% and 50±21% of total TF between events, respectively. The mean canopy storage capacity (S)

was 2.4±0.7 mm. The coefficient of variability (CV) of TF rate decreased asymptotically with increasing P_G amount, ranging from 16% to 56% with median 26%. The CV of TF rate was not significantly correlated with canopy cover (r=0.152, p=0.521, n=20) and distance from the nearest trunk (r=0.196, p=0.408, n=20). Based on the revised Gash analytical model, total simulated E_i was close to observed, with a general underestimation magnitude 5.7%. The E_i components were quantified, and most of the interception loss (62.9%) was evaporated during rainfall, of which 26.8% evaporated after rainfall ceased. Climatic and forest structural parameters required by the model were identified and analyzed by sensitivity analysis, implying that the revised Gash analytical model is robust and reliable enough for the abandoned Japanese cypress plantation in a maritime climate. The present study may improve understanding of water resources of forested watersheds and provides a basis for future studies of forest management and rainfall partitioning interaction.

5-1-2 Partitioning of the total evapotranspiration in an abandoned Japanese cypress stand during the growing season

The partitioning of ET into E_i, E_t and E_f were quantified in an abandoned Japanese cypress plantation. Monitoring primarily focused on the growing season of July – October 2011. Total ET during the monitoring period was 446.3 mm accounting for 47.5% of the total precipitation of 938.8 mm. E_i was the dominant evaporation flux and accounted for 53.6% of ET or 25.5% of rainfall, followed by E_t with 33.7% of ET or 16.0% of rainfall. The average E_t was 1.5 ± 0.6 mm d^{-1}. It was well correlated with soil moisture at a depth of 5 – 15 cm, which reflected the forest properties, i.e., tree roots were exposed on the forest floor. E_f accounted for 12.7% of ET or 6.0% of rainfall with a daily mean of 0.55 ± 0.26 mm d^{-1}, and was best correlated with soil moisture in the upper 5 cm of soil. The interactions between soil moisture and evaporation fluxes can be used to predict ET more accurately when estimates of ET are based only on averaged soil moisture in the root zone. These findings can improve the understanding of water budget in forested watershed and also be used to

build and validate hydrologic models for water resource managements.

5-1-3 The effect of strip thinning on canopy interception

The changes in P_g partitioning into *TF*, *SF* and E_i were quantified by thinning in the pre-thinning period (November 2010 – October 2011) and the post-thinning period (November 2011 – October 2012). The results revealed that after thinning, annual *TF* rate increased from 61.4 to 73.0% whereas annual *SF* rate decreased from 9.8 to 6.1% and annual E_i rate decreased from 28.7 to 20.8%. Thinning treatment resulted in the water availability an increase in the soil matrix, especially in dry season. The reduction in E_i rate by strip thinning tended to be smaller than that by selective thinning, which may be related to the different changes in canopy cover by the two thinning methods. This study is one of case studies, however, it is important to accumulate data related to changes in E_i caused by different forest practices to acquire an integrated understanding of canopy water balance. Based on summarizing the findings of previous studies, the degree of decline in E_i loss/rate caused by thinning was related to P_g and ratio of thinning. These results provide useful information for assessing the effects of forest practice on water resources in forested watershed.

5-1-4 The effect of strip thinning on tree transpiration

Tree-to-tree and radial variation in xylem sapflow density (F_d) were measured in the pre- and post-thinning periods. The results revealed that the F_d at the outer xylem (0-20 mm) increased remarkably, whereas the F_d at the inner xylem (20-40 mm) had no significant change after thinning. Mean stand sap flow density (J_S) values were higher in the post-thinning period, and the differences significantly increased with increasing vapor pressure deficit (*VPD*) values. Furthermore, the daily E_{t-tree} increased, particularly in the small tree class. Unlike the daily E_{t-tree}, the daily $E_{t-stand}$ decreased from 1.29 ± 0.60 to 1.00 ± 0.40 mm d^{-1} during the growing season or decreased from 1.23 ± 0.48 to 0.74 ± 0.42 mm d^{-1} on the annual scale. The total $E_{t-stand}$ decreased by 23.0%, from 214.9 to 165.5 mm, during the growing season or decreased by 38.3%, from 441.0 to 272.1 mm, on the annual scale. G_c decreased after thinning, which implies lower stand E_t and photosynthesis. G_c

was primarily related to the *VPD* and would be an effective model to predict E_t from these Japanese cypress plantations. This study provides useful information for understanding the E_t responses at individual tree and stand levels to strip thinning and contributes to obtaining a thorough understanding of the change in tree water use under different management strategies.

5-1-5 The effect of strip thinning on forest floor evaporation

Daily variations in E_f of three lysimeters located at different points had no significant differences in both periods. The spatial variations in E_f in the post-thinning period corresponded to solar radiation measured at the forest floor. That indicates spatial differences in E_f are independent on the location and are homogeneousness at the forest floor even after thinning treatment. These results provide useful information for understanding the changes in spatial variations in E_f and solar radiation by thinning, and will be used to analyze and model the energy balance at the forest floor. Additionally, changes in E_f by thinning were quantified. Daily E_f increased by 99.3% from 0.34 ± 0.23 to 0.68 ± 0.47 mm d^{-1}, which was due to the increase in solar radiation. Annual E_f increased by 97.6% from 124.0 (8.6% of P_g) to 245.0 mm (19.3% of P_g). The quantification of changes in E_f by thinning could improve the understanding of hydrological processes at the forest floor and develop predictive and management tools to improve water use and water-use efficiency in forest ecosystems.

5-1-6 The effect of strip thinning on partitioning of evapotranspiration

The changes in partitioning of ET by thinning were quantified in pre- and post-thinning periods. The results showed that thinning caused the annual ET decreased by 15.5% (corresponding 200.1 mm) from 980.2 to 780.1 mm. The ratio of ET to PET decreased from 109.6% to 82.5%. Thinning efficiently increased the water availability and highlighted the positive thinning effects on water resources in the forested watershed. ET partitioned into E_i, E_t and E_f was 42.3%, 45.3% and 12.4%, respectively, in the pre-thinning period. After thinning, ET partitioned into E_i, E_t and E_f was 33.7%, 34.9% and 31.4%, respectively. Thinning resulted in decreases in E_i and E_t, and an increase

in E_f. Furthermore, thinning changed the relative contribution of individual flux components to total ET. Although E_t was the dominant component of ET in both periods, the relative contributions of the three components to ET were changed to be very close after thinning. The quantification of changes in partitioning of ET response to thinning could guide us for predicting the effect of thinning on forest stand water balance, and achieving an optimized water and forest management in forested watersheds.

5-2 Further research

Because of the uncertainty of estimations of each component, further measurements should be applied to validate the total ET. There are two methods: eddy covariance system and water balance approach. The eddy covariance system coupled with meteorological data allows analysis of the factors controlling ET for short/long-term periods. By contrast, the water balance approach cannot allow researchers to determine the factors controlling ET or their influences on the characteristics of ET; so, a long-term period of time is needed to evaluate ET. The two methods have been proved to be close to estimate total ET in forested watershed for a long time scale (e.g., Kosugi and Katsuyama, 2007).

This study was conducted only one-year before and after thinning without soil water stress. Thus, measurement studies at a multi-year scale are recommended to examine the temporal changes in partitioning of ET for the succeeding years after thinning due to the temporal changes in stand characteristics (e.g., stand growth, forest cover recovery, and understory vegetation growth).

Furthermore, we didn't examine the resultant changes in partitioning of ET between strip thinning and other forestry practices (e.g., afforestation, partial cutting and selective thinning), because few studies elucidated the effect of forestry practices on partitioning of ET in Japanese coniferous plantations. The different forestry practices could result in different effects on components of forest water cycle (e.g., E_t, ET, runoff). Therefore, further research should evaluate

thinning effects on hydrological processes for different management plans to identify those practices that are most optimized for water and forest management in forest watersheds.

Acknowledgements

I would like to take this opportunity to thank my supervisor Dr. Yuichi Onda, professor from Graduate of Life and Environmental Sciences, University of Tsukuba, for his endless support, knowledge, and guidance throughout my graduate work, which has led me attracted to the forest hydrology research.

I would like to thank my colleagues in University of Tsukuba for their help and encouragement. Drs. Hiroaki Kato, Jeremy Patin, Akiko Hirata, M. Teramage Tesfaye and Cristobal Padilla provided fruitful comments and plentiful guidance that improved the quality of the research. Drs. Marino Hiraoka and Yoshitaka Komatsu, and Mr. Tomohiro Narisawa provided valuable support in installing and maintaining field measurements in Mt. Karasawa, Tochigi Prefecture, Japan. They deserve my sincere appreciation.

I would like to thank Professor Kyoichi Otsuki, and Drs. Yoshinori Shinohara, Kenji Tsuruta, and Makiko Tateishi, from Kyushu University, for providing valuable guide and support in sap flow measurements and analysis.

My thanks also go to Dr. Takashi Gomi of Associate Professor and Dr. Bui Xuan Dung from Tokyo University of Agriculture and Technology, for their cooperation in my research as well as support in climatic data in Mt. Karasawa, Tochigi Prefecture.

I also appreciate all my friends in Japan and China for their help and encouragement.

Finally, I wish to express my special thanks to my dear family for their endless love to support me to conduct this study in Japan.

References

Aboal, J.R., Jimenez, M.S., Morales, D., Gil, P., 2000. Effects of thinning on throughfall in Canary Islands pine forest - the role of fog. *Journal of Hydrology* **238**: 218-230.

Allen, S.J., 1990. Measurement and estimation of evaporation from soil under sparse barley crops in northern Syria. *Agricultural and Forest Meteorology* **49**: 291-309.

Anderson, H.W., Hoover, M.D., Reinhart, K.G., 1976. Forests and water. Effects of forest management on floods, sedimentation, and water supply. *USDA Forest service general technical report* **1-3**.

Andre, F., Jonard, M., Jonard, F., Ponette, Q., 2011. Spatial and temporal patterns of throughfall volume in a deciduous mixed-species stand. *Journal of Hydrology* **400**: 244-254.

Andreassian, V., 2004. Waters and forests: from historical controversy to scientific debate. *Journal of Hydrology* **291**: 1-27.

Aussenac, G., Granier, A., 1988. Effects of thinning on water-stress and growth in Douglas-fir. *Canadian Journal of Forest Research* **18**: 100-105.

Aussenac, G., Granier, A., Naud, R., 1982. Influence of thinning on the growth and water-balance of a young-population of douglas firs (*Pseudotsuga-Menziesii* (Mirb) Franco). *Canadian Journal of Forest Research* **12**: 222-231.

Baker, M.B., 1986. Effects of ponderosa pine treatments on water yield in Arizona. *Water Resources Research* **22**: 67-73.

Baldocchi, D.D., Law, B.E., Anthoni, P.M., 2000. On measuring and modeling energy fluxes above the floor of a homogeneous and heterogeneous conifer forest. *Agricultural and Forest Meteorology* **102**: 187-206.

Baldocchi, D.D., Meyers, T.P., 1991. Trace gas-exchange above the floor of a deciduous forest. 1. Evaporation and CO_2 efflux. *Journal of Geophysical Research-Atmospheres* **96**: 7271-7285.

Black, T.A., Tan, C.S., Nnyamah, J.U., 1980. Transpiration rate of Douglas-fir trees in thinned and un-thinned stands. Canadia Journal of Soil Science **60**: 625-631.

Boast, C.W., Robertson, T.M., 1982. A micro-Lysimeter method for determining evaporation from bare soil - Description and laboratory evaluation. *Soil Science Society of America Journal* **46**: 689-696.

Bond-Lamberty, B., Gower, S.T., Amiro, B., Ewers, B.E., 2011. Measurement and modelling of bryophyte evaporation in a boreal forest chronosequence. *Ecohydrology* **4**: 26-35.

Bosch, J.M., Hewlett, J.D., 1982. A review of catchment experiments to determine the effect of vegetation changes on water yield and evapo-transpiration. *Journal of Hydrology* **55**: 3-23.

Breda, N., Granier, A., Aussenac, G., 1995. Effects of thinning on soil and tree water relations, transpiration and growth in an oak forest (*Quercus-Petraea* (Matt) Liebl). *Tree Physiology* **15**: 295-306.

Bristow, K.L., Campbell, G.S., Papendick, R.I., Elliott, L.F., 1986. Simulation of heat and moisture transfer through a surface residue soil system. *Agricultural and Forest Meteorology* **36**: 193-214.

Castro, N.M.D., Auzet, A.V., Chevallier, P., Leprun, J.C., 1999. Land use change effects on runoff and erosion from plot to catchment scale on the basaltic plateau of Southern Brazil. *Hydrological Processes* **13**: 1621-1628.

Cavanaugh, M.L., Kurc, S.A., Scott, R.L., 2011. Evapotranspiration partitioning in semiarid shrubland ecosystems: a two-site evaluation of soil moisture control on transpiration. *Ecohydrology* **4**: 671-681.

Cienciala, E., Kucera, J., Malmer, A., 2000. Tree sap flow and stand transpiration of two Acacia mangium plantations in Sabah, Borneo. *Journal of Hydrology* **236**: 109-120.

Clausnitzer, F., Kostner, B., Schwarzel, K., Bernhofer, C., 2011. Relationships between canopy transpiration, atmospheric conditions and soil water availability-Analyses of long-term sap-flow measurements in an old Norway spruce forest at the Ore Mountains/Germany. *Agricultural and Forest Meteorology* **151**: 1023-1034.

Crockford, R.H., Richardson, D.P., 1990. Partitioning of rainfall in a eucalypt forest and pine plantation in Southeastern Australia. 4. The relationship of interception and canopy storage capacity, the interception of these forests, and the effect on interception of thinning the pine plantation. *Hydrological Processes* **4**: 169-188.

Crockford, R.H., Richardson, D.P., 2000. Partitioning of rainfall into throughfall, stemflow and interception: effect of forest type, ground cover and climate. *Hydrological Processes* **14**: 2903-2920.

Daikoku, K., Hattori, S., Deguchi, A., Aoki, Y., Miyashita, M., Matsumoto, K., Akiyama, J., Iida, S., Toba, T., Fujita, Y., Ohta, T., 2008. Influence of evaporation from the forest floor on evapotranspiration from the dry canopy. *Hydrological Processes* **22**: 4083-4096.

Deguchi, A., Hattori, S., Daikoku, K., Park, H.T., 2008. Measurement of evaporation from the forest floor in a deciduous forest throughout the year using microlysimeter and closed-chamber systems. *Hydrological Processes* **22**: 3712-3723.

Deguchi, A., Hattori, S., Park, H.T., 2006. The influence of seasonal changes in canopy structure on interception loss: Application of the revised Gash model. *Journal of Hydrology* **318**: 80-102.

Delzon, S., Sartore, M., Granier, A., Loustau, D., 2004. Radial profiles of sap flow with increasing tree size in maritime pine. *Tree Physiology* **24**: 1285-1293.

Dodson, E.K., Peterson, D.W., Harrod, R.J., 2008. Understory vegetation response to thinning and burning restoration treatments in dry conifer forests of the eastern Cascades, USA. *Forest Ecology and Management* **255**: 3130-3140.

Dung, B.X., Gomi, T., Miyata, S., Sidle, R.C., Kosugi, K., Onda, Y., 2012. Runoff responses to forest thinning at plot and catchment scales in a headwater catchment draining Japanese cypress forest. *Journal of Hydrology* **444**: 51-62.

Dung, B.X., Miyata, S., Gomi, T., 2011. Effect of forest thinning on overland flow generation on hillslopes covered by Japanese cypress. *Ecohydrology* **4**: 367-378.

Dykes, A.P., 1997. Rainfall interception from a lowland tropical rainforest in Brunei. *Journal of Hydrology* **200**: 260-279.

Eltahir, E.A.B., 1998. A soil moisture rainfall feedback mechanism. 1.Theory and observations. *Water Resources Research* **34**: 765-776.

Fang, C., Moncrieff, J.B., 1996. An improved dynamic chamber technique for measuring CO_2 efflux from the surface of soil. *Functional Ecology* **10**: 297-305.

Frost, W.E., Edinger, S.B., 1991. Effects of tree canopies on soil characteristics of annual rangeland. *Journal of Range Management* **44**: 286-288.

Gash, J.H.C., 1979. Analytical model of rainfall interception by forests. *Quarterly Journal of the Royal Meteorological Society* **105**: 43-55.

Gash, J.H.C., Wright, I.R., Lloyd, C.R., 1980. Comparative estimates of interception loss from three coniferous forests in Great-Britain. *Journal of Hydrology* **48**: 89-105.

Gash, J.H.C., Lloyd, C.R., Lachaud, G., 1995. Estimating sparse forest rainfall interception with an analytical model. *Journal of Hydrology* **170**: 79-86.

Ganatsios, H. P., Tsioras, P.A., Pavlidis, T., 2010. Water yield changes as a result of silvicultural treatments in an oak ecosystem. *Forest Ecology and Management* **260**: 1367-1374.

Gebauer, R., Volarik, D., Urban, J., Borja, I., Nagy, N.E., Eldhuset, T.D., Krokene, P., 2011. Effect of thinning on anatomical adaptations of Norway spruce needles. *Tree Physiology* **31**: 1103-1113.

Gomi, T., Sidle, R.C., Miyata, S., Kosugi, K.i., Onda, Y., 2008. Dynamic runoff connectivity of overland flow on steep forested hillslopes: Scale effects and runoff transfer. *Water Resources Research* **44**: W08411.

Goulden, M.L., Crill, P.M., 1997. Automated measurements of CO_2 exchange at the moss surface of a black spruce forest. *Tree Physiology* **17**: 537-542.

Granier, A., 1987. Evaluation of transpiration in a Douglas-fir stand by means of sap flow measurements. *Tree Physiology* **3**: 309-320.

Granier, A., Biron, P., Breda, N., Pontailler, J.Y., Saugier, B., 1996a. Transpiration of trees and forest stands: Short and longterm monitoring using sapflow methods. *Global Change Biology* **2**: 265-274.

Granier, A., Biron, P., Kostner, B., Gay, L.W., Najjar, G., 1996b. Comparisons of xylem sap flow and water vapour flux at the stand level and derivation of canopy conductance for Scots pine. *Theoretical and Applied Climatology* **53**: 115-122.

Granier, A., Biron, P., Lemoine, D., 2000a. Water balance, transpiration and canopy conductance in two beech stands. *Agricultural and Forest Meteorology* **100**: 291-308.

Granier, A., Huc, R., Barigah, S.T., 1996c. Transpiration of natural rain forest and its dependence on climatic factors. *Agricultural and Forest Meteorology* **78**: 19-29.

Granier, A., Loustau, D., Breda, N., 2000b. A generic model of forest canopy conductance dependent on climate, soil water availability and leaf area index. *Annals of Forest Science* **57**: 755-765.

Guswa, A.J., Celia, M.A., Rodriguez-Iturbe, I., 2002. Models of soil moisture dynamics in ecohydrology: A comparative study. *Water Resources Research* **38**: 1166.

Haibara, K., Aiba, Y., 1982. The nutrient circulation and budget for a small catchment basin of an established Sugi (*Cryptomeria japonica*) and Hinoki (*Chamaecyparis obtusa*) stand. *Journal of Japanese Forest Society* **64**: 8-14. (in Japanese with English summary)

Hanchi, A., Rapp, M., 1997. Stemflow determination in forest stands. *Forest Ecology and Management* **97**: 231-235.

Hattori, S., 1983. The seasonal variation of evaporation from the forest floor in a hinoki stand. *Journal of Japanese Forest Society* **65**: 9-16. (in Japanese with English abstract)

Hattori, S., Chikaarashi, H., Takeuchi, N., 1982. Measurement of the rainfall interception and its micrometeorological analysis in a Hinoki stand. *Bulletin of the Forestry and Forest Products Research Institute* **318**: 79-102. (in Japanese with English summary)

Hattori, S., Chikaarashi, H., 1988. Effect of thinning on canopy interception in a hinoki stand. *Journal of the Japanese Forest Society* **70**: 529-533. (in Japanese with English summary)

Hormann, G., Branding, A., Clemen, T., Herbst, M., Hinrichs, A., Thamm, F., 1996. Calculation and simulation of wind controlled canopy interception of a beech forest in northern Germany. *Agricultural and Forest Meteorology* **79**: 131-148.

Huber, A., Iroume, A., 2001. Variability of annual rainfall partitioning for different sites and forest covers in Chile. *Journal of Hydrology* **248**: 78-92.

Iwamoto, J., 2002. The development of Japanese forestry, Chapter 1. In Forestry and the Forest Industry in Japan, Iwai Y (ed). UBC Press, Vancouver, 3-9

Iwatsubo, G., Tsutsumi, T., 1967. On the amount of plant nutrients supplied to the ground by rainwater in adjacent open plot and forests (2). *Bulletin of the Kyoto University Forests* **39**: 110-124. (in Japanese with English summary)

Jackson, N.A., 2000. Measured and modelled rainfall interception loss from an agroforestry system in Kenya. *Agricultural and Forest Meteorology* **100**: 323-336.

Jackson, N.A., Wallace, J.S., 1999. Soil evaporation measurements in an agroforestry system in Kenya. *Agricultural and Forest Meteorology* **94**: 203-215.

Jansson, P.E., Cienciala, E., Grelle, A., Kellner, E., Lindahl, A., Lundblad, M., 1999. Simulated evapotranspiration from the Norunda forest stand during the growing season of a dry year. *Agricultural and Forest Meteorology* **98**: 621-628.

Jarvis, P.G., Mcnaughton, K.G., 1986. Stomatal control of transpiration - Scaling up from leaf to region. *Advances in Ecological Research* **15**: 1-49.

Keim, R.F., Skaugset, A.E., Weiler, M., 2005. Temporal persistence of spatial patterns in throughfall. *Journal of Hydrology* **314**: 263-274.

Kimmins, J.P., 1973. Some statistical aspects of sampling throughfall precipitation in nutrient cycling studies in British Columbian coastal forests. *Ecology* **54**: 1008-1019.

Kelliher, F.M., Hollinger, D.Y., Schulze, E.D., Vygodskaya, N.N., Byers, J.N., Hunt, J.E., McSeveny, T.M., Milukova, I., Sogatchev, A., Varlargin, A., Ziegler, W., Arneth, A., Bauer, G., 1997. Evaporation from an eastern Siberian larch forest. *Agricultural and Forest Meteorology* **85**: 135-147.

Kelliher, F.M., Leuning, R., Raupach, M.R., Schulze, E.D., 1995. Maximum conductances for evaporation from global vegetation types. *Agricultural and Forest Meteorology* **73**: 1-16.

Kelliher, F.M., Leuning, R., Schulze, E.D., 1993. Evaporation and canopy characteristics of coniferous forests and grasslands. *Oecologia* **95**: 153-163.

Kelliher, F.M., Whitehead, D., Mcaneney, K.J., Judd, M.J., 1990. Partitioning evapotranspiration into tree and understorey components in two young *Pinus Radiata* D. Don Stands. *Agricultural and Forest Meteorology* **50**: 211-227.

Komatsu, H., 2004. A general method of parameterizing the big-leaf model to predict the dry-canopy evaporation rate of individual oniferous forest stands. *Hydrological Processes* **18**: 3019-3036.

Komatsu, H., Hotta, N., 2007. Relationship between stem density and dry-canopy evaporation rates in coniferous forests. *Journal of Hydrology* **332**: 271-275.

Komatsu, H., Kang, Y.H., Kume, T., Yoshifuji, N., Hotta, N., 2006. Transpiration from a *Cryptomeria japonica* plantation, part 2: responses of canopy conductance to meteorological factors. *Hydrological Processes* **20**: 1321-1334.

Komatsu, H., Maita, E., Otsuki, K., 2008a. A model to estimate annual forest evapotranspiration in Japan from mean annual temperature. *Journal of Hydrology* **348**: 330-340.

Komatsu, H., Onozawa, Y., Kume, T., Tsuruta, K., Kumagai, T., Shinohara, Y., Otsuki, K., 2010. Stand-scale transpiration estimates in a Moso bamboo forest: II. Comparison with coniferous forests. *Forest Ecology and Management* **260**: 1295-1302.

Komatsu, H., Onozawa, Y., Kume, T., Tsuruta, K., Shinohara, Y., Otsuki, K., 2012. Canopy conductance for a Moso bamboo (*Phyllostachys pubescens*) forest in western Japan. *Agricultural and Forest Meteorology* **156**: 111-120.

Komatsu, H., Shinohara, Y., Kume, T., Otsuki, K., 2008b. Relationship between annual rainfall and interception ratio for forests across Japan. *Forest Ecology and Management* **256**: 1189-1197.

Komatsu, H., Tanaka, N., Kume, T., 2007. Do coniferous forests evaporate more water than broad-leaved forests in Japan? *Journal of Hydrology* **336**: 361-375.

Komatsu, H., Shinohara, Y., Nogata, M., Tsuruta, K., Otsuki, K., 2013. Changes in canopy transpitation due to thinning of a *Cryptomeria japonica* plantation. *Hydrological Research Letters* **7**: 60-65.

Kostelnik, K.M.,, Lynch, J.A., Grimm, J.W., Corbett, E.S., 1989. Sample size requirements for estimation of throughfall chemistry beneath a mixed hardwood forest. *Journal of Environmental Quality* **18**: 274-280.

Kosugi, Y., Katsuyama, M., 2007. Evapotranspiration over a Japanese cypress forest. II. Comparison of the eddy covariance and water budget methods. *Journal of Hydrology* **334**: 305-311.

Kucera, J., Bednarova, E., Kamlerova, K., 2002. Vertical profile of needle biomass and penetration of radiation through the spruce stand. *Ekologia Bratislava* **21**: 107-121.

Kuraji, K., 2003. Effects of forests on stabilizing streamflow. Nihon Chisan-chisui Kyokai, Tokyo. (in Japanese)

Kumagai, T., 2001. Modeling water transportation and storage in sapwood - model development and validation. *Agricultural and Forest Meteorology* **109**: 105-115.

Kumagai, T., Aoki, S., Otsuki, K., Utsumi, Y., 2009. Impact of stem water storage on diurnal estimates of whole-tree transpiration and canopy conductance from sap flow measurements in Japanese cedar and Japanese cypress trees. *Hydrological Processes* **23**: 2335-2344.

Kumagai, T., Aoki, S., Nagasawa, H., Mabuchi, T., Kubota, K., Inoue, S., Utsumi, Y., Otsuki, K., 2005a. Effects of tree-to-tree and radial variations on sap flow estimates of transpiration in Japanese cedar. *Agricultural and Forest Meteorology* **135**: 110-116.

Kumagai, T., Aoki, S., Shimizu, T., Otsuki, K., 2007. Sap flow estimates of stand transpiration at two slope positions in a Japanese cedar forest watershed. *Tree Physiology* **27**: 161-168.

Kumagai, T., Aoki, S., Nagasawa, H., Mabuchi, T., Kubota, K., Inoue, S., Utsumi, Y., Otsuki, K., 2005b. Effects of tree-to-tree and radial variations on sap flow estimates of transpiration in Japanese cedar. *Agricultural and Forest Meteorology* **135**: 110-116.

Kumagai, T., Nagasawa, H., Mabuchi, T., Ohsaki, S., Kubota, K., Kogi, K., Utsumi, Y., Koga, S., Otsuki, K., 2005c. Sources of error in estimating stand transpiration using allometric relationships between stem diameter and sapwood area for *Cryptomeria japonica* and *Chamaecyparis obtusa*. *Forest Ecology and Management* **206**: 191-195.

Kumagai, T., Saitoh, T.M., Sato, Y., Morooka, T., Manfroi, O.J., Kuraji, K., Suzuki, M., 2004. Transpiration, canopy conductance and the decoupling coefficient of a lowland mixed dipterocarp forest in Sarawak, Borneo: dry spell effects. *Journal of Hydrology* **287**: 237-251.

Kumagai, T., Tateishi, M., Shimizu, T., Otsuki, K., 2008. Transpiration and canopy conductance at two slope positions in a Japanese cedar forest watershed. *Agricultural and Forest Meteorology* **148**: 1444-1455.

Kume, T., Otsuki, K., Du, S., Yamanaka, N., Wang, Y.L., Liu, G.B., 2011. Spatial variation in sap flow velocity in semiarid region trees: its impact on stand-scale transpiration estimates. *Hydrological Processes* **26**: 1161-1168.

Kume, T., Tsuruta, K., Komatsu, H., Kumagai, T., Higashi, N., Shinohara, Y., Otsuki, K., 2010. Effects of sample size on sap flux-based stand-scale transpiration estimates. *Tree Physiology* **30**: 129-138.

Kurc, S.A., Small, E.E., 2004. Dynamics of evapotranspiration in semiarid grassland and shrubland ecosystems during the summer monsoon season, central New Mexico. *Water Resources Research* **40**: W09305.

Kuuluvainen, T., Pukkala, T., 1989. Simulation of within-tree and between-tree shading of direct-radiation in a forest canopy - Effect of crown shape and sun elevation. *Ecological Modelling* **49**: 89-100.

Lagergren, F., Lankreijer, H., Kucera, J., Cienciala, E., Molder, M., Lindroth, A., 2008. Thinning effects on pine-spruce forest transpiration in central Sweden. *Forest Ecology and Management* **255**: 2312-2323.

Lagergren, F., Lindroth, A., 2004. Variation in sapflow and stem growth in relation to tree size, competition and thinning in a mixed forest of pine and spruce in Sweden. *Forest Ecology and Management* **188**: 51-63.

Lai, C.T., Katul, G., Oren, R., Ellsworth, D., Schafer, K., 2000. Modeling CO_2 and water vapor turbulent flux distributions within a forest canopy. *Journal of Geophysical Research-Atmospheres* **105**: 26333-26351.

Laio, F., Porporato, A., Ridolfi, L., Rodriguez-Iturbe, I., 2001. Plants in water-controlled ecosystems: active role in hydrologic processes and response to water stress - II. Probabilistic soil moisture dynamics. *Advances in Water Resources* **24**: 707-723.

Lane, P.N.J., Mackay, S.M., 2001. Streamflow response of mixed-species eucalypt forests to patch cutting and thinning treatments. *Forest Ecology and Management* **143**: 131-142.

Lauenroth, W.K., Sala, O.E., 1992. Long-term forage production of North-American shortgrass Steppe. *Ecological Applications* **2**: 397-403.

Law, B.E., Cescatti, A., Baldocchi, D.D., 2001a. Leaf area distribution and radiative transfer in open-canopy forests: implications for mass and energy exchange. *Tree Physiology* **21**: 777-787.

Law, B.E., Goldstein, A.H., Anthoni, P.M., Unsworth, M.H., Panek, J.A., Bauer, M.R., Fracheboud, J.M., Hultman, N., 2001b. Carbon dioxide and water vapor exchange by young and old ponderosa pine ecosystems during a dry summer. *Tree Physiology* **21**: 299-308.

Lesch, W., Scott, D.F., 1997. The response in water yield to the thinning of *Pinus radiata*, *Pinus patula* and *Eucalyptus grandis* plantations. *Forest Ecology and Management* **99**: 295-307.

Leyton, L., Reynolds, E., Thompson, F.B., 1967. Rainfall interception in forest and moorland. In, Sopper, W.E., Lull, H.W. (Eds), Proceedings of the International Symposium on Forest Hydrology, Pergamon Press, New York.

Levia, D.F., Frost, E.E., 2003. A review and evaluation of stemflow literature in the hydrologic and biogeochemical cycles of forested and agricultural ecosystems. *Journal of Hydrology* **274**: 1-29.

Levia, D.F., Frost, E.E., 2006. Variability of throughfall volume and solute inputs in wooded ecosystems. *Progress in Physical Geography* **30**: 605-632.

Li, Q., Cheng, J., Li, T., Liu, F.J., 2007. Ecological function of artificial conifers timber forests in water conservation. *Jinlin Forest of Sciences and Technique* **36**: 14-20

Limousin, J.M., Rambal, S., Ourcival, J.M., Joffre, R., 2008. Modelling rainfall interception in a Mediterranean *Quercus ilex* ecosystem: Lesson from a throughfall exclusion experiment. *Journal of Hydrology* **357**: 57-66.

Lin, Y., Wang, G.X., Guo, J.Y., Sun, X.Y., 2012. Quantifying evapotranspiration and its components in a coniferous subalpine forest in Southwest China. *Hydrological Processes* **26**: 3032-3040.

Link, T.E., Unsworth, M., Marks, D., 2004. The dynamics of rainfall interception by a seasonal temperate rainforest. *Agricultural and Forest Meteorology* **124**: 171-191.

Llorens, P., 1997. Rainfall interception by a Pinus sylvestris forest patch overgrown in a Mediterranean mountainous abandoned area. 2. Assessment of the applicability of Gash's analytical model. *Journal of Hydrology* **199**: 346-359.

Llorens, P., Domingo, F., 2007. Rainfall partitioning by vegetation under Mediterranean conditions. A review of studies in Europe. *Journal of Hydrology* **335**: 37-54.

Llorens, P., Poch, R., Latron, J., Gallart, F., 1997. Rainfall interception by a *Pinus sylvestris* forest patch overgrown in a Mediterranean mountainous abandoned area. 1. Monitoring design and results down to the event scale. *Journal of Hydrology* **199**: 331-345.

Lloyd, C.R., Gash, J.H.C., Shuttleworth, W.J., Marques, A.D., 1988. The measurement and modeling of rainfall interception by Amazonian rain-forest. *Agricultural and Forest Meteorology* **43**: 277-294.

Loustau, D., Berbigier, P., Granier, A., 1992a. Interception Loss, Throughfall and stemflow in a maritime pine stand. 2. An application of Gash analytical model of interception. *Journal of Hydrology* **138**: 469-485.

Loustau, D., Berbigier, P., Granier, A., Moussa, F.E., 1992b. Interception loss, throughfall and stemflow in a Maritime pine stand. 1. Variability of throughfall and stemflow beneath the pine canopy. *Journal of Hydrology* **138**: 449-467.

Lu, P., Muller, W.J., Chacko, E.K., 2000. Spatial variations in xylem sap flux density in the trunk of orchard-grown, mature mango trees under changing soil water conditions. *Tree Physiology* **20**: 683-692.

Mahendrappa, M.K., 1990. Partitioning of rainwater and chemicals into throughfall and stemflow in different forest stands. *Forest Ecology and Management* **30**: 65-72.

Maleque, M.A., Ishii, H.T., Maeto, K., Taniguchi, S., 2007a. Line thinning enhances diversity of Coleoptera in overstocked *Cryptomeria japonica* plantations in central Japan. *Arthropod-Plant Interactions* **1**: 175-185.

Maleque, M.A., Ishii, H.T., Maeto, K., Taniguchi, S., 2007b. Line thinning fosters the abundance and diversity of understory Hymenoptera (Insecta) in Japanese cedar (*Cryptomeria japonica* D. Don) plantations. *Journal of Forest Research* **12**: 14-23.

Mazza, G., Amorini, E., Cutini, A., Manetti, M.C., 2011. The influence of thinning on rainfall interception by *Pinus pinea* L. in Mediterranean coastal stands (Castel Fusano-Rome). *Annals of Forest Science* **68**: 1323-1332.

McNaughton, K.G., Black, T.A., 1973. A study of evapotranspiration from a Douglas fir forest using the energy balance approach. *Water Resources Research* **9**: 1579-1590.

Medhurst, J.L., Battaglia, M., Beadle, C.L., 2002. Measured and predicted changes in tree and stand water use following high-intensity thinning of an 8-year-old *Eucalyptus nitens* plantation. *Tree Physiology* **22**: 775-784.

Meinzer, F.C., Grantz, D.A., 1990. Stomatal and hydraulic conductance in growing sugarcane - stomatal adjustment to water transport capacity. *Plant, Cell and Environment* **13**: 383-388.

Mitsudera, M., Satomi, S., Terashima, I., 1984. Effect of fire on water and major nutrient budgets in forest ecosystems. 3. Rainfall interception by forest canopy. *Japanese Journal of Ecology* **34**: 15-25.

Miyata, S., Kosugi, K., Nishi, Y., Gomi, T., Sidle, R.C., Mizuyama, T., 2010. Spatial pattern of infiltration rate and its effect on hydrological processes in a small headwater catchment. *Hydrological Processes* **24**: 535-549.

Mizugaki, S., Nanko, K., Onda, Y., 2010. The effect of slope angle on splash detachment in an unmanaged Japanese cypress plantation forest. *Hydrological Processes* **24**: 576-587.

Mizugaki, S., Onda, Y., Fukuyama, T., Koga, S., Asai, H., Hiramatsu, S., 2008. Estimation of suspended sediment sources using ^{137}Cs and ^{210}Pb$_{ex}$ in unmanaged Japanese cypress plantation watersheds in southern Japan. *Hydrological Processes* **22**: 4519-4531.

Molina, A.J., del Campo, A.D., 2012. The effects of experimental thinning on throughfall and stemflow: A contribution towards hydrology-oriented silviculture in Aleppo pine plantations. *Forest Ecology and Management* **269**: 206-213.

Moore, K.E., Fitzjarrald, D.R., Sakai, R.K., Goulden, M.L., Munger, J.W., Wofsy, S.C., 1996. Seasonal variation in radiative and turbulent exchange at a deciduous forest in central Massachusetts. *Journal of Applied Meteorology* **35**: 122-134.

Monteith, J.L., Unsworth, M.H., 1990. Principles of Environmental Physics. Edward Arnold, UK.

Moren, A.S., Lindroth, A., Flower-Ellis, J., Cienciala, E., Molder, M., 2000. Branch transpiration of pine and spruce scaled to tree and canopy using needle biomass distributions. *Trees-Structure and Function* **14**: 384-397.

Morikawa, Y., Hattori, S., Kiyono, Y., 1986. Transpiration of a 31-year-old *Chamaecyparis obtusa* Endl. stand before and after thinning. *Tree Physiology* **2**: 105-114.

Murai, H., 1970. Studeis on precipitation interception by forest vegetations. *The Japanese Forestry Society* **232**:25-64. (in Japanese)

Murai, H., Kumagai, N., 1989. Studies on effects of some treatments to forest so as to control steam flow in small mountian watershed. 3. Inlfuences on hydrological cycle in forest land and runoff and sediment discharge in steam. *Bulletin of the Shizuoka University Forests* **13**: 1-25.

Murakami, S., Tsuboyama, Y., Shimizu, T., Fujieda, M., Noguchi, S., 2000. Variation of evapotranspiration with stand age and climate in a small Japanese forested catchment. *Journal of Hydrology* **227**: 114-127.

Nagaike, T., Masaki, T., Ito, S., 2006. Special feature: ecology and management of conifer plantations in Japan: control of tree growth and maintenance of biodiversity. *Journal of Forest Research* **11**: 215-216.

Nanko, K., Mizugaki, S., Onda, Y., 2008. Estimation of soil splash detachment rates on the forest floor of an unmanaged Japanese cypress plantation based on field measurements of throughfall drop sizes and velocities. *Catena* **72**: 348-361.

Nanko, K., Onda, Y., Ito, A., Ito, S., Mizugaki, S., Moriwaki, H., 2010. Variability of surface runoff generation and infiltration rate under a tree canopy: indoor rainfall experiment using Japanese cypress (*Chamaecyparis obtusa*). *Hydrological Processes* **24**: 567-575.

Nanko, K., Onda, Y., Ito, A., Moriwaki, H., 2011. Spatial variability of throughfall under a single tree: Experimental study of rainfall amount, raindrops, and kinetic energy. *Agricultural and Forest Meteorology* **151**: 1173-1182.

Nanko, K., Onda, Y., Kato, H., Gomi, T., 2013. Immediate change in throughfall saptial distribution and canopy interception after heavy thinning in a dense mature Japanese cypress plantation. *Ecohydrology* under review.

National Astronomical Observatory, 2009. Chronological Environmental Tables 2009/2000. Maruzen, Tokyo.

National Research Council, 2008. Hydrologic effects of a changing forest landscape. National Academies Press: 15-17.

Norman, J.M., Garcia, R., Verma, S.B., 1992. Soil Surface CO_2 fluxes and the carbon budget of a grassland. *Journal of Geophysical Research-Atmospheres* **97**: 18845-18853.

Onda, Y., Gomi, T., Mizugaki, S., Nonoda, T., Sidle, R.C., 2010. An overview of the field and modelling studies on the effects of forest devastation on flooding and environmental issues. *Hydrological Processes* **24**: 527-534.

Onda, Y., Yukawa, N., 1994. The influence of understories and litter layer on the infiltration of forested hillslopes. *Proceedings of the International Symposium of Forest Hydrology*: 107-114.

Oren, R., Phillips, N., Ewers, B.E., Pataki, D.E., Megonigal, J.P., 1999. Sap-flux-scaled transpiration responses to light, vapor pressure deficit, and leaf area reduction in a flooded Taxodium distichum forest. *Tree Physiology* **19**: 337-347.

Pataki, D.E., Oren, R., 2003. Species differences in stomatal control of water loss at the canopy scale in a mature bottomland deciduous forest. *Advances in Water Resources* **26**: 1267-1278.

Phillips, N., Oren, R., 1998. A comparison of daily representations of canopy conductance based on two conditional time-averaging methods and the dependence of daily conductance on environmental factors. *Annals of Forest Science* **55**: 217-235.

Phillips, N., Oren, R., Zimmermann, R., 1996. Radial patterns of xylem sap flow in non-, diffuse- and ring-porous tree species. *Plant, Cell and Environment* **19**: 983-990.

Pielke, R.A., 2001. Influence of the spatial distribution of vegetation and soils on the prediction of cumulus convective rainfall. *Reviews of Geophysics* **39**: 151-177.

Porporato, A., Laio, F., Ridolfi, L., Rodriguez-Iturbe, I., 2001. Plants in water-controlled ecosystems: active role in hydrologic processes and response to water stress. III. Vegetation water stress. *Advances in Water Resources* **24**: 725-744.

Price, A.G., Carlyle-Moses, D.E., 2003. Measurement and modelling of growing-season canopy water fluxes in a mature mixed deciduous forest stand, southern Ontario, Canada. *Agricultural and Forest Meteorology* **119**: 69-85.

Raupach, M.R., 1995. Vegetation atmosphere interaction and surface conductance at leaf, canopy and regional scales. *Agricultural and Forest Meteorology* **73**: 151-179.

Raz-Yaseef, N., Rotenberg, E., Yakir, D., 2010. Effects of spatial variations in soil evaporation caused by tree shading on water flux partitioning in a semi-arid pine forest. *Agricultural and Forest Meteorology* **150**: 454-462.

Raz-Yaseef, N., Yakir, D., Schiller, G., Cohen, S., 2012. Dynamics of evapotranspiration partitioning in a semi-arid forest as affected by temporal rainfall patterns. *Agricultural and Forest Meteorology* **157**: 77-85.

Reid, D.E.B., Silins, U., Lieffers, V.J., 2006. Sapwood hydraulic recovery following thinning in lodgepole pine. *Annals of Forest Science* **63**: 329-338.

Roberts, J., 1983. Forest transpiration - a conservative hydrological process. *Journal of Hydrology* **66**: 133-141.

Rodriguez-Iturbe, I., 2000. Ecohydrology: A hydrologic perspective of climate-soil-vegetation dynamics. *Water Resources Research* **36**: 3-9.

Ruprecht, J.K., Schofield, N.J., Crombie, D.S., Vertessy, R.A., Stoneman, G.L., 1991. Early hydrological response to intense forest thinning in Southwestern Australia. *Journal of Hydrology* **127**: 261-277.

Rutter, A.J., Kershaw, K.A., Robins, P.C., Morton, A.J., 1971. A predictive model of rainfall interception in forests, 1. Derivation of the model from observations in a plantation of Corsican pine. *Agricultural and Forest Meteorology* **9**: 367-384.

Rutter, A.J., Morton, A.J., 1977. A predictive model of rainfall interception in forests. 3. Sensitivity of model to stand parameters and meteorological variables. *Journal of Applied Ecology* **14**: 567-588.

Rutter, A.J., Morton, A.J., Robins, P.C., 1975. A predictive model of rainfall interception in forests. 2. Generalization of the model and comparison with observations in some coniferous and hardwood stands. *Journal of Applied Ecology* **12**: 367-380.

Sado, S., Kurita, M., 2004. Long-term measurements on changes in throughfall induced by thinning for a hinoki plantation. *Report of Yamaguchi forestry* **17**: 14-18.

Sato, Y., Otsuki, K., Ogawa, S., 2003a. Estimation of annual canopy interception by lithocarpus edulis Nakai. *Bulletin of the Kyoto University Forests* **83**: 15-29. (in Japanese with English summary)

Sato, Y., Kume, A., Otsuki, K., Ogawa, S., 2003b. Effects of difference in canopy structure on the distribution of throughfall - A comparison of throughfall characteristics between the coniferous forest and the broad-leaved forest. *Joural of Japan Society of Hydrology and Water Resources* **16**: 605-616. (in Japanese with English summary)

Schaap, M.G., Bouten, W., 1997. Forest floor evaporation in a dense Douglas fir stand. *Journal of Hydrology* **193**: 97-113.

Schellekens, J., Scatena, F.N., Bruijnzeel, L.A., Wickel, A.J., 1999. Modelling rainfall interception by a lowland tropical rain forest in northeastern Puerto Rico. *Journal of Hydrology* **225**: 168-184.

Serengil, Y., Gokbulak, F., Ozhan, S., Hizal, A., Sengonul, K., Balci, A.N., Ozyuvaci, N., 2007. Hydrological impacts of a slight thinning treatment in a deciduous forest ecosystem in Turkey. *Journal of Hydrology* **333**: 569-577.

Shachnovich, Y., Berliner, P.R., Bar, P., 2008. Rainfall interception and spatial distribution of throughfall in a pine forest planted in an arid zone. *Journal of Hydrology* **349**: 168-177.

Shi, Z.J., Wang, Y.H., Xu, L.H., Xiong, W., Yu, P.T., Gao, J.X., Zhang, L.B., 2010. Fraction of incident rainfall within the canopy of a pure stand of *Pinus armandii* with revised Gash model in the Liupan Mountains of China. *Journal of Hydrology* **385**: 44-50.

Shimizu, A., Shimizu, T., Miyabuchi, Y., Ogawa, Y., 2003. Evapotranspiration and runoff in a forest watershed, western Japan. *Hydrological Processes* **17**: 3125-3139.

Shinohara, Y., Ide, J., Higashi, N., Komatsu, H., Kume, T., Chiwa, M., Otsuki, K., 2010. Observation of canopy interception loss in an abandoned coniferous plantation. *Journal of Japanese Forest Society* **92**: 54-59 (in Japanese with English summary)

Shinohara, Y., Tsuruta, K., Ogura, A., Noto, F., Komatsu, H., Otsuki, K., Maruyama, T., 2013. Azimuthal and radial variations in sap flux density and effects on stand-scale transpiration estimates in a Japanese cedar forest. *Tree Physiology* **33**: 550-558.

Sidle, R.C., Kim, K., Tsuboyama, Y., Hosoda, I., 2011. Development and application of a simple hydrogeomorphic model for headwater catchments. *Water Resources Research* **47**: W00H13.

Sidle, R.C., Tsuboyama, Y., Noguchi, S., Hosoda, I., Fujieda, M., Shimizu, T., 2000. Stormflow generation in steep forested headwaters: a linked hydrogeomorphic paradigm. *Hydrological Processes* **14**: 369-385.

Silva, I.C., Rodriguez, H.G., 2001. Interception loss, throughfall and stemflow chemistry in pine and oak forests in northeastern Mexico. *Tree Physiology* **21**: 1009-1013.

Silva, I.C., Okumura, T., 1996. Throughfall, stemflow, and interception loss in mixed white oak forest (*Quericus serrata* Thunb.). *Journal of Forest Research* **1**: 123-129.

Simonin, K., Kolb, T.E., Montes-Helu, M., Koch, G.W., 2006. Restoration thinning and influence of tree size and leaf area to sapwood area ratio on water relations of *Pinus ponderosa*. *Tree Physiology* **26**: 493-503.

Simonin, K., Kolb, T.E., Montes-Helu, M., Koch, G.W., 2007. The influence of thinning on components of stand water balance in a ponderosa pine forest stand during and after extreme drought. *Agricultural and Forest Meteorology* **143**: 266-276.

Staelens, J., De Schrijver, A., Verheyen, K., Verhoest, N.E.C., 2006. Spatial variability and temporal stability of throughfall water under a dominant beech (*Fagus sylvatica* L.) tree in relationship to canopy cover. *Journal of Hydrology* **330**: 651-662.

Stednick, J.D., 1996. Monitoring the effects of timber harvest on annual water yield. *Journal of Hydrology* **176**: 79-95.

Stogsdill, W.R., Wittwer, R.F., Hennessey, T.C., Dougherty, P.M., 1989. Relationship between throughfall and stand density in a *Pinus taeda* plantation. *Forest Ecology and Management* **29**: 105-113.

Stogsdill, W.R., Wittwer, R.F., Hennessey, T.C., Dougherty, P.M., 1992. Water-use in thinned loblolly pine plantations. *Forest Ecology and Management* **50**: 233-245.

Stomph, T.J., De Ridder, N., Steenhuis, T.S., Van de Giesen, N.C., 2002. Scale effects of Hortonian overland flow and rainfall-runoff dynamics: Laboratory validation of a process-based model. *Earth Surface Processes and Landforms* **27**: 847-855.

Suleiman, A.A., Ritchie, J.T., 2003. Modeling soil water redistribution during second-stage evaporation. *Soil Science Society of America Journal* **67**: 377-386.

Sawano, S., Komatsu H., Suzuki, M., 2005. Differences in annual precipitation amounts between forested area, agricultural area, and urban area in Japan. *Joural of Japan Society of Hydrology and Water Resources* **18**: 435-440. (in Japanese with English summary)

Takagi, M., 2013. Evapotranspiration and deep percolation of a small catchment with a mature Japanese cypress plantation. *Journal of Forest Research* **18**: 73-81.

Tanaka, N., Kuraji, K., Suzuki, Y., Suzuki, M., Ohta, T., Suzuki, M., 2005. Throughfall, stemflow and rainfall interception at mature *Cryptomeria japonica* and *Chamaecyparis obtusa* stands in Fukuroyamasawa watershed. *Bulletin of the Tokyo University Forests* **113**: 197-240. (in Japanese with English summary)

Taniguchi, S., 1999. A case study of practicing the line-thinning with the help of high-efficiency forestry machines. *Applied Forestry Sciences*: 181–184. (in Japanese)

Taniguchi, M., Tsujimura, M., Tanaka, T., 1996. Significance of stemflow in groundwater recharge. 1. Evaluation of the stemflow contribution to recharge using a mass balance approach. *Hydrological Processes* **10**: 71-80.

Teklehaimanot, Z., Jarvis, P.G., Ledger, D.C., 1991. Rainfall interception and boundary-layer conductance in relation to tree spacing. *Journal of Hydrology* **123**: 261-278.

Teramage, M.T., Onda, Y., Kato, H., Wakiyama, Y., Mizugaki, S., Hiramatsu, S., 2013. The relationship of soil organic carbon to $^{210}Pb_{ex}$ and ^{137}Cs during surface soil erosion in a hillslope forested environment. *Geoderma* **192**: 59-67.

Thomas, S.C., Halpern, C.B., Falk, D.A., Liguori, D.A., Austin, K.A., 1999. Plant diversity in managed forests: Understory responses to thinning and fertilization. *Ecological Applications* **9**: 864-879.

Tian, F.X., Zhao, C.Y., Feng, Z.D., 2011. Simulating evapotranspiration of Qinghai spruce (*Picea crassifolia*) forest in the Qilian Mountains, northwestern China. *Journal of Arid Environments* **75**: 648-655.

Tsujimura, M., Tanaka, T., 1998. Evaluation of evaporation rate from forested soil surface using stable isotopic composition of soil water in a headwater basin. *Hydrological Processes* **12**: 2093-2103.

Valente, F., David, J.S., Gash, J.H.C., 1997. Modelling interception loss for two sparse eucalypt and pine forests in central Portugal using reformulated Rutter and Gash analytical models. *Journal of Hydrology* **190**: 141-162.

van Dijk, A.I.J.M., Bruijnzeel, L.A., 2001. Modelling rainfall interception by vegetation of variable density using an adapted analytical model. Part 2. Model validation for a tropical upland mixed cropping system. *Journal of Hydrology* **247**: 239-262.

Van Pelt, R., Franklin, J.F., 2000. Influence of canopy structure on the understory environment in tall, old-growth, conifer forests. *Canadian Journal of Forest Research* **30**: 1231-1245.

Vellak, K., Paal, J., Liira, J., 2003. Diversity and distribution pattern of bryophytes and vascular plants in a boreal spruce forest. *Silva Fennica* **37**: 3-13.

Vertessy, R.A., Benyon, R.G., Osullivan, S.K., Gribben, P.R., 1995. Relationships between stem diameter, sapwood area, leaf-area and transpiration in a young mountain ash forest. *Tree Physiology* **15**: 559-567.

Viville, D., Biron, P., Granier, A., Dambrine, E., Probst, A., 1993. Interception in a mountainous declining spruce stand in the srengbach catchment (Vosges, France). *Journal of Hydrology* **144**: 273-282.

Wallace, J., McJannet, D., 2006. On interception modelling of a lowland coastal rainforest in northern Queensland, Australia. *Journal of Hydrology* **329**: 477-488.

Waterloo, M.J., Bruijnzeel, L.A., Vugts, H.F., Rawaqa, T.T., 1999. Evaporation from *Pinus caribaea* plantations on former grassland soils under maritime tropical conditions. *Water Resources Research* **35**: 2133-2144.

Whitehead, D., 1998. Regulation of stomatal conductance and transpiration in forest canopies. *Tree Physiology* **18**: 633-644.

Whitehead, D., Kelliher, F.M., 1991. A canopy water-balance model for a *Pinus radiata* stand before and after thinning. *Agricultural and Forest Meteorology* **55**: 109-126.

Williams, D.G., Cable, W., Hultine, K., Hoedjes, J.C.B., Yepez, E.A., Simonneaux, V., Er-Raki, S., Boulet, G., de Bruin, H.A.R., Chehbouni, A., Hartogensis, O.K., Timouk, F., 2004. Evapotranspiration components determined by stable isotope, sap flow and eddy covariance techniques. *Agricultural and Forest Meteorology* **125**: 241-258.

Wilson, K.B., Hanson, P.J., Baldocchi, D.D., 2000. Factors controlling evaporation and energy partitioning beneath a deciduous forest over an annual cycle. *Agricultural and Forest Meteorology* **102**: 83-103.

Wilson, K.B., Hanson, P.J., Mulholland, P.J., Baldocchi, D.D., Wullschleger, S.D., 2001. A comparison of methods for determining forest evapotranspiration and its components: sap-flow, soil water budget, eddy covariance and catchment water balance. *Agricultural and Forest Meteorology* **106**: 153-168.

Wullschleger, S.D., King, A.W., 2000. Radial variation in sap velocity as a function of stem diameter and sapwood thickness in yellow-poplar trees. *Tree Physiology* **20**: 511-518.

Wullschleger, S.D., Wilson, K.B., Hanson, P.J., 2000. Environmental control of whole-plant transpiration, canopy conductance and estimates of the decoupling coefficient for large red maple trees. *Agricultural and Forest Meteorology* **104**: 157-168.

Zang, D.Q., Beadle, C.L., White, D.A., 1996. Variation of sapflow velocity in Eucalyptus globulus with position in sapwood and use of a correction coefficient. *Tree Physiology* **16**: 697-703.

Zhang, L., Dawes, W.R., Walker, G.R., 2001. Response of mean annual evapotranspiration to vegetation changes at catchment scale. *Water Resources Research* **37**: 701-708.

Zhang, Z., Fukushima, T., Onda, Y., Mizugaki, S., Gomi, T., Kosugi, K.i., Hiramatsu, S., Kitahara, H., Kuraji, K., Terajima, T., 2008. Characterisation of diffuse pollutions from forested watersheds in Japan during storm events — Its association with rainfall and watershed features. *Science of The Total Environment* **390**: 215-226.

Zimmermann, B., Zimmermann, A., Lark, R.M., Elsenbeer, H., 2010. Sampling procedures for throughfall monitoring: A simulation study. *Water Resources Research* **46**: W01503.